Universidade de Évora - Instituto de Investigacão e Formacão Avançada

Programa de Doutoramento em Bioquímica

Tese de Doutoramento

Identification of protein-based materials in Cultural Heritage: Immunodetection of Paint Binders

Aditya Sandeep Goyal

Orientador(es) | Ana Teresa Caldeira

António José Candeias

Carole Mathe de Souza

Évora 2023

Universidade de Évora - Instituto de Investigacão e Formacão Avançada

Programa de Doutoramento em Bioquímica

Tese de Doutoramento

Identification of protein-based materials in Cultural Heritage: Immunodetection of Paint Binders

Aditya Sandeep Goyal

Orientador(es) | Ana Teresa Caldeira

António José Candeias

Carole Mathe de Souza

Évora 2023

A tese de doutoramento foi objeto de apreciação e discussão pública pelo seguinte júri nomeado pelo Diretor do Instituto de Investigacão e Formacão Avançada:

Presidente | António Manuel Pereira (Universidade de Évora)

Vogais | Ana Teresa Caldeira (Universidade de Évora)
Carole Mathe de Souza (Avignon Universite)
Gérald Culioli (Avignon Universite)
Maria Rosário Martins (Universidade de Évora)
Maria da Conceição Fernandes (Centro de Biotecnologia Agrícola e Agro-Alimentar do Alentejo-CEBAL)
Nathalie Dupuy (Aix-Marseille Universite)
Paula Cristina de Sério Branco (Universidade Nova de Lisboa - Faculdade de Ciências e Tecnologias)

Évora 2023

Declaration

I hereby declare that the contents and organization of this dissertation constitute my own original work and does not compromise in any way the rights of third parties, including those relating to the security of personal data.

Aditya Sandeep Goyal 2023

* This dissertation is presented in partial fulfilment of the requirements for **Ph.D. degree** in Biochemistry at the University of Évora and for **Ph.D. degree** in Chemistry at Université d'Avignon et des Pays de Vaucluse.

I would like to dedicate this thesis to my loving family, friends, and people that helped me, as well as those working in this field.

Acknowledgments

This PhD project has been carried out under the European Joint Doctorate in "Archaeological and Cultural Heritage Materials Science" - ED- ARCHMAT, awarding a joint Double Doctorate degree in *Biochemistry (Bioquimica)* by University of Evora (UEVORA), in cotutelle with the degree in *Chemistry (Chemie)* by Université d'Avignon et des Pays de Vaucluse (UAPV).

This project has received funding from the European Union's Horizon 2020 research and innovation programme H2020-MSCA- ITN-2017- EJD: Marie Skłodowska-Curie Innovative Training Networks (European Joint Doctorate) – Grant agreement no: 766311 – ED-ARCHMAT.

Sample collection in the research was by special permission of the Centre de Conservation et de Restauration du Patrimoine – CCRP in Perpignan and Perpignan Museum authorities. The collaboration was organised by Prof. Carole Mathe, my co-supervisor from the IMBE - UMR 7263 – CNRS, Ingénierie de la restauration des patrimoines naturel et culturel, Avignon Université - UFR-ip STS.

The ELISA immunoassays and synthesis of silica nanoparticles in this research was conducted in the Departamento de Química e Bioquímica in University of Evora & Bio-LAB at HERCULES Laboratory with the supervision from my Supervisor Prof. Ana Teresa Cardeira and Dr. Catia Salvador.

The Pyrolysis-GC-MS, FTIR Microcompression and development of paint model replicas with heritage materials was conducted at IMBE- Ingénierie de la restauration des patrimoines naturel et culturel, Avignon Université - UFR-ip STS under the supervision of Prof. Carole Mathe De Souza.

A special thanks to my second supervisor, Prof. Antonio Candeias for giving his expert opinion in the area of nanotechnology and providing special analysis provisions for the characterisation of the silica nanoparticles, in particular for the Nitrogen porosimetry, SEM analysis and the calcination of the nanoparticles. It was a pleasure to work and learn from him and a privilege to have his guidance.

The instruments used in this research particularly the orbital agitator, the ultrasonic bath, the Microplate reader, The dry-air oven were from the Departamento de Química e Bioquímica in University of Evora & Bio-LAB at HERCULES Laboratory.

A very special thanks to my Supervisor Prof. Ana Teresa Caldeira for being generous in procuring and providing any and all materials required for my research analysis in Évora, in particular the primary & secondary antibodies, the ELISA plates, the silica precursors & surfactants and commercial proteins. Furthermore, I am thankful for her trust in me to synthesize the silica nanoparticles and perform ground-breaking research with nanobiotechnological application with protein-nanoparticle interactions. I cannot forget her kindness in every sense to me and I will always be grateful for the flexibility she gave to me in performing the experiments.

A big thank you to my colleague & friend Dr. Catia Salvador for helping me throughout my research from the beginning till the end and guiding me through tough times. It would have been almost impossible to be on the right track without her support. I was able to work independently in the lab just in a couple of months from the beginning of my research journey due to her advice during my research work at Évora.

Many thanks to Celine Joliot for helping me at every stage of my research in the lab at Avignon and teaching me a bit of French while we were at it. I'm pretty sure that the amount of research I did in the final year of my PhD would not have been stress-free without her support.

A special thanks to Mr. Herve Giocanti for his help to develop the paint models at Avignon and to Mrs Isabelle Jubal Desperamont (Responsable du Centre de conservation et de restauration du patrimoine du Conseil Départemental, Direction des patrimoines) for providing the artistic samples for the case study analysis in the final chapter.

Many thanks to the professors and researchers in the Hercules Lab at University of Evora and at University of Avignon for encouraging me to go ahead at every stage of my research.

A very special thanks to my wife, Vanessa Santos Pereira who was present at every step during my PhD journey. We started as friends back in 2019 when I begun my PhD journey and then as a couple over the course of the research and now we are finally married at the time of submission. I'm a better man today than I was when we met and all credit goes to you. I cherish every moment with you.

I'd also like to a very special thanks to my closest friends during this research work which includes Sriradha Bhattacharya, Yufan Ding and Paladugu Roshan. Without them, it would not have been so much fun while sailing through this long voyage. Those coffee breaks, 1am discussions on life and being there for each other during the COVID pandemic would have been unbearable without all your love and support.

Sincerest thanks to my supervisors – Prof. Ana Teresa Caldeira, Prof. Antonio Candeias and Prof. Carole Mathe De Souza for their great effort and selfless support in my study and research during this PhD.

In the end, gratefulness to my family and friends, for cheering up and accompanying with me in any difficult times.

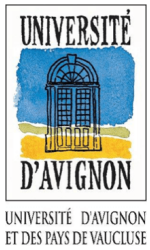

Abstract

Identification of protein-based materials in Cultural Heritage: Immunodetection of Paint Binders

This PhD thesis aims to investigate the identification of proteinaceous materials in particular used in paintings and artworks by immunodetection and other complimentary methodologies. The thesis is divided into two parts. The first part (chapters 1-3) goes in depth on the detection of proteins with ELISA and its optimization with silica nanoparticles. The second (chapters 4-5) investigates the development of paint model replicas to imitate real artworks with proteinaceous binders, application of other complimentary techniques to detect proteins and the comparison with ELISA on real artworks. In particular, chapter 1 focuses the use of proteins in artworks and bibliographical literature on the particular use of ELISA as a method for detection and investigates the different complimentary techniques such as stratigraphy, Naphthalene Blue black and Pyrolysis GC-MS and how they have been applied in the past to detect proteins in artworks and the use of standard markers for characterization with chromatography. Chapter 2 provides an in-depth case study of ELISA based immunoassays to detect proteins from previously developed paint models. Chapter 3 investigates the optimisation of ELISA with silica nanoparticles for protein detection. Chapter 4 illustrates the development of paint model replicas with the use of heritage materials and proteinaceous binders and their characterization to detect proteins with Pyrolysis GC-MS. Chapter 5 portrays four case studies from the samples obtained at the Perpignan museum in France and their characterization with stratigraphy, Pyrolysis GC-MS and ELISA while comparing the results of protein detection between the latter two.

Keywords: ELISA, immunoassays, proteins, collagen, casein, ovalbumin, pyrolysis, silica nanoparticles, MCM-41

Resumo

Identificação de materiais à base de proteínas no Património Cultural: Imunodetecção de ligantes de tintas

Este projeto visa investigar a identificação de materiais proteicos, nomeadamente utilizados em pinturas e obras de arte pora imunodetecção e outras metodologias complementares. A tese está dividida em duas partes. A primeira parte (capítulos 1-3) desenvolve de forma detalhada a deteção de proteínas com ELISA e a sua otimização com nanopartículas de sílica. A segunda parte (capítulos 4-6) investiga o desenvolvimento de réplicas de modelos de pintura que mimetizam obras reais, com diferentes ligandos proteicos, e utilizam-se diversas técnicas complementares para detetar proteínas. Faz-se ainda uma comparação com a deteção por ELISA em obras de arte reais. Em particular, o capítulo 1 centra-se na utilização de proteínas em obras de arte e literatura bibliográfica sobre a utilização particular da ELISA como método de deteção. O capítulo 2 fornece um estudo aprofundado de caso de imunoensaios baseados em ELISA para detetar proteínas de modelos de pintura previamente desenvolvidos. O Capítulo 3 investiga a otimização da ELISA com nanopartículas de sílica para deteção de proteínas. O capítulo 4 investiga as diferentes técnicas complementares, tais como a estratigrafia, a naftalina azul e a pirólise GC-MS e como foram aplicadas no passado para detetar proteínas em obras de arte e a utilização de marcadores padrão para caracterização com cromatografia. O Capítulo 5 ilustra o desenvolvimento de réplicas de modelos de pintura com a utilização de materiais patrimoniais e aglutinantes proteicos e a sua caracterização para detetar proteínas com Pirólise GC-MS. O capítulo 6 retrata quatro estudos de caso das amostras obtidas no museu de Perpignan em França e a caracterização com estratigrafia, Pirólise GC-MS e ELISA, comparando os resultados da deteção de proteínas entre os dois últimos.

Palavras-Chave: ELISA, imunodetecção, proteínas, colagénio, caseína, ovalbumina, pirólise, nanopartículas de sílica, MCM-41

Résumé

Identification des matériaux à base de protéines dans le patrimoine culturel : immunodétection des liants de peinture

Ce projet vise à étudier l'identification des matériaux protéiques en particulier utilisés dans les peintures et les œuvres d'art par Immunodetection et d'autres méthodologies complémentaires. La thèse est divisée en deux parties. La première partie (chapitres 1-3) approfondit la détection des protéines avec ELISA et son optimisation avec les nanoparticules de silice. Le second (chapitres 4-6) étudie le développement de répliques de modèles de peinture pour imiter de vraies œuvres d'art avec des liants protéiques, l'application d'autres techniques complémentaires pour détecter les protéines et la comparaison avec ELISA sur des œuvres d'art réelles. En particulier, le chapitre 1 met l'accent sur l'utilisation des protéines dans les œuvres d'art et la littérature bibliographique sur l'utilisation particulière du test ELISA comme méthode de détection. Le chapitre 2 fournit une étude de cas approfondie des immunoessais basés sur ELISA pour détecter les protéines à partir de modèles de peinture précédemment développés. Le chapitre 3 étudie l'optimisation d'ELISA avec des nanoparticules de silice pour la détection des protéines. Le chapitre 4 examine les différentes techniques complémentaires telles que la stratigraphie, le bleu de naphtalène noir et la GC-MS de pyrolyse et comment elles ont été appliquées dans le passé pour détecter les protéines dans les œuvres d'art et l'utilisation de marqueurs standard pour la caractérisation par chromatographie. Le chapitre 5 illustre le développement de répliques de modèles de peinture avec l'utilisation de matériaux patrimoniaux et de liants protéiques et leur caractérisation pour détecter les protéines avec la GC-MS par pyrolyse. Le chapitre 6 présente quatre études de cas à partir des échantillons obtenus au musée de Perpignan en France et la caractérisation avec stratigraphie, Pyrolyse GC-MS et ELISA tout en comparant les résultats de détection des protéines entre les deux derniers.

Mots Clés: ELISA, Immunodetection, protéines, collagène, caséine, ovalbumine, pyrolyse, nanoparticules de silice, MCM-41

Contents

List of Figures

List of Tables

List of Abbreviations

1. **BSA**- Bovine Serum Albumin
2. **CTAB**- Cetyltrimethylammonium bromide
3. **ELISA**- Enzyme-Linked Immunosorbent Assay
4. **HMDS**- Hexamethyldisilane
5. **MCM-41**- Mobil Composition of Matter hexagonal structure mesoporous silica
6. **NPSiO$_2$-** Monodisperse Silica Nanoparticles
7. **PBS**- Phosphate Buffer Solution
8. **pnPP**-4-Nitrophenyl phosphate disodium salt hexahydrate
9. **Py-GC-MS**- Pyrolysis with Gas chromatography and Mass Spectroscopy
10. **SEM-** Scanning Electron Microscope
11. **TMAH**- Tetramethylammonium hydroxide
12. **TEOS**-Tetra Ethyl Ortho Silicate
13. **XRD-** X-Ray Diffraction

Chapter 1

State of The Art

Cultural heritage (CH) is an interdisciplinary field of research. It involves history, archaeology, geology, science and engineering combined with each other [1-5]. The protection of cultural artefacts such as monuments and works of art and craft can be traced back to the 15th century in Europe [6, 7]. Janet Blake states that "CH artefacts can be considered within an extensive list of objects such as monuments and complexes of buildings, sites of archaeological or historic significance, ancient works of art (including rock carvings and cave paintings), ethnographic items, places associated with the development of a technology or industry, landscapes and topographical features, grave sites, sacred places and ritual sites, natural features endowed with special cultural significance to a people, items of clothing or jewellery, weapons, daily utensils, ritual items, musical instruments, objects associated with certain historical characters, coins, carved obsidian or ivory, fossils, skeletal remains, pollen samples, ancient copper or tin mines" [8]. The economic impact on any modern country's revenue with cultural heritage and its protection outweigh the investments for its conservation [9]. Some of the salient features of cultural heritage research as part of any economy are more jobs, tourism, preserving the cultural history of the region/place and upgrading the monumental constructs [9,10]. Marta de la Torre states that "The narrow view of heritage presented in 1964 in the Charter of Venice still reflected eighteenth- and nineteenth-century ideas developed in England and France. Traditionally conservation focused on the preservation of fabric and was equated with interventions and legal protection [11]." Moreover, CH artefacts have an immediate need to be preserved and therefore require to undergo vast amount of investigation at the scientific level. In fact, it is the materials in these artefacts that require attention and therefore make up the core of better understanding the needs of cultural heritage conservation.

The impact of conservation has serious implications on the natural values of a place and the protection of the heritage for future generations. Heritage as a modern scientific field and area of research only came to light about 50 years ago when the United Nations held the 1972 UNESCO World Heritage Convention. The preservation of heritage have become an important field of academic study and research in recent times. Though heritage as a field of research

started off as a hobby from archaeology and conservation, the wide diversity in ideas comes from it being quite multidisciplinary in nature. This interdisciplinary approach branches from different ideologies that arise from the different views and opinions about how to tackle a particular problem [11].

Although the presence of experts from different areas of research provide a unique opportunity for Heritage as a field to grow, it also possesses significant challenges to mutual understanding. Going further into the near future, a transdisciplinary approach is one that could benefit largely the conservation and preservation of artefacts. Both tangible and intangible heritage have been at the centre of cultural tourism [12]. It is important to identify the knowledge gap and the issues in accomplishing solutions for different types of cultural heritage to attract tourism and recently to effects on climate change. In terms of the methodology used to promote research into finding solutions, there are different models based on demographic locations. The funding that is derived for the purpose of cultural heritage can also largely differ based on the place from where this model has been derived. The North American model of cultural tourism involves research via academic institutions, museums or private groups that are funded by philanthropic contributions from private and wealthy individuals. In the European model, the main difference lies in funding that comes mostly from governmental institutions. Whereas both have its pros and cons, the transparency in functioning and communication within the Heritage research environment almost always leads seems to be the most efficient [12].

When it comes to cultural heritage research, the artefacts that help uncover or rediscover a particular finding, it is the proper scientific tools applied to the artefacts that finally provides the right result. To dwell further deep into the artefact, it is the materials from which the artefacts are made of that determine what scientific methodology would be the most appropriate. Therefore, it is the materials from which cultural heritage artefacts uncover information about its past [13]. Generally, these materials fall under the category of metals, ceramics, polymers or composites with more often than not being a combination of two or more types of materials. The study of materials in cultural heritage artefacts has given rise to a new area of research known as archaeological materials science, or simply known as archaeometry [14]. Moreover, the combination of biological sciences with materials science as an area has been widely popular over the past decade. Therefore, the term archaeometry can be broadened further to describe the scientific study of cultural heritage artefacts with interdisciplinary fields intertwined and stitched to work as one research unit.

Different cultures from around the world, in different ways, endeavour to safeguard their cultural heritage, as it is the principal component of their character inside present day human advancement. The various headings and manners by which these cycles are acknowledged rely upon the particular progressive phase of science and innovation, government assistance of society, and experienced risks of this character. Vital objects of cultural heritage are material endlessly objects of art created by all networks. The physical and mechanical properties of material objects are dependably of prime worry to archaeometry and science-based studies in archaeology. The protection of material objects for people in the future with the most ideal devotion expects top to bottom information, to help the most reasonable reclamation, conservation, stockpiling, and possible exhibition hall show. An insightful usage of present day techniques for substance examination is a huge component of exploration studies into such objects giving data on the most reasonable strategies for their rebuilding and conservation. There is wide energy among conservators and keepers for the use of logical instruments to improve the administration of assortments.

According to the perspective of use to an examination of archaeological and art objects, it is frequently vital to utilize both non-destructive (which can be now and again completely harmless) techniques as well as destructive strategies for present day microanalysis for investigation of little examples. As data about given objects or artistic procedures dependent just upon authentic sources may frequently prompt serious misinterpretations, there are various purposes for the use of chemical examination in archaeometric studies. They might be very important in showing the provenance of an item and the beginning of the materials used for its production, and likewise in deciding degradation state and checking the changes occur during the maturing system. They are additionally helpful while picking the most reasonable techniques for rebuilding and conservation, the sort of materials for conservation, and furthermore in checking the advancement of conservation processes. The use of analytical techniques to improve the management of collections has received a lot of support from curators and conservators.

Different insightful techniques can likewise be employed for dating of materials and recognizable proof of phony art objects. Prior works in this field focused basically on examination of inorganic materials [15]; nonetheless, over the most recent twenty years significant advancement in elite execution partition methods has permitted definite conclusions

of different gatherings of organic mixtures fundamental for materials studies (colours, saps, oils, waxes, starches, and proteins).

Non-destructive strategies find a particular spot among scientific techniques utilized for archaeometric purposes due to the one of a kind worth of the vast majority of the objects examined. Their chief benefit is the absence of need for sampling from objects, and on account of present day versatile instrumentation there is additionally the chance of performing estimations on location. Most regularly these techniques are utilized for essential examination, however in late many years they have additionally been utilized for assurance of different gatherings of mixtures. For essential examination of such objects, e.g., glasses, paintings, metallic objects, and verifiable compositions, microbeam procedures, for example, electron microscopy with energy dispersive X-ray spectrometry are usually utilized [9-11]. [12].

Various other spectroscopic strategies are likewise utilized in non-destructive mode in the examination of artifacts. In the UV-vis range one can utilize reflectance spectroscopy, yet substantially more data is given by, e.g., Raman spectroscopy with a fibreoptic microprobe, which is broadly utilized for ID of organic shades and colours, e.g., in paintings or coloured objects. To non-destructive techniques ought to likewise be added the immunofluorescence strategy utilized for the portrayal of proteins in paint media, which uses binding of fluorescent marked antibodies on the surface of the objects analysed. The analysis of archaeological samples by chemical and/or biological techniques is of valuable interest for adding knowledge to the historical context and for obtaining information about daily life, human-environment interactions, historical transition periods, dietary habits, and so on. On the other hand, characterizing ancient artworks is of interest, not only for shedding light on the manufacturing techniques used, but also to detect previous restoration interventions and in view of conservation strategies [14].

From the different cultural heritage artefacts that have been encountered before, this thesis will discuss about artworks and the identification of proteinaceous binders (binding media) via different scientific methodologies that have been put into perspective from a biological, chemical and archaeological point of view.

1.1 Artworks and paint media

Since ancient times, natural organic materials have been utilized as paint binders, adhesives, waterproofing materials, etc. The conservation and restoration of easel paintings is a highly skilled discipline that requires artistic skills combined with an understanding of different physical and chemical processes. This profession links art history with a knowledge of different painting techniques attributed to different artistic periods. The process of conservation and restoration also demands a deep understanding of the properties of the original and modern materials and techniques used to enable a precise evaluation of the possible irreversible effects on a particular painting [15].

At the time of their creation all old paintings looked different than they do today. This is because paintings are delicate by nature and subject to the natural aging process, deterioration or accidental damage. Changes become particularly apparent in the paint layer, and are determined by such factors as the picture support, the ground, and the chemical composition of the paint layer and varnish. Pigments may fade or change colour, crack patterns develop as the paint dries, contracts and moves with the support. At the same time the varnish layer becomes discoloured. Paintings may also be obscured by unprofessional renovation treatments that conceal the original paint and which can seriously mislead [16].

with the exception of the fresco technique, in which pigments are applied to fresh plaster and subsequently trapped in the developing calcium carbonate, All other painting techniques use an organic binder to disperse pigments and ensure their cohesion into the paint layers and adhesion to the support,. Some physico-chemical criteria must be met by an effective organic binder.

- be clear and colourless;
- have filmmaking properties: when applied, the binder must dry, giving rise to a resistant sold layer that is elastic but not sticky;
- be stable to aging.
- be fluid when mixed with pigments, generating an impasto stable, which is homogeneous and easy to apply.

The proteinaceous ingredients (egg, animal glue, and casein or milk), polysaccharide gums (Arabic, tragacanth, and fruit tree gums), drying oils (linseed, walnut, and poppy seed oils),

and beeswax over the years have best satisfied these needs. The painting methods have several names depending on the binder used:

• oil painting, where the binder is a vegetable drying oil;

• tempera grassa, where the binder is a mixture of a vegetable oil and a proteinaceous material;

• proteinaceous tempera, where the binder is a proteinaceous material, most notably egg;

• polysaccharide tempera, where the binder is a polysaccharide material (in watercolours pigments are dispersed in a plant gum, and in gouache technique in addition (beeswax partially hydrolysed by means of a base, to favour its solubilisation).

Each painter used a different method, therefore each approach required a separate set of additions to make the binding medium, leading to a variety of formulations. For instance, it is thought that fig latex (a white liquid secreted by the fig tree) and animal or plant resins were frequently added to egg tempera and oil- and wax-based binders, respectively. These substances were utilized not only as paint binders but also as consolidants in restorations, as components of varnishes used to finish paintings, and as components of mordants to add metallic leaf decorations due to their sticky characteristics.

Easel artworks have long been known for their importance in art history and are known to contain binders & adhesives [17]. These artworks are very popular and provide an insight into the materials used to produce the paints, binders, adhesive and supports in the medieval times. Out of these, natural organic materials and biopolymers have been used as adhesives, binders or supports [13-16]. These organic materials are constituted by proteins, triglycerides, alcohols, sterols, free acids, among others [17].

Most artworks consist of different layers that constitute the painting media. These layers are more often than not characterized to produce a visual model about what needs to be analysed and assessed. The layering starts with a bottom layer being a support on which the artwork is produced [18]. The following other layers can be adhesives, binders, fillers that will increase the strength of the artwork in some way or the other [18, 19]. On top of this strong layer the artist would add the pigment or colour that is depicted in the painting [19].

In the last 10 years some improvements in analytical procedures used by the scientific community for the analysis of organic materials in art samples have been proposed. Particular focus has been on both understanding and removing analytical interference caused by inorganic

constituents and on developing methods for the simultaneous detection of more than one class of organic materials in the same micro-sample [20]. Although many artists have used these modern paints and explored their handling and optical properties, ‘‘tempera’’, a classic painting technique using a protein based binder, has also been rediscovered in the twentieth century [21]. New editions of historical treatises increased the debate on technical issues and the use of tempera was a key topic among those artists involved in the renewal of a classicist style and traditional working methods. Consequently, numerous formulations containing proteinaceous binders were developed and commercialised. Identifying modern tempera techniques is much more complex than in classical art [22].

Deterioration of artistic materials caused by environmental agents is one of the main problems concerning the preservation of cultural heritage. The optimum strategy for the examination/restoration of an artistic work could require a detailed knowledge of the composition of the materials employed by the artist [23]. Among these, binders are particularly difficult to characterise being complex mixtures of organic substances, subjected to various biological and chemical degradation paths capable to modify the original composition.

Binders are important constituents of painting layers. In the Renaissance period painting layers were often based on tempera. Organic ligands used by Italian artists in the Renaissance period were primarily proteinaceous materials available from animal sources, such as eggs, animal glues and milk.
Proteins, glycerolipids, and polysaccharides are the main binders found in art samples. In addition, natural waxes, lacquers, and terpenoid resins have been used as additives, varnish ingredients, and consolidants. These materials are mixed together with pigments and fillers. They are then subjected to ageing. All this results in extremely complex samples with a variety of molecules with different chemical reactivities [24].

The proteins are usually present in the binding layer of an artwork. A technique of staining of cross-sections can detect the presence of certain materials in the various painting layers such as lipids (suggesting an oil-containing medium), or proteins (signifying a gum-, casein- or animal glue-based medium) but it is more often than not that these strategies tend to be tedious and do not provide accurate information [25, 26]. Animal proteins are found in both art and archaeology as organic remnants of trade, human or animal tissues, fabrics, leather and parchment, paint binders, and adhesives. Aged proteins are denaturized; internal links between

functional groups are rearranged as a result of water loss and aging, changing the tertiary and quaternary structures. As a result, they are less soluble and reactive than the native ones, albeit in some circumstances the makeup of the amino acids can largely remain the same. Proteins frequently exist in quite a good condition of conservation in the paint layers of paintings, but microbiological protein destruction occurs relatively quickly in the burial environment.

In some circumstances, the differentiation and identification of proteins in paint samples can be accomplished by determining the amino acid profile of proteins following the hydrolysis of peptide bonds [28]. Animal proteins were commonly utilized in paintings as binders for pigments in the tempera process, including glue, egg, and casein. Most commonly, whole eggs and egg yolks were used. A full dry hen egg has 2% cholesterol, 41% fat, and 45% protein [2, 8]. Dry cow milk includes around 26% protein, 26% lipid, and carbohydrates, making milk an aqueous emulsion of proteins and lipids [29]. Casein is produced by treating milk with acids, enzymes, or heat. Boiling the skin, bones, or cartilaginous components of fish and mammals produced animal glue. Collagen, a protein with a high concentration of glycine, proline, and hydroxyproline, makes up its composition [30].

1.2 Protein binders

Proteins are often found in cultural heritage materials. Protein materials are important signatures in paintings because they provide information about the workshop or art heritage, and the state of conservation [31]. Proteins binders are quite often found in the form of animal glues & bovine bones (collagen), eggs (ovalbumin), and cow's milk (casein) serving as the backbone of providing stability to the painting [32]. The quantity, kind, and order of the amino acids influence the surface charge, molecular structure, and special chemical and physical properties of the protein. Concerning the three-dimensional structure numerous factors, such as variations in pH, temperature, salt content, and the presence of reducing chemicals, can denaturize this structure and disrupt it [33,34].

During aging, proteins may also undergo condensation and cross-linking reactions with glycer-olipids, among other interactions with other elements in the historical/archaeological artefact. A potential by-product of the oxidative breakdown of serine, phenylalanine, and cysteine is amino malonic aldehyde [35]. This compound's continued oxidation can lead to the creation of amino malonic acid. This chemical has been identified in paint samples, and its concentration rises with time. Changes in pH, which, in the presence of water, can lead to the hydrolysis of peptide bonds, are a further essential element in protein breakdown. As a result, the molecular

weight can shift, and serine and threonine might dehydrate. Alkaline treatments (often employed in restoration) can partially hydrolyse proteins and convert cysteine into cystine and dehydroalanine [36]. The production of oxalate salts on paint surfaces has also been seen, indicating the presence of photooxidation [37]. The decreased solubility of proteins in ancient samples is attributable to denaturation and cross-linking activities that occur during aging; cations may act as catalysts for protein oxidation, so accelerating this event. Microorganisms' can also promote breakdown of proteins that result in the creation of compounds such piperidone, benzoic acid, and p-hydroxyphenylacetic acid [38, 39].

Relatively to proteins, when an organism dies, it begins to naturally convert L-amino acids to the D-form via a process known as racemization. The ratio of D/L isomers measures the degree of racemization, which rises with time and temperature. The longer racemization continues, the closer the proportion of D- to L-forms approaches. Although it is not an absolute dating method, the degree of amino acid racemization has been used to date organic materials such as well-preserved fossils, teeth, bones, egg and mollusk shells, plants, calcium-rich soil sediments, and rock paintings, as well as to assess the state of protein degradation. The racemization of particular amino acids can also be used to estimate the age of deceased animals. The most commonly found animal proteins found in paintings are collagen, casein and ovalbumin [40].

Animal glues are obtained by boiling animal tissues such as bones, skin, and cartilaginous parts of animals and fish. The constituent protein is collagen, characterised in the peptidic chain by a high content of glycine and proline and by the presence of hydroxyproline, an amino acid which is absent in the other proteinaceous materials commonly used as paint media [41]. Apart from its use as a paint medium and adhesive, animal glue was mixed with gypsum for the preparation of the priming in easel paintings. Animal glue has a relatively high solubility in water, compared to other proteinaceous media, even after ageing [42].

Whole egg and egg yolk have been the most widespread media in tempera paintings, and have also been used as fixatives and consolidants in restoration. Since egg yolk contains a consistent fraction of lipids (dried whole hen egg contains about 45% protein, 41% lipids, and 2% cholesterol [43]), as it dries it forms a particularly resistant and elastic film, whose permeability and solubility decreases in the course of curing and ageing due to the denaturation of globular

hydrophilic proteins. Egg glair alone was not as frequently used because it forms less impermeable films that tend to be brittle.

Milk and casein were a valid alternative to egg tempera for artists of the past, and though their use is not as widely documented as that of egg tempera, these materials have been used in many recipes both as binders and as fixatives. Milk is an aqueous emulsion of proteins and lipids (dried whole cow milk contains around 26% protein, 26% lipids, and 39% sugars[44]). Casein, obtained by the acidic, enzymatic, or heating treatment of milk, is soluble in basic aqueous solutions. Ammonium caseinate has been used as a binder, mainly in mural paintings, while calcium caseinate is a strong viscous glue widely used in restoration work .

1.2.1 Collagen

Collagen is an abundant protein found in most animals [45]. The characteristic feature of collagen is a structural motif defining in which three parallel polypeptide strands form a coil with each other and form a right-handed triple helix (Fig. 1.5). Proline, Glycine and Hydroxyproline is the most common triplet (10.5%) in collagen [46]. Collagen has wide applications in artefacts present in museums as a strong gluing adhesive for wood, as a pigment binder in paint and as a binder in the preparation of grounds. It is produced by the treatment of certain animal or fish tissues with hot water. On cooling the leached material, the solution sets to a jelly. The components which are responsible for this gelling are a result of the partial breakdown of tissues [45, 46].

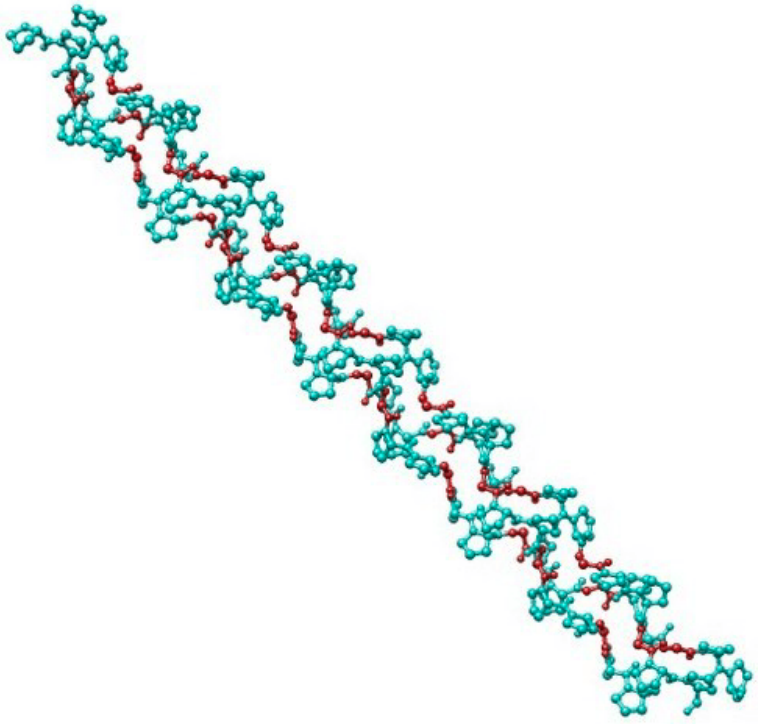

Fig 1.1: Triple Helix Structure of Collagen (Source: Protein Data bank)

Less drastic treatment, for example extraction at lower temperatures generally results in gelatins of light colour and giving a clear solution. Glues tend to be darker, thicker, more turbid and certainly contain more impurities than gelatin [46].

Fig 1.2: Collagen as an animal glue

1.2.2 Ovalbumin from Eggs

The egg consists of three major portions; a) eggshell, b) egg white, and c) egg yolk. Protein is one of the major component present in all three parts of the egg, and egg white is the prime source of proteins [47].

The egg white is made up of four individual layers: chalaziferous layer, thin layer, thick layer, and the chalazae cord. The outer and inner thin layers are separated by the thick or viscous layer which accounts for the most substantial portion of egg white, i.e., 57.3% Water is the primary constituent of egg white which accounts for about 84% to 89% of the total egg white or albumen weight [47]. Among albumen solids, proteins are the major constituents (10%–11%), while the minor components include carbohydrates (0.9%), lipids (0.03%), vitamins and minerals. Egg albumen consists of several different protein components which have been identified and characterized through modern high-resolution analytical techniques. The major egg white proteins studied due to their abundance are ovalbumin, ovotransferrin, ovomucoid, ovomucin, and lysozyme [47]. Ovalbumin constitutes about 54% of the total egg albumen and thus it is the primary protein present in egg white. It is a phosphorylated glycoprotein made up of complete three subunits having different phosphate groups along with a carbohydrate group attached to its N-terminal [47].

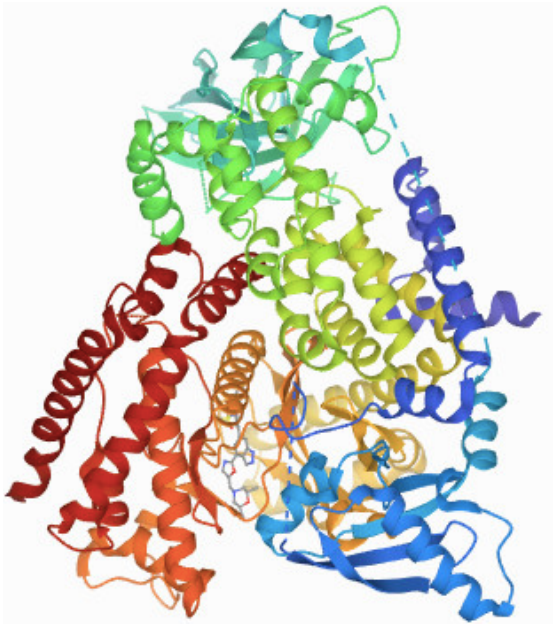

Fig 1.3: Crystallographic structure of Ovalbumin (Source: Protein Data Bank)

Egg yolk is composed of plasma and granules, located between the thin and thick albumen, supported by the chalazae. Yolk plasma constitutes 80% of the yolk fraction, and its protein content is of 23% on a dry basis composed of Low-Density Lipoprotein (LDL) (15%) and globular glycoproteins (15%). Yolk granules nonetheless have a higher concentration of lipids (33%) and proteins (58%) in comparison with plasma. Their structure formation is mainly composed of non-soluble HDL-phosvitin complexes. Although the egg proteins are present in all parts of the eggs, but the major concentration lies in the egg white (50%) and egg yolk (40%) [48].

Egg albumen and yolk has been used as a pigment binder and when used in this way, the paint is called tempera. The white of the egg can be used, in which case it is called glair. It has also found application as temporary varnish and as a sealant or priming over grounds. Whole egg can be beaten to form an emulsion and used as medium or just the yolk to give a somewhat richer medium. The use of the latter should lead to the detection of cholesterol in the sample and so would provide an alternative indicator [49].

Fig 1.4: Egg tempera being mixed with a pigment

1.2.3 Casein

Cow's milk contains about 5.5% fat, 4.9% lactose and between 3% and 5% protein. Unlike egg white, which contains but one non-glycoprotein (lysozyme), milk has been found to contain K-a-caseins and immunoglobulin G. Amongst the glycoproteins we may enumerate ß-, y- caseins, albumin, a-lactalbumin and ß-lactoglobulin [50]. Clearly when whole milk has been used, in addition to the information afforded by amino acid analysis, examination of the fatty acid components should reveal augmented lauric and myristic acids with respect to palmitic and stearic acids.

Historically, binders were mixed and combined with the pigments in various proportions to obtain the right amount of strength required for the painting [51]. The major constituent of binders are proteins from various animal origin sources such as collagen from animal glue, albumin from eggs, casein from milk, etc. [51,52]. The binders are mixed and combined with the pigments in pre-determined proportions to imbibe strength and colours [52].

Due to the relevance of proteinaceous materials in artefacts, especially as the artist's materials, particularly as binders and adhesives, their identification and quantification is of great interest to characterize the artistic technique and for conservation/restoration purposes, but, the co-presence of different proteins, environmental contaminants and previous addition of restoring materials make this task particularly difficult to be accomplished [52,53]. Consequently, binders while being extremely important to the painting, over time, might also affect the painting due to degradation (biodegradation, microbiological interactions, biodeterioration) [52, 53].

1.3 Characterization of proteinaceous binders

Raymond White in his article says that "Perhaps one of the most taxing problems for a museum analyst to face is that of attempting to characterize adhesives and paint media based on proteinaceous material" [54]. Because materials used as binding media are highly complex organic substances containing the same common elements, there is no general analytical technique for identifying paint media and finishes. These materials also degrade significantly over long periods of time. Furthermore, analyses are difficult due to the limitations imposed

on the number and size of samples due to the artwork's unique and inimitable character. Although non-invasive/non-destructive techniques would be preferable, the most useful analysis is currently obtained using high-sensitivity techniques that necessitate the removal of sub-milligram artwork samples [55].

The principal applications of chemical analysis in the assessment of historical objects showed up toward the start of the 20th century with the advent of micro-chemical methods and various spot tests giving data about particular inorganic and organic constituents. They are average destructive methods of analysis, requiring testing of material and typically its disintegration. In spite of critical advancement in analytical instrumentation, these methods actually assume a fundamental part in examination of historical objects. Nonetheless, the organic materials present in artworks degrade quickly, resulting in the overlapping of exhibited solubility parameters, obstructing the identification of binding media [55, 56].

The majority of the microchemical tests used in painting analyses are derived from general histology practice. This technique takes advantage of specific functional groups' affinity for certain highly coloured biological stains, allowing for organic binding differentiation. Aside from their ease of use, another advantage of microchemical tests is the ability to identify the paint media within the picture's structure because these tests can be performed on cross-sections and the reaction can be observed using a stereomicroscope [58]. This technique, however, is limited by its low specificity due to poor discrimination between different materials within the same group (i.e., albuminoids, casein or gelatine within proteinaceous materials).

Despite the fact that UV-vis spectrophotometry has been used to study organic compounds such as dyes used as artists' materials, its use in the identification of binding media and protective coatings is severely limited due to the non-specific spectra provided by these materials [59]. In contrast, when excited by ultraviolet light, the fluorescence exhibited by the organic compounds present in paintings as binding media and protective coatings has been widely used in the field of art conservation to examine painted surfaces [60].

In the field of art and art conservation, infrared spectroscopy is one of the most widely used techniques [61]. Its versatility and ability to provide structural information of both inorganic and organic materials, as well as the minimal sample preparation requirement, are some of the factors that justify the importance of this analytical approach in the field of art and art conservation. FTIR microscopy imaging in the reflection mode has been used to obtain two-

dimensional images of the functional group distribution of pigments and lead carboxylates formed from oil media among the different paint layers of a cross-section [62]. Using this technique to study ancient objects yields intriguing results, such as the identification of an altered drying oil-egg binding medium in Medieval paintings [63].

Chromatographic techniques have been widely used in labs specializing in the analysis of artworks due to their ability to separate the organic components of complex mixtures found in paint layers and coatings [64]. Much consideration in the use of these methods is in many cases zeroed in on optimisation of significant techniques of extraction of given analytes from the artefacts analysed, as can be exemplified by the assurance of colours by liquid chromatography [65] or the examination of extraction of proteins in their identification in renaissance paintings. The majority of traditional painting binding media are complex mixtures of natural products, some of which are polymeric in nature. As a result, one or more pre-treatment steps are required prior to the separation of the released monomers in the chromatographic system.

One can track down various applications of molecular spectroscopy in recent archeometric studies. In molecular analysis, particularly much consideration as of late has zeroed in, be that as it may, on different applications of elite execution chromatographic methods and MS [66]. The primary area of use of gas chromatography (GC), utilized most ordinarily with MS recognition, is in the assurance of such a gathering of mixtures as waxes, lipids, and resinous and proteinaceous materials [67], and furthermore colours and amino acids. Despite the fact that GC is all the more normally used in ongoing many years a quick expansion in the employment of high-performance liquid chromatography with normal recognition methods, for example, spectrophotometric or fluorometric identification has been noticed [68]. This is particularly significant for the recognizable proof of obscure mixtures and displays extremely low restrictions of identification when combined with MS recognition [69]. This mix is utilized regularly in the assurance of amino acids and peptides of proteinaceous matter and colours. The simultaneous application of numerous procedures with variable selectivity, sensitivity, and detection limits in the study of a certain historical sample is, as in many other fields, the analytical strategy that yields the most information about things.

In medieval paintings, proteinaceous binders play a significant role in understanding the state of art; helping the process of conservation & restoration [70]. In most paintings, these binders (albumin from chicken eggs, collagen from animal glues and bones, casein from bovine milk,

gelatine from crustaceans) constitute about 5-10% of the overall paint matter[70, 71]. Hence, they are minute and require a multi-analytical approach to determine their origin and properties.

Conservation scientists and conservators innovate numerous techniques to tackle several issues of protein optimization, quantification, binder degradation, but often, find themselves involved in complexities which are beyond the scope of materials science characterization [71]. The methodologies mentioned above (i.e. microchemical tests, UV-vis, FTIR) have been limited in the characterisation of protein binders and difficult to conclude and expensive [72, 73]. Analytical techniques such as Mass Spectrometry give a lot of information, but require huge amounts of data processing to interpret on these paint samples [74]. FTIR also can give some information but most of the data obtained by these methods are for the pigments, support and varnish or previous restorations, but little information is available about the binders; and if present, interpreting the source of protein origin is not easy [75].

The identification of organic paint constituents and in particular of proteinaceous paint media in works of art is still considered a difficult challenge for the chemist for the following reasons: i) aged proteins are denaturised and scarcely soluble in water and organic solvents; ii)several organic natural and synthetic substances may be simultaneously present in the layered structure; iii) degradation compounds, formed as a result of ageing, restoration treatment, and pollution may also be pre- sent and iv) a low protein content (at most 0.1 mg) is generally encountered in small heterogeneous paint samples (1 mg).

In paint media, several sources of protein can be present which makes analysis tedious. Immunological techniques were proposed as an alternative to traditional histological techniques. Immunological methods rely on the reaction of a specific antibody that binds to specific areas of the antigen molecule known as epitopes. Because proteins are the most potent immunogens, immunological techniques are primarily used in heritage conservation to identify proteinaceous media. Because of the high specificity of the antigen-antibody reaction, the same protein from different species can be distinguished. Furthermore, multiple antigens can be detected in the same sample. Immunological techniques are divided into three categories based on the labelling mechanism used to reveal the presence of the antigen: (a) immunofluorescence microscopy (IFM), (b) enzyme-linked immunosorbent assays (ELISA), and (c) techniques based on the use of opaque markers such as colloidal (nanoparticles) gold or radioactive

markers (radio-immunoassay), which allow for the detection of proteins by microscopy. Only the first two have reported applications to artwork analysis.

A fluorescence microscope is used in IFM to detect secondary antibodies that have been conjugated to a fluorophore. The main advantage of this technique is that the analysis can be performed directly on cross-sections, allowing for direct localization of the antigen in a specific region or layer of the painting. Another advantage of this technique is that no protein solubilisation is required because the test is performed on the surface of the cross-section. This technique was first used to recognize casein, ovalbumin, and egg proteins in general.

The ELISA technique employs an enzyme-conjugated secondary antibody to amplify the immunoreactive response of the primary antibody. The reaction between the enzyme-tagged secondary antibody and the substrate produces a reaction group that the colorimetric assay can detect. The main advantage of the ELISA method is its high sensitivity to sub-nanogram order. A single extraction can also be used in multiple assays. Furthermore, a sequence of primary antibodies can be used to perform multiple assays until a positive reaction is detected. Therefore, in recent times, immunodetection has been employed for characterization of protein binders [71-75]. Furthermore, immunodetection has been rarely explored in the field of heritage and this work aims to contribute a deeper insight into the identification of protein binders via ELISA and compare it with previously discussed complimentary techniques.

Since the first reported analytical studies and technical examinations of art and archaeological objects in the late 18th century, analytical techniques and methods used to study artworks have steadily improved. Thus, in addition to the traditional and simpler microchemical tests, a variety of instrumental techniques have been gradually introduced in an attempt to improve the detection limit, sensitivity, resolution, and, in general, the repeatability and accuracy of the analytical results. At the moment, the most useful analysis comes from high-sensitivity techniques that necessitate the removal of sub-milligram art samples. Nonetheless, non-invasive/non-destructive technique optimization, as well as the development of novel methods for providing not only chemical but also morphological/spatial information on the organic materials composing the object, are current trends in the art and art conservation fields.

1.4. The panorama for identification of proteins in cultural heritage artefacts

A series of complimentary methods were used to identify proteins in cultural heritage artefacts. Table 1.1 shows the four more typical methodologies.

Table 1.1 Complimentary techniques for the Identification of Protein in CH Artefacts

Name of Technique	Type of Analysis
Stratigraphy	Microscopy
Naphthalene Amido Black	Microchemical Tests
Pyrolysis-GC-MS	Chromatography

1.4.1 Stratigraphy

Stratigraphic studies are one of the standard examination methods that provides very precise information about the complexity of paint layers that make up a painting or decorative finish. It is the key method to assess the extent and condition of different painting layers. Stratigraphic studies can reveal the way the paint layers are applied and consequently, they tell us how the artist worked [76]. Tiny samples of paint are taken from discrete and representative areas and mounted in clear resin. Such prepared samples are observed under a binocular microscope at high magnification between 50x and 200x depending on the thickness of the examined layer [77, 78].

Thorough observation of the various layers enables the conservator to determine the history of the object and whether interventions have occurred by inspecting layers of dirt, varnish and paint. Additionally the media analysis can be carried out on the cross-sections which provide important information about an artist's technique, and helps to determine the most appropriate conservation treatments to use. The information revealed using the stratigraphic analysis can be recorded using microphotography and then compared with UV, IR and X-ray examination (non-invasive techniques), consequently providing reliable information on the object's history and artist's technique [78, 79]. The only drawback of stratigraphy is that it is a destructive technique from which there is no returning back to the original form of any sample [80].
There are three crucial steps for the sample preparation in stratigraphy given in Annex I.

1.4.2 Naphthalene Blue Black

Naphtol Blue Black (also called Amido Black 10B) or 4-amino-5-hydroxy-3-(p-nitrophenylazo)-6-(phenylazo)-2,7-sodium naphthalenedisulfonate according to IUPAC nomenclature is a coloured molecule displaying specifically proteic binders. Moreover, according to the pH value of used coloured solution, it is possible to determine the corresponding protein identity. The difference of reactivity of these reagents can be rationalised mainly by the effect of the pH on the ionisation state of a given protein and its average amino acid composition [81, 82]. In this method a resin is added to some paint microsamples and reacted with a Naphthol Blue solution and based on the intensity of the colour on the microsamples, it is possible to detect the proteins. (Anex I)

1.4.3 Pyrolysis GC-MS

Chemical investigations on ancient paintings are often focused on two basic goals. On the one hand, they intend to understand painter techniques (choice of pigments, binders, mixtures, applications, and so on); on the other hand, it can enable the following of painting evolutions, such as pigment synthesis across centuries; or it can date a painting, thanks to the identification of constitutive pigments. Some studies, on the other hand, are aimed at improving our understanding of modification mechanisms (pigment whitening or blackening, the appearance of fissures, efflorescence, and so on) [83-89].

Analytical studies on the composition of paint binders have been based heavily on gas chromatography and mass spectrometry (GC-MS) for about 13 years, starting in 1979 [96–100]. Chromatography is a powerful technique to separate organic components from one another For binding media, this means a three-step pre-treatment that starts with hydrolysis followed by the suppression of interferences and ends with derivatisation[97-105]. Although, each technique has its advantages and disadvantages, GC is by far the most widely used technique for the identification of organic media and varnishes because it can analyse almost every traditional organic materials present in artworks while also having a high sensitivity and versatile as an instrument in general[106-112]. When Pyrolysis is combined with a MS, similar to chromatograms, it produces pyrograms. These pyrograms are quite complex in comparison to the GC-MS chromatograms [113]. Therefore, even though pyrolysis is a major time-saver, the pyrograms can void that difference in time. In recent times though, the Pyrolysis step is completed with a GC-MS to form Py-GC-MS[114-116]. This indeed is an excellent way to

benefit from both the avoidance of sample preparation with Pyrolysis and the much simple chromatograms with the GC. In recent studies, chromatography coupled with mass spectrometry has often been used as a complementary method to identify proteins. Overall, although complex, chromatography is a powerful tool in the identification of proteins.

Recent studies have shown the feasibility of performing pyrolysis in combination with gas chromatography and mass spectrometry (Py-GC-MS) to characterize proteinaceous binding media. Indeed, Py-GC-MS was used to identify the paint layer binder in the heritage context.

Characterization of proteinaceous binders by determining the amino acid composition of the binding medium using gas chromatography (GC) or high performance liquid chromatography (HPLC) of pre-treated samples. A major drawback of these methods is related to the need for time-consuming chemical steps (hydrolysis, extraction, derivatization) that can lead to loss of amino acids [117]. Since analytical pyrolysis does not require chemical processing and a minimal amount of sample is sufficient for analysis, the technique has been applied to analyze complex organic materials in the fields of art and archeology [118]. . Recent studies have shown the feasibility of performing pyrolysis in combination with gas chromatography and mass spectrometry (Py-GC-MS) to characterize proteinaceous binding media.

Interpretation of pyrolysis data is based on analysis of chromatographic profiles and detection of molecular markers. However, the interpretation of pyrograms is important and requires experience. The co-occurrence of different organic substances, the relative abundance of one substance compared to others, the presence of inorganic substances, the morphology of the sample, and many other factors can affect the resulting pyrogram in different ways. may contribute [119,120]. Various molecular markers and thermal decomposition profiles have been proposed for each material. This is due to several factors:

(i) **pyrolizer for analysis**-The most frequently used ones are: the Curie point (the sample is rapidly heating), and a resistive heating filament (the sample is heated by an initial pulse of high voltage, which causes a current to flow through the metal filament) or the micro-furnace (a micro-furnace rapidly raises the temperature of the sample until it reaches the pyrolysis temperature and then maintains that temperature for the desired pyrolysis time),

(ii) **Sample composition** – the co-existence of multiple substances, both organic and inorganic, in the sample contributes to the formation of the final pyrolysis product, label formation, chromatographic profile, and possibly derivatization yield. can affect

(iii) **Instrument set-up** – This includes sample introduction techniques (samples can be introduced into quartz tubes of various dimensions or placed directly on metal wires, etc.), pyrolyzer geometry, and GC/MS interfaces (temperature and dimensions) and connection between pyrolyzer and GC injection port)

(iv) **Deactivated silica pre-columns** are also an essential tool when performing pyrolysis, as they help partially avoid contamination of analytical columns with underivatized polar compounds. Blanking (i.e. thermal decomposition of the derivatizing agent without sample) should be performed between runs to ensure that the chromatogram does not contain signals that do not belong to the sample.

(v) **temperature of pyrolysis**

The molecular markers reported in the literature for the identification of proteinaceous binding media are listed in Table below.

Table 1.2 Molecular markers suggested in the literature for the identification of proteinaceous binding media [121, 122]

Protein	Derivatising agent	Marker
Animal glue	none	Pyrrole, pyrocoll, 3,6-(2-methylpropyl)-2,5-diketopiperazine
	TMAH	Pyrrole
	HMDS	Pyrrole,2-methylpyrrole, 3-methyl pyrrole, 2,4,6-trimethylpyrrole
Egg Yolk	none	Palmitic and oleic acids
	TMAH	Methyl esters of palmitic and oleic acids
	HMDS	Hexadecanonitrile, heptadecanonitrile, cholesterol derivatives, tetradecanoic acid, hexadecanoic and octadecanoic TMS ester

Egg Glair	none	Indole, methylindole
Calcium Caseinate	none	Pyrroline, 2,5-diketopiperazines
Casein	None HMDS	4-ethyl-2,5-dimethylisoxalidine, 3-nitro-2-pentanol, 6-methyl-tetrahydro-*2H*-pyran-2-one, O-(3-methylbutyl)hydroxylamine, tetrahydro-6,6-dimethyl-2H-pyran-2-one, 2-methyl-1-nitropropane indole

Pyrrole, diketodipyrrole (3-pyrroline), toluene, 3-Furanmethanol, 2-Furanmethanol, maltol, indole, 3-methyl indole, were used as standard compounds for the identification of pyrolysis products and were purchased from Aldrich [123].

In the absence of standard compounds, the identification of pyrolysis products is based on comparison or interpretation of their mass spectra with those of literature data. Various ratios have been proposed, for example gly/glu, gly/asp, pro/asp, glu/pro, glu/asp, glu/ala, ala/pro, ala/gly. Since this method usually relies on animal glues that have significantly higher amounts of Gly than eggs and milk, casein contains higher amounts of Glu than eggs, so Gly and Glu is always included in the most important proportions. Typically, collagen identification must be confirmed by the presence of Hyp. The amino acids chosen for the ratio may differ, but the underlying rationale remains the same. We use increasingly specific conditions to create block diagrams that lead to the identification of protein-containing binders. Identification by these flow charts is based on measurements of just a few amino acids [124, 125].

Methodologies such as Immunodetection involving immunoassays is one optimal solution to extract information present within proteinaceous materials. Immunoassays such as ELISA (Enzyme-linked immunosorbent assay) are highly efficient in selectively detecting proteins (antigens) present in aged paint binders and determining the origin of the sample under analysis. The antigen-antibody interactions in ELISA are specific while being highly sensitive, reliable, low cost and offers the possibility for multiple antigen recognition.

Immunoassays such as ELISA with specific antibodies work with high accuracy in identifying the biological origin of proteins. Since the binders contain protein based biological materials, they can be identified through immunodetection by antigen-antibody interactions. In

Immunoassays only the specific antigen, in this case a protein, would be identified in the presence of an antibody with the same source of origin. When these antigens encounter an antibody of the same origin, it binds to the antibody and a biochemical reaction (assay) occurs. In this way, ELISA helps to identify the biological source of the proteins present in these binders.

1.5 Role of nanoparticles in protein extraction of paint model microsamples

Many paint samples are too small to allow protein extraction for quantitative analysis. Hence, it is necessary to enhance the proteins present in such minute paint samples. To solve this disparity, the application of nanotechnology could be one possible solution. Nanotechnology is the study of objects/materials that fall in nanometre (10^{-9} m) size range using scientific principles and techniques while representing the design, production and application of materials at atomic, molecular and macromolecular scales for producing nano-sized materials [126, 127]. In previous studies, they have been used for several technological applications, but very few for the purpose of cultural heritage [128]. With this in mind, in recent times, nanomaterials have made the headlines constantly for having very large surface-to-volume ratios, and have been used in various applications and disciplines ranging from the medical and pharmaceutical industry [129], to being used in conservation and restoration processes [130].

Nanomaterials are materials which can be engineered from nanoparticles, nanotubes, nanorods or fibres [127-131]. A clearer definition could be that nanoparticles are the building blocks of nanomaterials [131]. These have distinct optical, mechanical, electrical or magnetic properties due to which they are highly employed in the field of pharmaceuticals, electronics, air and water purification technology, catalysis, drug-delivery, fuel-cells, etc. Examples include carbon nanotubes, graphene, fullerene, photo-catalyst composites, etc. Nano-sized particles or Nano-encapsulation has a lot of advantages over the traditional microencapsulation. In microcapsules, where the typical diameter range is 20-500 μm, nano-capsules have diameter ranges of 50-500 nm (0.05-0.5 μm) [131]. Furthermore, nanoparticles can be easily dispersed and are suitable for impregnation in aqueous suspension into the macrostructure of wood or other materials.

Nanoparticles are known to have large surface areas which allows bioactive agents to be imbibed on their surfaces [132, 133]. When nanoparticles containing bioactive agents are

dispersed in solutions, they undergo an explosive release initially [134,135]. Apart from this, nanoparticles have several advantages that particles in bulk materials cannot provide. The most significant difference between the bulk material particles and nanoparticles is the extremely large surface areas obtained with nanoparticles. The large surface areas are with respect to the overall volume of the material. It is due to this property of nanoparticles that they exhibit several unexpected properties such as optical transitions. This is mostly due to the confinement of electrons within the small size which helps to reproduce quantum effects [136-139]. Also, in a lot of inorganic materials the melting temperature of nanoparticles is reduced immensely. For example, gold nanoparticles have a melting point of ~300°C and appear deep-red to black in supsensions, compared to gold slabs which have a melting point of 1064°C.

Silicon is present in different forms in the environment such as in silica, where it is present in combination with oxygen or hydroxides as in silicic acid. Silica is also present in living organisms such as algae (such as diatoms), sponges, etc [131, 134]. When the chemical structure of silica is observed, it occurs as orthosilicates or silicates (SiO_4) tetrahedrons interlinked with each other through siloxane (Si-O-Si) bridges (Fig. 1.10). Therefore, sometimes the term silica refers to the silicate tetrahedral structures and vice-e-versa. This macromolecule ends with the formation of silanol groups (Si-OH), whose nature, distribution and accessibility affects the properties of the material and the possibility of functionalization and of interaction with other molecules [128].

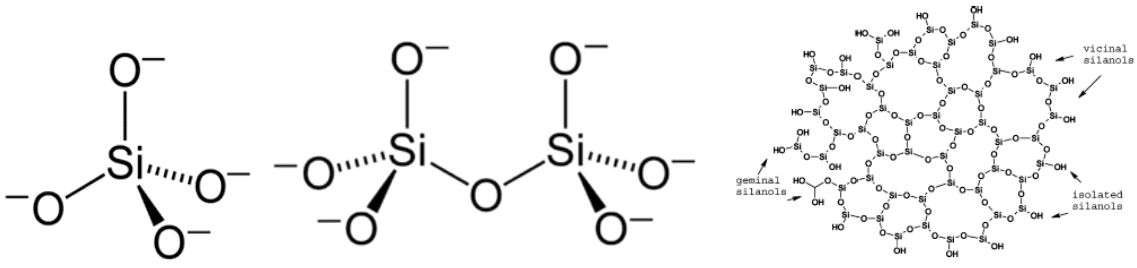

Figure 1.6 Molecular representation of Silica

In the beginning, some scientists found that silica had sieving properties to adsorb specific molecules on their surface. This developed an increased inclination towards these materials due to the ability of selective adsorption consequence of small differences in size of the

adsorbed molecules. Therefore, it was extensively used for the purpose of selective adsorption. Furthermore, when the petrochemical industries flourished the need of selective adsorption materials like zeolites became an interest for the cracking process during refining. Silica based materials found its place as one of the best zeolites for this purpose. Nowadays, various applications require a specific predefined shape and size of the pores, the synthesis of materials such as silica which have a controlled structure is quite important for both industrial and academic studies [130,134].

Ordered mesoporous structures have proved to be effective support carriers because of excellent adsorption properties, a high specific surface area and porosity, tuneable pore size with narrow distribution, biocompatibility, easy functionalization [135]. These advantages are contributed due to their high stability and possibility to modulate the pore size and modify the surface properties by connecting various functional organic groups to the support. Moreover, mesoporous silica based on MCM classes have been thoroughly investigated as carriers in the form of hollow spheres, films or coated supports for a large number of applications [136]. Three different mesophases from the MCM family have been identified i.e. lamellar (MCM-50), cubic (MCM-48), hexagonal (MCM-41) as shown in the figure 1.12 [137]

The MCM (Mobil Composition of Matter) class of mesoporous supports was developed by researchers at Mobil Oil Corporation. Within the MCM class of mesoporous materials, the MCM- 41 is best known for its controlled release properties. This can be attributed to the well-organized structure of channels (mesopores), with well-defined shape and variable sizes depending on the synthesis conditions. The high pore volume and the high surface area coupled to the ease of modification of surface properties, guarantee an extraordinary adsorption capacity. MCM-41 silica supports present a hexagonal array with pore sizes around 30–45 Å (2-10 nm), with a high porosity (0.6–0.8), BET surface area (760–1260 m^2 g^{-1}), and pore volume (0.7–1.25 cm^3g^{-1}) [138]

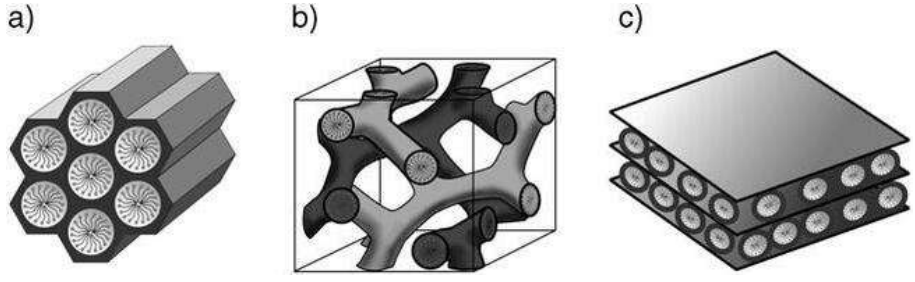

Figure 1.7 Representation of MCM Structures (Closer view) a) MCM-41 (hexagonal), b) MCM-48 (cubic), c) MCM-50 (lamellar)

Ordered mesoporous materials like MCM-41 can be obtained by hydrothermal synthesis and a liquid templating mechanism [139]. These materials can be synthesized using anionic, cationic, neutral surfactant or non-surfactant templates [140]. The diameter of the pores can be controlled by changing the length of the template molecule. Moreover, changing the silica sources, surfactants or reaction conditions leads to the development of new mesoporous systems [141]. The MCM class of materials was originally developed by using cetyltrimetylammonium bromide (CTAB) as the template surfactant and altering the amount to produce the cubic, lamellar and hexagonal structures.

The use of supramolecular aggregates of ionic surfactants (long-chain alkyltrimethylammonium halides) as structure-directing agents (SDAs) was a ground-breaking discovery in the synthesis of mesoporous materials. The SDAs facilitate the assembly of mesostructured materials during the condensation of silica sources under basic conditions [142]. An example of the formation of the MCM-41 is as shown below (Fig 1.9). In order for this method to work, there should be an attractive interaction between the silica precursor and the surfactant without phase separation taking place [143].

Therefore, under basic conditions, the surfactant is usually cationic quaternary ammonium salt with a negatively charged silica precursor. After the silica surrounds the surfactant template, through condensation of silica, the Mesoporous MCM-41 is formed.

The Stöber process is used in the preparation of monodisperse silica particles in which the simultaneous hydrolysis and condensation of alkyl silicates with ammonia as a catalyst [144]. The silica nanoparticles are individual silica particles with diameters in the range of 2-50 nm. The silica nanoparticles have very light weight and the density is very low in comparison to the MCM-41 [145]. Another suitable synthesis pathway takes the name of emulsion-condensation and involves the use of a hydrophobic supporting reaction component that generates an oil in water emulsion and modify the shape and dimensions of the micellar aggregates of the surfactant, inducing variations in the porosity of the final product. In this way hollow and mesoporous silica nanoparticles having around 20 nm of diameter are synthetized [153, 155]. The silica nanoparticles show lower surface area (around 200 $m2g^{-1}$) and pore can be radial [146, 147]. In particular, MCM-41 and silica monodisperse nanoparticles were exploited for the purpose of our investigation.

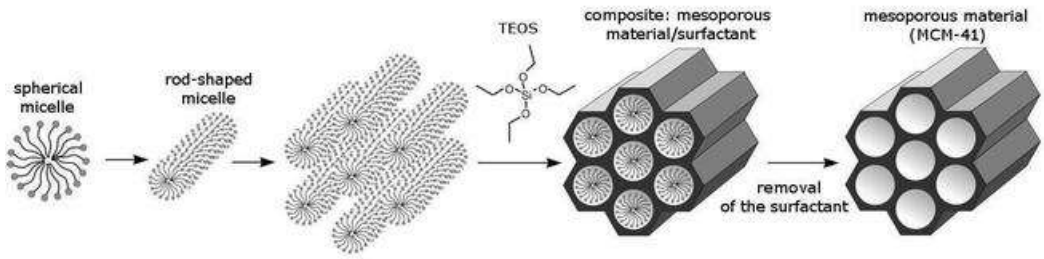

Figure 1.8 Process of formation of mesoporous material MCM-41 by surfactant (CTAB) [38]

Mesoporous silica-based nanoparticles (diameters between 2-50 nm) are extremely popular for reception of foreign materials within their pores [148-152]. These can range from monodisperse nanoparticles to the MCM class of mesoporous materials like MCM-41. Since nanoparticles come in various forms, for the purpose of protein applications, mesoporous (2-50nm) silica has some excellent properties with high surface adsorption capacities for a large number of bioactive substances.

This property of explosive release patterns can be exploited for increasing the limit of detection with ELISA at lower protein concentration. Furthermore, since the nanoparticles have a dynamic pharmacokinetics and ability for targeted delivery, it boosts the linking effect of the antigen with the antibodies, which would solve the issue of selectivity. The characterization of these nanoparticles would provide an insight and validate how they affect the antigen's properties. Finally, there is a strong motivation to reproduce the easel paintings with different paint models using ancient recipes. This would lead to an original set of research to help investigate and browse through a catalogue with various combinations of binders & pigments. It would also help reduce the use of micro-destruction in paintings when immunodetection is used for research purposes. Further contributions could lead to the evolution of new specific antibodies for archaeological proteinaceous materials while optimizing the protein extraction process using the nanoparticles.

AS mentioned earlier, many paint samples are too small and it is necessary to enhance the protein concentration present in such minute paint samples.. In previous studies, nanoparticles have been used for several technological applications, but very few for the purpose of cultural heritage [154]. Furthermore, nanoparticles can be easily dispersed and are suitable for impregnation in aqueous suspension into the macrostructure of wood or other materials.

For protein applications, mesoporous (2-50nm) silica has some excellent properties with high surface adsorption capacities for many bioactive substances [155]. Moreover, ordered mesoporous structures have proved to be effective support carriers because of excellent adsorption properties, a high specific surface area and porosity, tuneable pore size with narrow distribution, biocompatibility, easy functionalization [156, 157]. These advantages are contributed due to their high stability and possibility to modulate the pore size and modify the surface properties by connecting various functional organic groups to the support [158, 159]. In particular, MCM-41 and silica monodisperse nanoparticles were exploited for the purpose of our investigation.

Chapter 2
Immunodetection of proteins with paint models

2.1 Introduction

The assay developed followed a step-wise process to identify the proteins. This process starts with an optimized process of protein extraction, quantification of protein, and ELISA (Enzyme-linked immunosorbent assay) to identify the protein within the protein extracts in the presence of specific primary and secondary antibodies. While, the procedure is straightforward, there are some important parameters to consider for optimizing the results. These parameters involve the protein extraction protocol, the size & quality of the paint microsample for the study, the detection limit & selectivity of ELISA and the protein concentration.
For this purpose, painting models were built and used in the optimization tests of this methodology.
In fact, the paint models play a crucial role in identifying strategies to tackle the problem of low sampling processes from real paintings [160]. When starting out with the identification of proteins with ELISA, the paint models with protein binders of ovalbumin, casein and collagen determine the effectiveness of the immunoassay [161]. The pigments added to the paint models undoubtedly make the identification of proteins more similar to real samples [162]. The materials and ELISA protocol used for the experiments have been explained thoroughly and further provide a blueprint for identifying the proteins from the paint models [163].

The sequence of the protein identification protocol involves the extraction of microsamples from paint models, the quantification of proteins and finally the ELISA immunoassays [160-163]. Consequently, to verify the results and completely uncover the entirety of ELISA the limit of detection and selectivity analysis sets the trend for the identification parameters in any immunoassay.

ELISA can be used with specific antibodies but involve a step of microsample preparation to be applied with success in heritage context. When extracting a sample from original paintings such as from museums the conservator is restricted to remove very small or minute quantity of

sample since it is micro destructive, but a lot of the times this is not enough to obtain a considerable amount of protein extract.

Therefore, for the optimization of ELISA representations of original paintings should be substituted by developing paint models which similar art preparations. Paint models can be developed with commercially available proteins along with certain pigments that have been found is medieval paintings. Certain ancient recipes can also be useful in determining the types of materials applied to original paintings in the past. For the support on which the paint model is developed, a glass or a canvas slab is appropriate.

2.1.1 ELISA Limit of detection and Selectivity

In immunoassays there is a limit of detection of the concentration of protein (ug/ml) at which the antibody activity can become negligible. Therefore, it is important to optimize the protein extraction process and develop techniques with higher sensitivity while estimating the limits of detection in each immunoassay. It is also important to perform a selectivity analysis for different antibodies to assess the reactivity of a particular antibody with the protein it is supposed to detect. The lowest possible protein concentration that can attains a detection signal is known as the limit of detection. Finally, the specificity of ELISA can be determined via the selectivity of several proteins in a single step as only the protein which is from the same source as the antibody present in the system will be detected. This filtering of proteins based on the biological source and identifying each of them individually provides an advantage over all current protein detection methods. The limit of detection and selectivity have not been explored in literature regarding immunodetection for cultural heritage artefacts such as paintings and protein binders. Therefore, in this chapter, the limit of detection of certain paint samples from proteins of ovalbumin, casein and collagen have been explored elaborately.

2.2. Preparation of Paint models

Paint models of ovalbumin, collagen and casein (Table 2.1) were prepared on glass slab supports with pigments of lead white and black bone pigments in various combinations and underwent ELISA immunodetection in the presence of primary and secondary antibodies.

Table 2.1: Paint models of ovalbumin (2,7,12,22, 29); casein (8,42, 46, 49) and collagen (5,32, 36, 39)

Paint model Number	Description
2	Egg albumin
7	Egg albumin +yolk
12	Whole egg + lead white
22	Egg albumin + lead white
29	Whole egg + lead white + blackbone
8	Egg albumin + egg yolk+ casein
42	Casein from cow's milk+ lead white
46	Casein from cow's milk+ blackbone
49	Cow's milk + lead white+ blackbone
5	Rabbit skin
32	Rabbit glue+ lead white
36	Rabbit glue + blackbone
39	Rabbit glue +lead white+ blackbone

A mixture of naturally available proteins from eggs, rabbit glues, commercially available casein and bovine milk were mixed with the pigments in a 3:1 pigment to binder ratio [160]. For the blanks, only the binder proteins were used.

The paint model materials were applied as a thin layer of 200-500nm thick. These paint models were artificially aged with a Relative Humidity of 85% for a period of 6 months.
The table above provides the details of each of the paint models with their pigment and binder composition used for the experiments.

2.3 Micro-extraction of proteins from Paint models

The protein was extracted from paint microsamples, using a previously optimised protocol [12]. Micro-samples were extracted (2-3mg) and dispersed into a PBS (150µl for each mg of sample) solution from each paint model into Eppendorf tubes. The protein was extracted by 3 consecutive cycles of orbital agitation (at 27° C) and ultrasonication (at 37° C) of 1h each. After the incubation period, three cycles more with the same structure were made the following day. Finally, the samples were centrifuged three times consecutively at 6000g for 1.5 min, and the supernatant was collected and used as antigen in ELISA.

2.4 Protein quantification

The extracted protein were quantified by Bradford Assay in the presence of Coomassie Blue solution using BSA as standard solution (1–40 µg mL^{-1}) (Annex II) Total protein content was expressed as µg of BSA equivalents per milligram or (µg/mg) of microsample.

2.5 Indirect ELISA immunodetection of antigens (proteins)

Commercial solutions of ovalbumin, casein and collagen were used to compare the outcome of ELISA with paint model samples while using commercial primary and secondary antibodies. Ovalbumin and collagen ELISA tests were performed with monoclonal primary and secondary antibodies, whereas, casein was done with polyclonal primary and secondary antibodies.

A step by step protocol was followed as given below:

i. ELISA is performed in a 96-well microtiter plate. Each well can hold volumes up to 500 µl. It is made from a special plastic good for the absorbance and protein attachments to the well. A buffer such as PBS (Phosphate-buffered saline) is used as a diluent for ELISA and a control is used to further ensure the assay's validity. Initially, the antigen (proteins) is filled into the wells. The 96 well plate containing the antigens were incubated for 1h at 37 ºC. This is done so that the binding of the proteins (antigens) to the wells occurs.

ii. After incubation, all microplate wells were rinsed with PBS (150 ul per well) 3 times. For this we used the microchannel which has the capacity to deliver 8 wells at the same time. Since each column consists of 8 wells, this helps save time during rinsing. (Note: during rinsing once, the PBS has been put into the wells, the microplate is turned upside down into a tray, and pressed onto a tissue to remove all the unbound antigen proteins from the well. This must be done at one go abruptly to not let the antigens from other wells mix with each other.)

iii. A blocking solution of 1% BSA solution in PBS (100 ul per well) is added. This is for discarding the unspecific sites of binding. After the addition it is incubated for 30mins at 37ºC.

iv. Addition of Primary antibody: Monoclonal anti-chicken egg (1:2000) antibodies (100µl per well) that were produced inside a mouse were used for the experiment. It was followed by an incubation for 1h at 37 C to allow the binding between antigens and antibodies.

v. Next, the microtiter wells are washed with PBS-T (150 ul per well) three times. To prepare PBS-T, we need to use the tween 20 at 0.05%.

vi. Addition of Secondary Antibody: The secondary antibodies have a conjugated alkaline phosphate enzyme attached to it which produces fluorescence when

activated. Anti-mouse IgG Monoclonal Ovalbumin (1:4000) was the secondary antibody which links with the primary antibody. These are diluted in BSA 0.1% in PBS-T. After adding the secondary antibody, it was incubated for 1h at 37 ºC to allow the binding between primary and secondary antibodies.

vii. Next, the washing was done once again with PBS-T (150ul per well) performed three times, further with water (150 ul per well), and finally the glycine buffer (100ul per well) is added with the p-NPP substrate (1mg/1ml) to the wells.

viii. The final incubation is for 10mins at 37 ºC of the substrate reaction with the secondary antibodies. The intensity of the fluorescence by this reaction shows the origin of the antigens present in the binder materials Finally, if the antigen matches the same biological origin of the primary antibody, it causes a chain reaction which is developed with a change in color of the co-enzyme substrate. The absorbance values (at 405nm) are read on a microreader corresponding to a positive/negative output.

2.6 Limit of detection of protein from ovalbumin paint models

The limit of detection is the lowest protein concentration of the any paint model that can be detected by ELISA. This is different for each protein, the type of pigments present and antibody sensitivity in the assay. The limit of detection for ovalbumin, collagen and casein were assessed along with whether they have a good sensitivity towards the selection of specific antibodies with the antigen. For each paint microsample, the proteins detection with Indirect ELISA has a limit of detection in terms of the concentration of protein (µg/ml) which depends on the microsample of the paint model. For this purpose, two experiments were designed for each of ovalbumin, casein and collagen.

2.7 Selectivity in protein analysis

It is also important to have a selectivity analysis for proteins of different biological origin. This means that each antibody should only detect the antigen of the same origin, for example, a collagen antibody should only detect a collagen antigen. If it detects casein or ovalbumin antigens, the selectivity of the antibody is not specific. When the detection of proteins is done with ELISA, it is important that the specific antibodies detect the specific antigen they are

meant to detect. In terms of absorbance values recorded, there needs to be a positive signal only for the protein that is under detection. For example, a primary ovalbumin antibody should only be able to detect ovalbumin proteins. If it detects also a purely casein or collagen protein, that means that the antibody is not specific. This is important because, if the antibody is not specific, the entire ELISA process is considered invalid. Therefore, it is important to assess the specificity of all primary antibodies irrespective of its origin. In our experiments, all the ELISA experiments were performed with an enhanced specificity before they were allowed to proceed to detect the protein under study. They were also combined together with and without the specific antigen needed to be detected.

2.8 Results and Discussion

2.8.1 Preparation of the Paint models

In cultural heritage artefacts such as easel paintings, it is important to reproduce these paint models with recipes depicted from the period in which the painting comes from. The paint models usually consist of a protein binder and a pigment and sometimes it can have multiple layers. Only a pigment of lead white was used in these experiments in order to have consistency in protein extraction. Samples were selected for the proteins of ovalbumin, casein and collagen from previously prepared paint models. Each of the paint models has a different combination of protein binders and pigments and the motivation was to assess the protein extraction protocol with different paint models in the presence of nanoparticles.

Fig. 2.1 shows some examples of used paint models

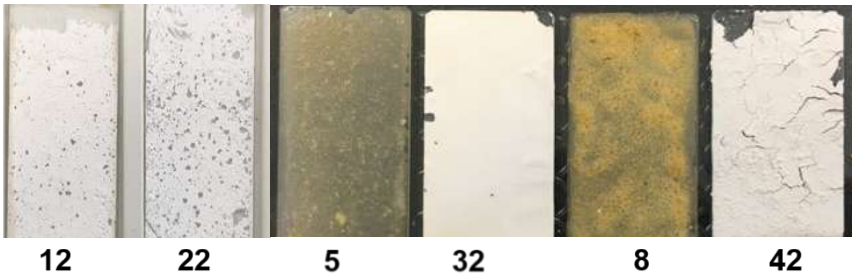

Figure 2.1 Paint models of ovalbumin, casein and collagen

Once these paint models were developed and dried, the microextraction process was followed and the protein supernatants were finally removed from the paint model extracts. Following

this, the protein supernatant was quantified by the Braford assay in the presence of Coomassie Blue. The protein quantification is discussed in the next subsection.

2.8.2 Protein quantification from the paint models

The protein present in the paint models were quantified and normalised in terms of ug/ml of protein in each sample. The Fig. 2.2 below shows the graphical representation of this amount of protein while it is possible to make a comparative study.

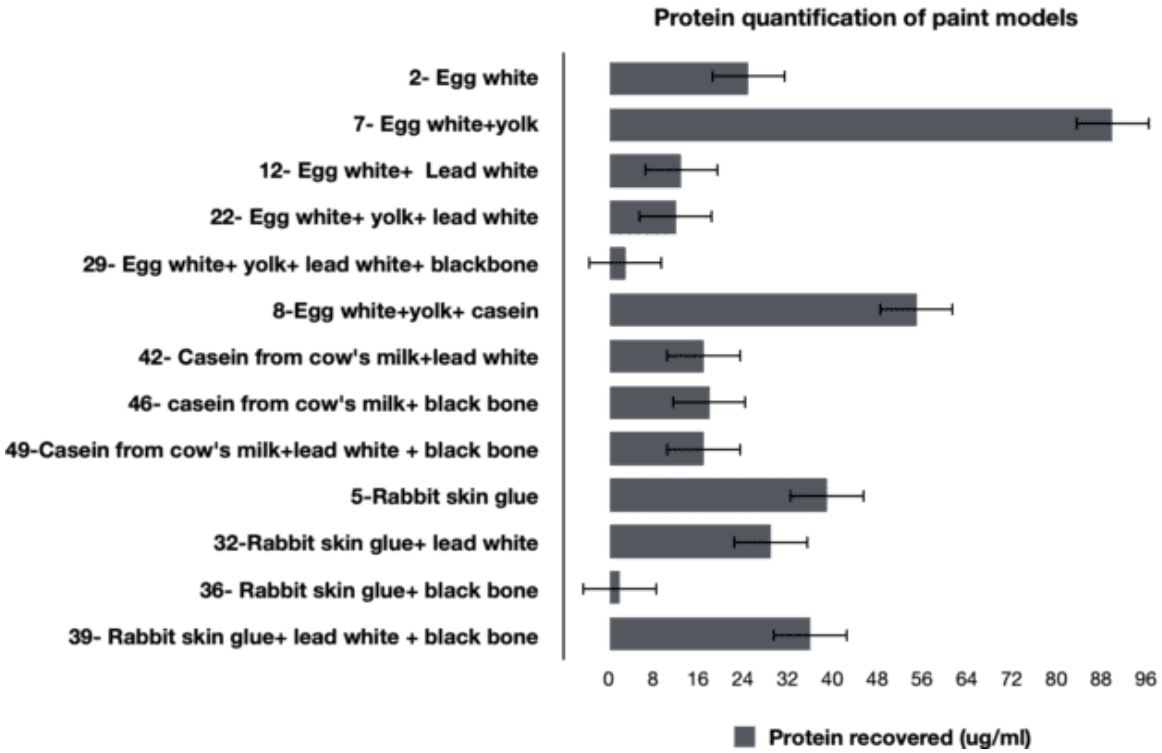

Figure 2.2 Protein quantification from paint models in ug/ml

From Fig. 2.2 it can be observed that there is a difference in protein quantified in the different paint models. Sample 7, which is a paint model of ovalbumin has the highest protein recovery from the system (around 90 ug/ml). The recovery of protein from paint models with pigments is much lower than paint models without any pigments. This is quite evident due to the high concentration of pigments in comparison to the binder content. Although, pigments differ from one another in terms of protein being recovered as each pigment binds with the binder differently. In the above graph, lead white and blackbone were used as the pigments, and the amount of protein recovered from these pigments is different even if they have the same pigment to binder ratio (3:1). Paint models of ovalbumin and collagen that have blackbone as

the pigment, i.e. 29 and 36, when quantified portrays the lowest protein recovery amounts in comparison to the other paint models (around 1-1.5 ug/ml). The micro-extracts of protein quantified with pigments of lead white demonstrate a larger amount of protein recovery in all samples of ovalbumin and collagen. In casein paint models, the blackbone based model (i.e. 46) had a slightly higher protein value in comparison to the lead white model (i.e. 42). Overall it was possible to quantify the paint models based on their protein content and eventually represent them individually.

After quantifying the protein based on the ug/ml, the paint models were further quantified based on the weight of each microsample used for extraction. This is done in terms of the ug of protein present per milligram of microsample.

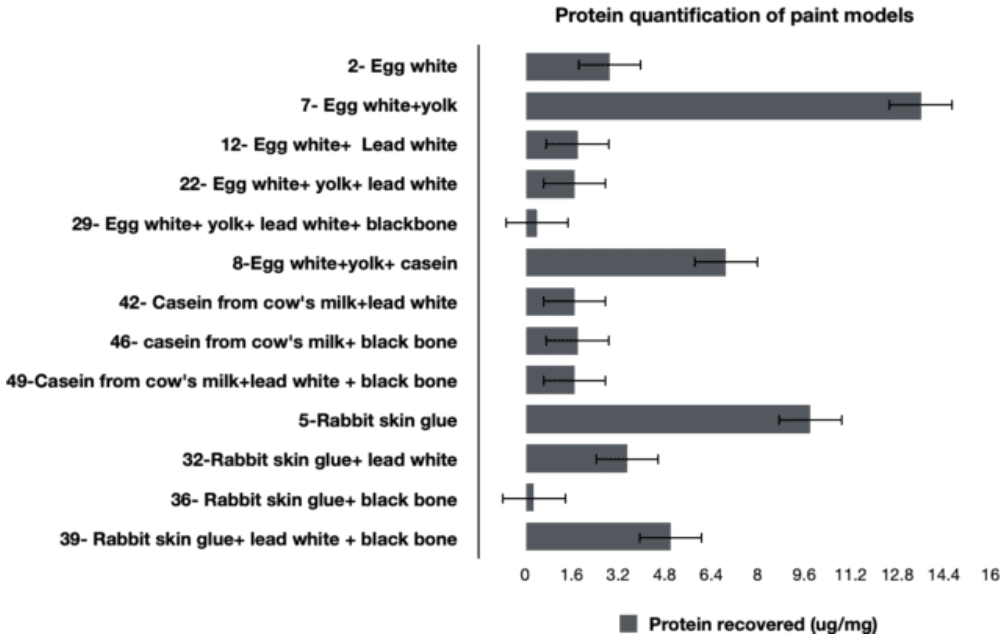

Figure 2.3 Protein quantification from paint models in ug/mg

In Fig. 2.3 the protein quantified in ug/mg of protein is given. These values give a better estimate of how much protein is present in every milligram of sample and represent the final value of the protein extraction step.

2.8.3 Immunodetection of the paint microsamples

The protein of the paint micro-extracts is detected via ELISA in the presence of primary and secondary antibodies. Initially, the concentration of primary and secondary antibodies for ovalbumin, casein and collagen were selected as mentioned in [161].

Table 2.2 gives the concentration of each primary and secondary antibodies.

Table 2.2 Primary and Secondary Antibody Concentrations

Protein	Primary Antibodies	Secondary Antibodies
Ovalbumin	Monoclonal Anti-chicken egg Albumin produced in mouse (1:2000)	Monoclonal Anti-mouse IgG (whole molecule)-Alkaline Phosphatase antibody produced in rabbit (1:4000)
Casein	Polyclonal Anti-Casein Kinase II antibody produced in rabbit (1:5000)	Monoclonal Anti-mouse IgG (whole molecule)-Alkaline Phosphatase antibody produced in rabbit (1:5000)
Collagen	Monoclonal Anti-Collagen antibody Type I produced in mouse (1:2000)	Polyclonal Anti-Rabbit IgG (whole molecule)-Alkaline Phosphatase antibody produced in goat (1:20000)

After the selection of the antibody concentrations, the ELISA immunoassays were carried out on each of the protein paint models and also commercial solutions of ovalbumin, casein and collagen according to the protocol discussed in Section 2.5. The detection of each paint model is given in U/ml which corresponds to the antigen-antibody activity within the ELISA immunoassay system. Given below, in Fig. 2.7 is the graphical representation for each paint model and commercial sol in U/ml.

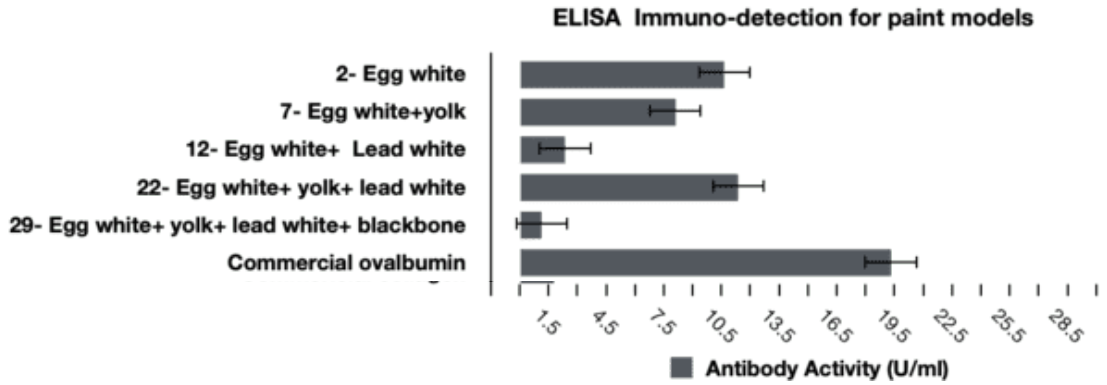

Figure 2.4 a)Antibody specific activity (U/ml) for ovalbumin

From Fig. 2.4 a) it can be seen that the commercial solution of ovalbumin has the highest antibody activity. The paint models 2,7 and 22 also have high antibody activity whereas 12 & 29 have lower detection.

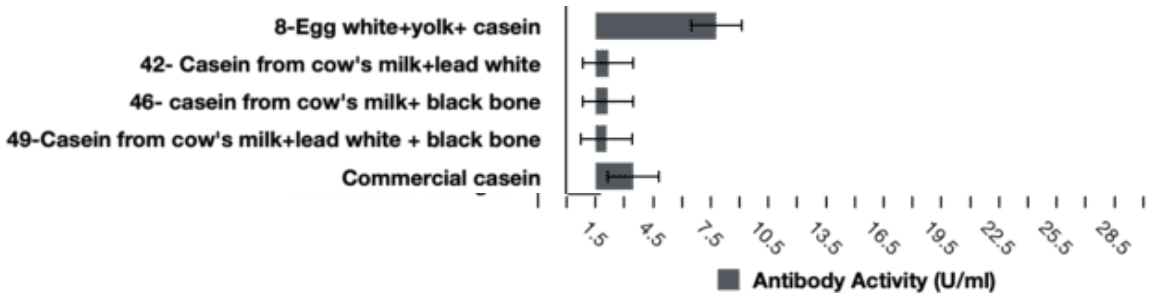

Figure 2.4 b)Antibody specific activity (U/ml) for casein

From Fig. 2.4 b) it can be seen that Sample 8 has the highest activity for the casein paint models including commercial casein. The other paint models of casein do not portray much antibody activity and it was hard to assess their sensitivity.

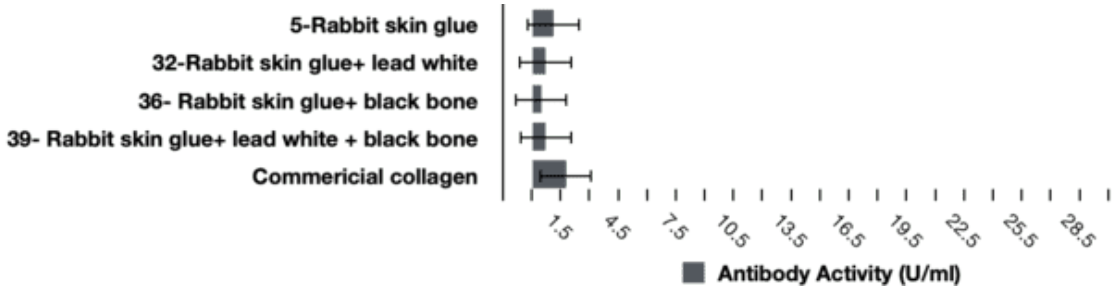

Figure 2.4 c)Antibody specific activity (U/ml) for collagen

From Fig. 2.4 c) The commercial collagen from rabbit skin has the highest activity for collagen detection. The detection of collagen in all samples was quite difficult overall and maybe this has to do with the presence of different types of collagen in the samples.

To further broaden this study, the limit of detection of the above paint models along with their selectivity were assessed which is explained in the section below.

2.9 Limit of Detection

The limit of detection was assessed for ovalbumin, casein and collagen with a starting concentration of 10µg/ml and then serially diluting it with each dilution being half the preceding concentration. Therefore, the concentrations in decreasing order are as follows: 10µg/ml, 5µg/ml, 2µg/ml, 1µg/ml, 0.5µg/ml, 0.25µg/ml, 0.12µg/ml, 0.06µg/ml. In Fig. 2.5a) to c), the concentrations above were plotted by the antibody activity.

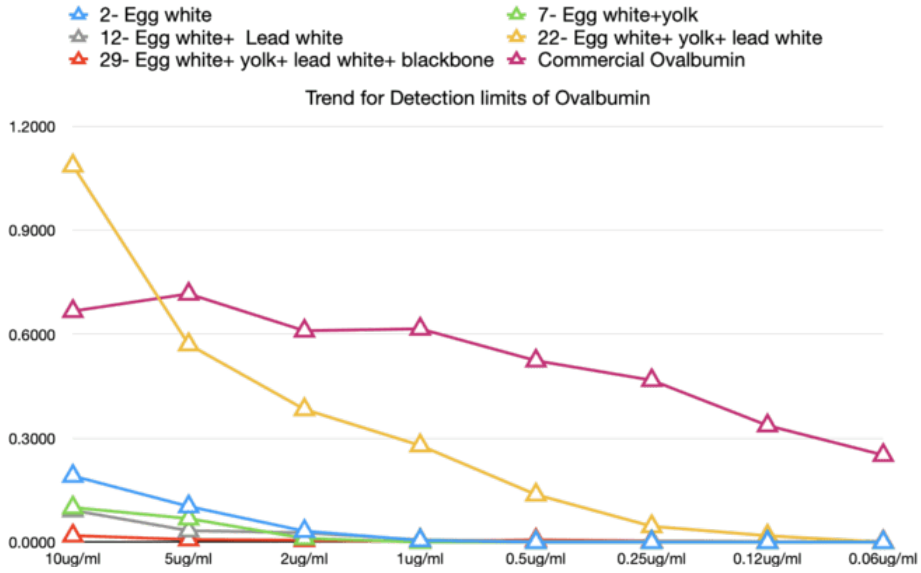

Figure 2.5 a) Trend of limit of detection for ovalbumin

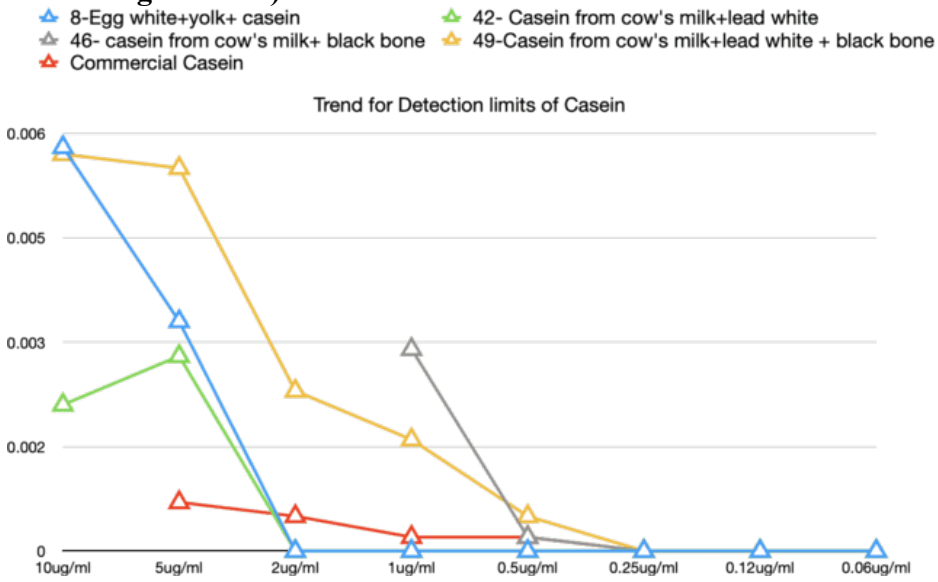

Figure 2.5b) Trend of limit of detection for casein

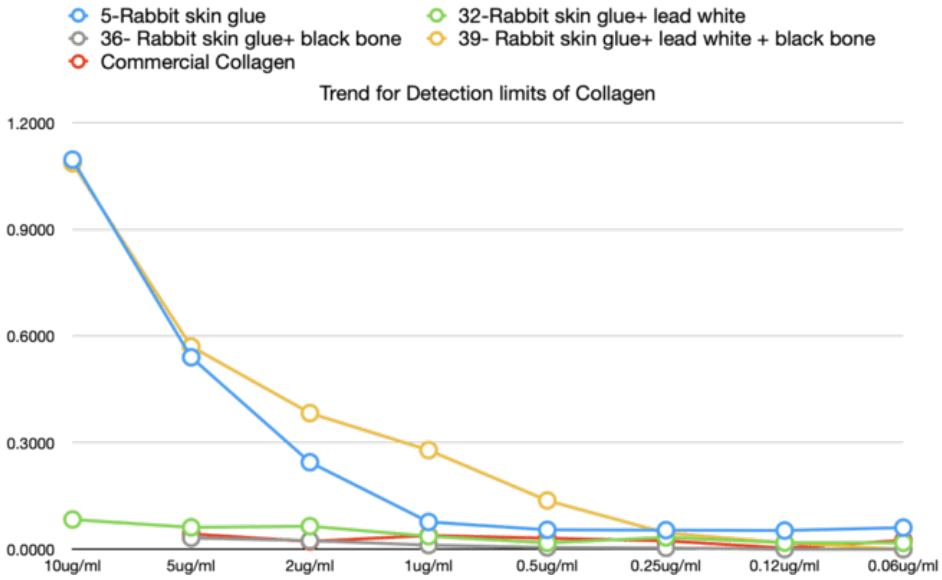

Figure 2.5 c) Trend of limit of detection for collagen

In Fig. 2.8 a) to c), the general trend of the detection is a decreasing curve as the concentration reduces. In some paint models the detection activity reduces drastically while in others the activity is almost negligible after a certain point. It is possible to visualize the effect of concentration on antibody activity and eventually the limit of detection is known via the end point of antibody activity at a particular concentration.

To have a quantitative measure of the limit of detection in each paint model, the Table 2.3 below provides the final output and defining point for the limits.

Table 2.3 Limit of detection of the paint models and commercial solutions

Sample	**Limit of detection in (µg/ml)**	**Sensitivity**
2- Egg white	1	+++
7- Egg white + yolk	2	++
12- Egg white+ Lead white	1	+
22- Egg white+ yolk+ lead white	0.12	++++
29- Egg white+ yolk+ lead white+ blackbone	0.5	+
Commercial Ovalbumin	Less than 0.06	+++++

8-Egg white + yolk+ casein	5	+
42- Casein from cow's milk + lead white	10	+
46- casein from cow's milk+ black bone	2	++
49-Casein from cow's milk + lead white + black bone	1	++
Commercial Casein	5	+
5-Rabbit skin glue	Less than 0.06	+++++
32-Rabbit skin glue+ lead white	Less than 0.06	+++++
36- Rabbit skin glue+ black bone	0.25	++
39- Rabbit skin glue+ lead white + black bone	0.06	++++
Commercial Collagen	0.06	++++

In Table 2.3 the protein limit of detection of all paint models and commercial solutions have been analysed. The lower the limit of detection here corresponds to the highest antibody activity which can be observed given in terms of '+' in the last column of table 3. The commercial ovalbumin, rabbit skin glue and rabbit skin glue with lead white have the lowest limits of detection overall with antibody detection even below 0.06 µg/ml. Commercial collagen and rabbit skin glue with lead white and blackbone together went down to 0.06 with a little less detectivity than the latter three. Sample 12 with egg white + yolk and lead white was realised with antibody activity at 0.12µg/ml. The least possible detection limit in casein was in sample 49 at 1µg/ml and 2µg/ml with sample 46. The other casein paint models along with the commercial casein did not show much activity below 5µg/ml, making casein the with very high limits of detection. The other paint models all showed limits of detection within the serial dilution range between 2-0.25 µg/ml.

2.10 Selectivity

The final step was to assess the selectivity of specific antibodies with the protein under study. In Table 2.4 a) the specificity study for each antibody is given individually for each protein and followed in Table 2.4 b) by the combination of two or more proteins in the same sample.

Table 2.4 a) Specificity analysis of antibodies in the presence of different proteins individually.

Antigen	**Response with Monoclonal Anti-Chicken Egg Ab**	**Response with Monoclonal Anti-Collagen Ab**	**Response with Polyclonal Anti-Casein Kinase Ab**
Casein commercial	-	-	+
Casein paint model	-	-	+
Collagen commercial	-	+++	-
Collagen paint model	-	++++	-
Ovalbumin commercial	++++	-	-
Ovalbumin paint model	+++	-	-

Table 2.4 b): Selectivity analysis of antibodies with proteins combined together

Antigen	**Response with Monoclonal Anti-Chicken Egg Ab**	**Response with Monoclonal Anti-Collagen Ab**	**Response with Polyclonal Anti-Casein Kinase Ab**
Casein + Ovalbumin	+	-	+
Collagen + Ovalbumin	+	+	-
Casein+ Collagen	-	+	+
Casein + Collagen + Ovalbumin	+	+	+

In Table 2.4 a) antibodies of ovalbumin, casein and collagen were tested for their specificity with commercial solutions and paint models of the above proteins. The response was highly selective for ovalbumin followed by collagen. For casein there was very less activity in terms of specificity. In Table 2.4 b), the same antibodies were assessed for their selective response to different proteins within the same solution. In this case, all antibodies were selective and they only showed activity when there was presence of the same protein corresponding to the antibody in the assay. Therefore, the antibodies are selectively able to identify proteins and have a specific response at the same time. This is quite advantageous because usually in cultural heritage artefacts, the proteins are not known and therefore, with ELISA immunoassays it would be possible to identify the proteins without knowing about them.

ELISA immunoassays are highly specific assays that have versatile applications. When such techniques are combined with other complementary techniques such as IR spectroscopy and mass spectrometry, a lot of information can be gathered about cultural heritage artefacts such as easel paintings. The protein quantification and immunodetection was able to show the possibility to identify the proteins, and further analysis with the selectivity broadened the scope of discussion.

Chapter 3

Optimization of protein extraction and immunodetection from protein-based paint models with Nanoparticles

**This Chapter has been published in the following proceedings:
1.Goyal, A.S., Salvador, C., Mathe, C. et al. "Optimization of protein extraction and ELISA immunodetection from protein-based paint models with mesoporous silica nanoparticles and MCM41", Eur. Phys. J. Plus 136, 691 (2021). https://doi.org/10.1140/epjp/s13360-021-01628-0
2. Aditya S. Goyal, Cátia Salvador, António Candeias, Carole Mathe, Ana Teresa Caldeira, "Mes oporous Silica based protein release systems", eCM Periodical, 2021, Collection 1; 2021 ScSB Abstracts (page P28), Scandinavian Society for Biomaterials 2021 13th annual meeting (ScSB 2021)
3. Aditya S. Goyal, Cátia Salvador, Ana Teresa Caldeira, António Candeias,"Recovering proteinaceous binders from Paint models of Medieval Paintings: A new Approach with Silica Nanoparticles and MCM41",Congress of Microbiology and Biotechnology MicroBiotec'19, Coimbra, 5th-7th December, 2019.

The aim of this study is to exploit silica nanoparticles in the microextraction process of proteins from paint model samples and realise the immunodetection of these proteins with ELISA. To further expand, the interaction of proteins with the nanoparticles could increase output yield of protein recovery.

3.1 Materials

The following reagents were used for sample preparation and ELISA experiments:
Phosphate-buffered saline solution (PBS, 137 mM NaCl, 10 mM phosphate (10,1 mM Na_2HPO_4, 1,8 mM KH_2PO_4), 2,7 mM KCl, pH 7,4) was used to dilute antigens and for washing step after the antigen incubation. PBS with Tween-20 (Sigma®), 0,05% solution (PBS-T) was used for the washing step after the incubation with primary and secondary antibodies.
Bovine serum albumin 1% (BSA, Acros Organics™) in PBS was used as a blocking solution, and solutions of BSA 0,1% in PBS and BSA 0,1% in PBS-T were used to dilute the primary and secondary antibodies, respectively.
Commercial standards of ovalbumin (albumin from chicken egg white, A5378, Sigma-Aldrich), commercial collagen from rabbit skin (Type I, Sigma-Aldrich), collagen from bovine

Achilles tendon (C9879, Sigma-Aldrich) and casein (C3400, Sigma-Aldrich) were used as specific controls for the primary antibodies.

Coomassie blue dye G-250 (Acros Organics™) [0,6% (m/v) in Hydrochloric acid 0.6 M (HCl)] was used for protein quantification.

The primary antibodies of Monoclonal Anti-chicken Egg Albumin (Ovalbumin) antibody produced in mouse (Reference A6075, Sigma-Aldrich), Monoclonal Anti-Collagen antibody Type I produced in mouse (Reference C2456, Sigma-Aldrich), Polyclonal Anti-Casein Kinase II antibody produced in rabbit (Reference SAB4500514, Sigma-Aldrich) were used after the addition of the antigens.

The secondary antibodies of Monoclonal Anti-mouse IgG (whole molecule)-Alkaline Phosphatase antibody produced in rabbit (Reference A2418, Sigma-Aldrich), Polyclonal Anti-Rabbit IgG (whole molecule)-Alkaline Phosphatase antibody produced in goat (Reference A3687, Sigma-Aldrich) were used to link the with the first antibodies.

Glycine buffer solution (0,1 M, pH 10,4, with 1 mM $MgCl_2$ and 1 mM $ZnCl_2$) was used to dilute the substrate p-NPP (1 mg mL-1) and for washing step immediately before the substrate addition.

4-Nitrophenyl phosphate disodium salt hexahydrate (p-nPP, Sigma-Aldrich) was the substrate that produces an optical signal for detection after the antigen-antibody interactions.

The following reagents were used for the synthesis of silica Nanoparticles:

Tetra Ethyl Ortho Silicate (TEOS) from Sigma Aldrich, Cetyltrimethylammonium Bromide (CTAB) from Sigma Aldrich, Ammonium Hydroxide (NH_4OH) from VWR Chemicals, Ethanol (100%) from VWR Chemicals and n-hexane from Aldrich.

All reagents were used and diluted in de-ionized Millipore water.

3.2 Apparatus

The following apparatus was used to perform ELISA and related experiments:

96-well Microtiter plates (maximum volume 500µl) from Nunc™, 96-well Microtiter plates (maximum volume 150µl) were used for performing the ELISA and Bradford experiments.

Micropipettes (100-1000µl, 10-100µl, 0.5-10µl), Microchannel (20-200µl), Standard Microtips (10µl, 200µl, 1000µl), Eppendorf tubes (1,5mL), 90mm disc plates, falcon tubes (50mL, 15mL), Magnetic stirrer, Nalgene Bottles (Thermo Scientific 250mL PPCO), High-speed Centrifuge (GYROZEN 2236R), Orbital Agitator (IKA KS 4000 I control) were the analytical tools used to perform ELISA in the microtiter plates.

Microplate reader (Thermo Scientific, Model Multiskan Go) was used to read the ELISA plates after the experiment was completed.

An incubator (Memmert, Model IN110) was used for accelerating the ELISA experimental procedure (at 37° C).

The nanoparticles were characterized by TESCAN MIRA-3 FEG-SEM in a vacuum chamber. The XRD images were produced by D8 advance Bruker and the Nitrogen porosimetry was done by Micromeritics Tristar II Plus.

3.3 Paint models

In real paintings, it is generally impossible to procure samples large enough for the purpose of research. Therefore, paint models represent and serve as a replacement for real paint samples. In cultural heritage artefacts such as easel paintings, it is important to reproduce these paint models with recipes depicted from the period in which the painting comes from. The paint models usually consist of a protein binder and a pigment and sometimes it can have multiple layers. Only a pigment of lead white was used in these experiments in order to have consistency in protein extraction. Samples were selected for the proteins of ovalbumin, casein and collagen from previously prepared paint models. These paint models are as given in Figure 3.4 below.

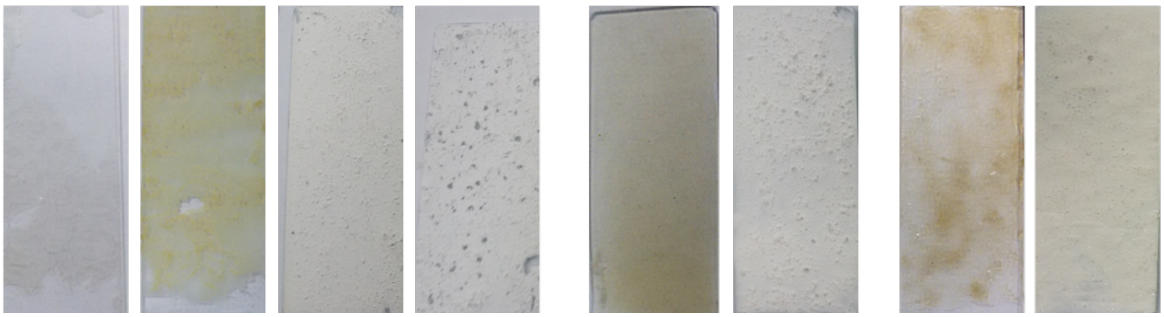

Figure 3.1 Paint models of ovalbumin (2,7,12,22); casein (8,42) and collagen (5,32)

Each of the paint models has a different combination of protein binders and pigments and the motivation was to assess the protein extraction protocol with different paint models in the presence of nanoparticles.

Table 3.1: Paint models of ovalbumin (2,7,12,22); casein (8,42) and collagen (5,32)

Paint model Number	Description
2	Egg albumin
7	Egg albumin +yolk
12	Whole egg + lead white
22	Egg albumin + lead white
8	Egg albumin + egg yolk+ casein
42	Casein from cow's milk+ lead white
5	Rabbit skin
32	Rabbit glue+ lead white

The table 3.1 above provides the details of each of the paint models with their pigment and binder composition used for the experiments.

3.4 Synthesis of Silica Nanoparticles

MCM-41 was synthesized following the emulsion-condensation route reported in [167]. This process uses oil in water emulsion consisting of water, n-hexane and the cationic surfactant CTAB. The Stöber process is used in the preparation of monodisperse silica particles in which the simultaneous hydrolysis and condensation of alkyl silicates with ammonia as a catalyst [168]. The synthesis of the silica nanoparticles were done in accordance with the "Stöber Method" for sol-gel formation. There were two different types of nanoparticles synthesized: i)Monodisperse silica nanoparticles ii)MCM-41 mesoporous silica nanoparticles.

The monodisperse silica nanoparticles ($NPSiO_2$) were prepared in accordance with by the following method [169]:

- The molar ratios of TEOS, Ethanol and Ammonium water were computed to prepare highly concentrated Silica nanoparticles. For this synthesis, the molar ratio of TEOS:Ethanol: H_2O (NH_3 25% by weight) was 1:126:9.
- TEOS (Tetraethyloxysilane) was used as the starting material. 2.6mL of TEOS was added to a Nalgene bottle. TEOS was dissolved in ethanol (72,56mL).

- Separately Ammonia water (4,05mL) and ethanol were mixed and added to the solution of TEOS and this entire sol mixture was stirred for 24h at room temperature.
- Next the sol was centrifuged and washed with ethanol three times to remove and unreacted TEOS. The resulting particles was dried in an incubator chamber for about 2 hours.

The experimental procedure for the synthesis of MCM-41 is as follows:

In a Nalgene bottle, 70 mL of distilled water, 0,80 mL of Ammonium hydroxide, 15 mL of n-hexane, 5 mL of ethanol and 0,5 g of CTAB are inserted in succession at room temperature. 2,6 mL of TEOS were added to the mixture. The molar ratios between the components are reported in the Table 3.2 below:

Table 3.2 Molar ratios of different compounds for the synthesis of Silica Mesoporous MCM-41

TEOS	Ethanol	n-Hexane	Water	CTAB	Ammonium hydroxide	HCl
1	8,7	13,9	311	0,11	1,8	0,22

Furthermore, the MCM-41 was calcined in a vacuum chamber at 550ºC for 6 hours. The calcination removes the surfactant CTAB which provides the morphological permanent structure and pores within MCM-41. It is these empty pores that can then adsorb proteins on the surface of the individual nanoparticles within MCM-41. The monodisperse silica nanoparticles $NPSiO_2$ was synthesised without any templating agents and therefore was kept in its uncalcined state.

The silica nanoparticles obtained from the modified Stöber method were characterized with SEM to understand the morphological characteristics of the nanoparticles. X-Ray Diffraction is performed to confirm the formation of silica nanoparticles with standard XRD images [170]. Finally, Nitrogen porosimetry was done on the mesoporous silica nanoparticles to identify their BET surface area, pore volume and Isotherms.

3.5 Micro-extraction of the paint models

The standard micro-extraction protocol for extracting proteins from the paint models was described in [161]. In this procedure, a paint sample of about 2-3 mg is added to an Eppendorf tube with around 300µl of PBS. This mixture then goes through a series of ultrasonic bath radiation and agitation alternatively three times of 1 hour each for two days with an overnight agitation at room temperature between day1 and day2. Through various trials it was postulated that the best way to have consistent results is to add 150µl per mg of sample. Therefore, throughout the experiments, depending on the weight in mg, an equal amount of PBS was added. After this process, the liquid supernatant containing the proteins is extracted carefully and transferred to a different Eppendorf which serves as samples to perform the ELISA experiments.

Micro-samples were extracted and dispersed into a PBS solution from each paint model, and the protein was extracted by 3 consecutive cycles of orbital agitation (at 27° C) and ultrasonication (at 37° C) of 1h each. Finally, the extracted protein were quantified.

3.6 Protein quantification of the paint models

The protein quantification is calculated in terms of the amount of protein recovered as a percentage of the theoretical value of the total protein present in a paint microsample which is also known as the yield of protein recovered. Finally, to understand the correctness of our research, the statistical ANOVA analyses was computed with SPSS on software by taking into consideration 3 different trials (SET A, B and C) that were performed separately with each extraction method.

3.7 Indirect ELISA immunodetection of antigens (proteins)

The paint binders have one or more proteins which serve as the antigen. When these antigens encounter an antibody of the same origin, it binds to the antibody and a biochemical reaction

(assay) take place. The protocol followed for ELISA is as given from Salvador et. al. [161]. Commercial solutions of ovalbumin, casein and collagen were used to compare the outcome of ELISA with paint model samples while using commercial primary and secondary antibodies. Ovalbumin and collagen ELISA tests were performed with monoclonal primary and secondary antibodies, whereas, casein was done with polyclonal primary and secondary antibodies.

3.8 Results and Discussions

3.8.1 Characterization of silica nanoparticles and MCM-41

The characterisation of the silica nanoparticles was first compared between macroscopic imaging, optical microscopy imaging and SEM imaging.

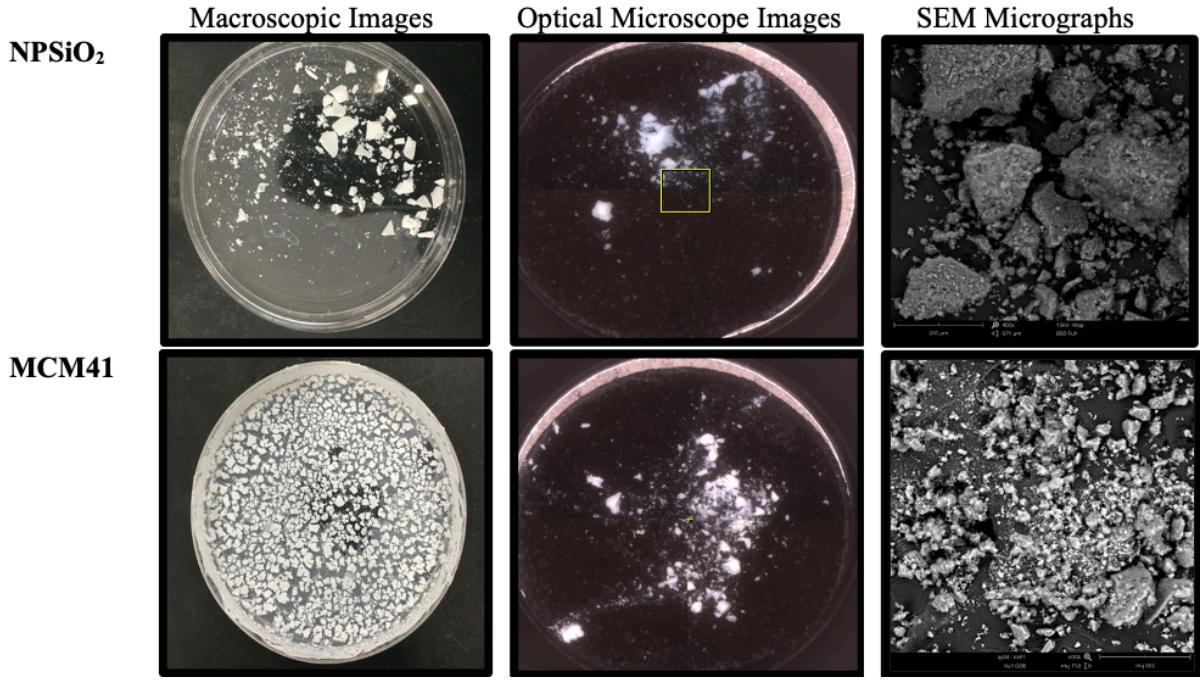

Figure 3.2 Characterization of $NPSiO_2$ & MCM41

The comparative characterization of the silica nanoparticles and MCM-41 shows the differences while going from macro to micro analysis.

The Fig. 3.3 below shows the SEM images of these materials at various resolutions. It is possible to compare between the real particle size as the magnification increases. For $NPSiO_2$, the particles seem to be spherical in shape often producing aggregates, whereas, for the MCM-41, large aggregates are formed but the particle morphology its undefined varying from small

particles to larger foiled shapes. In both cases the aggregates seem to have low adhesion between particles.

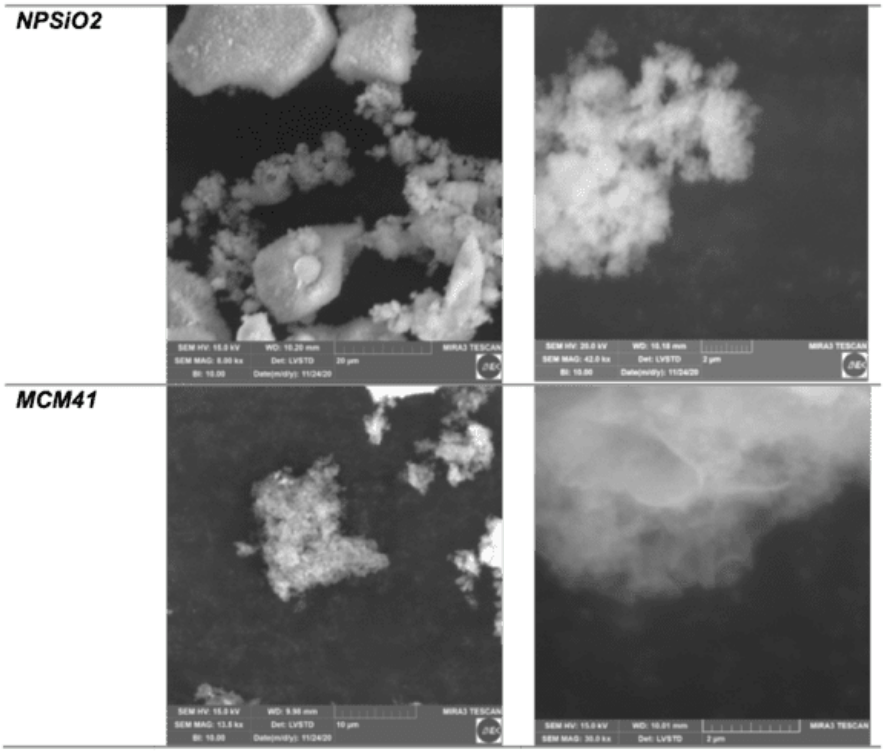

Figure 3.3 High Resolution SEM images of $NPSiO_2$ and MCM-41

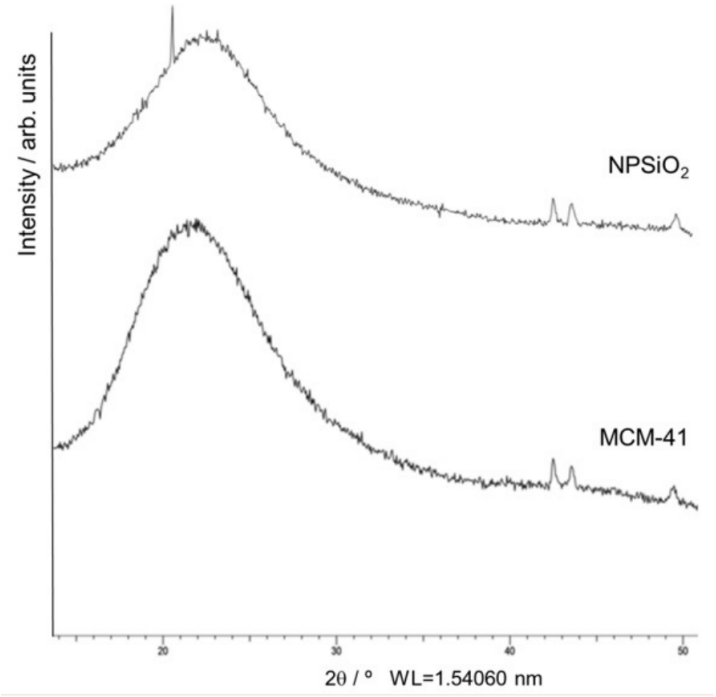

Figure 3.4 XRD images of $NPSiO_2$ and MCM-41

In Fig. 3.4 the XRD patterns of uncalcined MCM-41 and $NPSiO_2$ are as shown. The diffraction pattern for both materials exhibit the typical pattern of amorphous silica with a broad peak from 16-28º. Furthermore, $NPSiO_2$ shows a sharp peak at 21º typical of monodisperse silica nanoparticles. This indicates that even though they both are forms of silica nanoparticles, they are different from one another.

The nitrogen N_2 porosimetry was done at 77K in a vacuum after degasification at 255K for 4h with an equilibration interval of 10s and sample density of 1.000 g/cm^3. The isotherm of $NPSiO_2$ is type II typical of a non-porous samples and multilayer physical adsorption while the isotherm for calcined MCM-41 is type IV typical of mesoporous samples presenting an hysteresis loop due to capillary condensation (Annex III). The simplified surface area values given by the application of the BET equation (BET surface area) are given in the Table 3.3 below.

Table 3.3 BET Surface Area of the silica based nanoparticles

Property	**$NPSiO_2$**	**MCM-41 uncalcined**	**MCM-41 Calcined**
BET Surface Area	6,96 m^2/g	201,85 m^2/g	788,52 m^2/g

From Table 3.3 it can be noted that the BET surface area is highest in the Calcined MCM-41 with 788,5232 m^2/g and lowest in $NPSiO_2$ with 6,9630 m^2/g. The value of BET surface area for uncalcined MCM-41 might be overestimated due to degasification conditions that might have degraded part of the template surfactant. The isotherms and the BET surface area plot can be referred to in Appendix A. As we will see further that the surface area and pore volume would be correlated to the protein recovery % from the paint models.

3.8.2 Protein recovery and comparison of micro-extraction techniques

As discussed previously, there were different micro-extraction techniques utilized for the comparison of the protein recovered in each method. The purpose was to investigate whether the nanoparticles provide an added advantage for recovering proteins from paint microsamples more efficiently than the original extraction procedure. We started with the original procedure and then ventured into silica nanoparticles and MCM-41 in both uncalcined and calcined states. In Fig. 3.5 it is possible to see the difference in protein recovered in each extraction (1st,2nd and

3rd) from the paint models of ovalbumin (2,7,12,22), collagen (5,32), and casein (8,42) with and without the presence of nanoparticles for each of the four techniques.

The percentage of protein recovery for each extraction was performed according to the formulas in Section 2.3.4. After calculating each extraction for each paint microsample, it was possible to portray how the micro-extraction kinetics vary for the three extractions and also compare the differences for each sample with the different techniques.

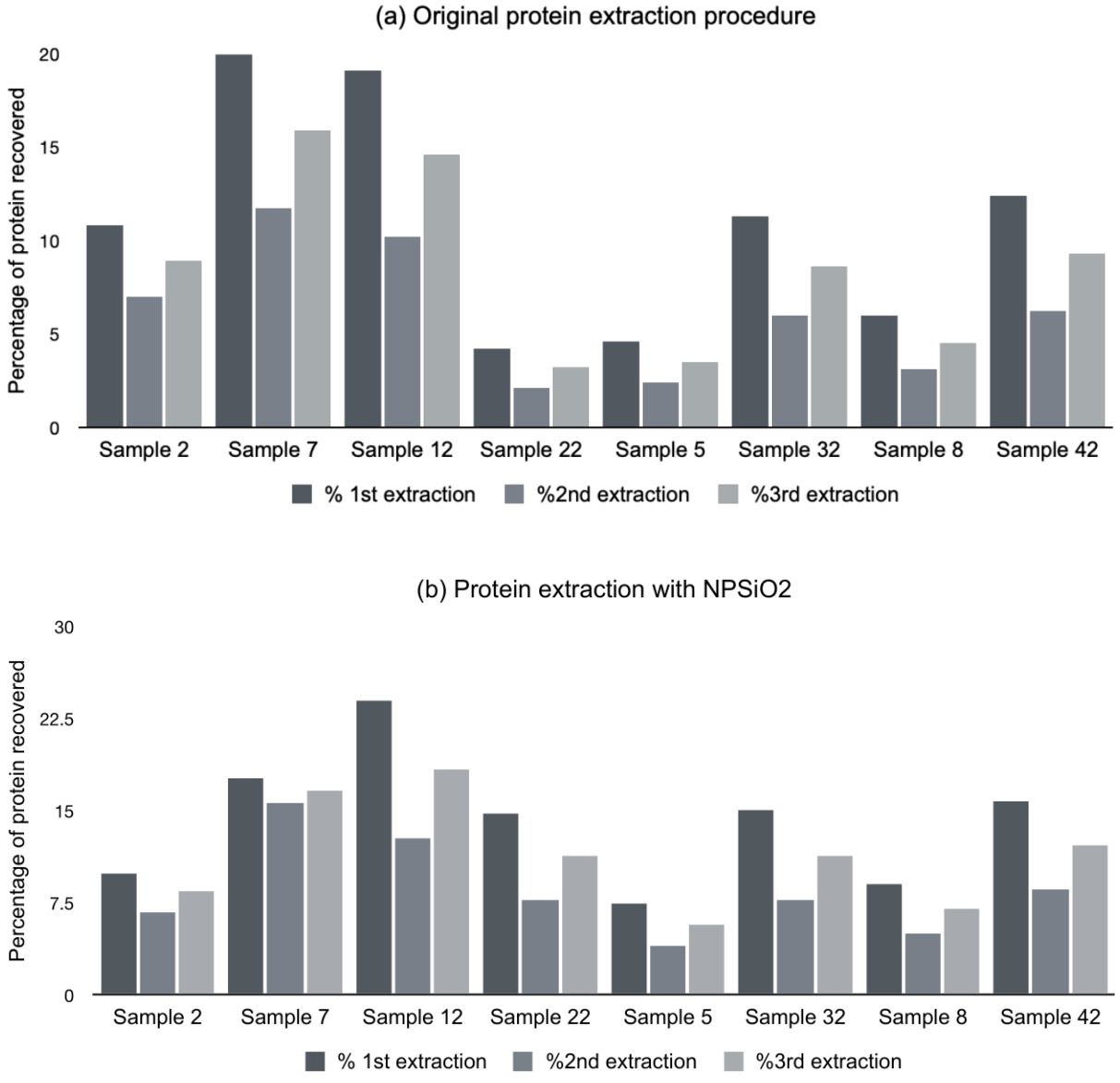

Figure 3.5 Percentage of Protein recovery for each extraction from Paint microsamples a) Original extraction b) with $NPSiO_2$

In Fig. 3.5a) the % of protein recovered from the original extraction procedure shows a general trend of increase-decrease-increase during the 1^{st}-2^{nd}-3^{rd} extractions in all paint models. The protein recovery of sample 2 is the highest among other extraction techniques. In all the paint models, the first extraction has the highest % protein recovery with respect to the other extractions. Sample 7 has the highest percentage for the 1^{st}, 2^{nd} and 3rd extraction and sample 22 has the least among all paint models. Sample 12 which is an ovalbumin based paint model has a high recovery percentage even though it contains a pigment. Sample 32 and 42 contain pigments and have a better recovery than their protein binders (collagen & casein) without any pigments (sample 5 and 8).

In Fig. 3.5b) the protein recovery with $NPSiO_2$ shows a general trend of increase-decrease-increase during the 1^{st}-2^{nd}-3^{rd} extractions in all paint models. Sample 2 has a similar pattern to the original procedure, but with a little bit lower content of protein in the three extractions. Sample 7 also follows the similar pattern of the original technique but with bit lower values. The first extraction of sample 12 is the highest protein recovery among all other paint models while it reaches an even higher percentage of recovery than the original extraction at about 24%. The third extraction of the sample 12 is also higher than the original extraction technique. Sample 5, 32, 8, 42 all have a slight increase in the protein recovery than the original technique. The second extraction of sample 5 has the lowest protein recovery in this technique.

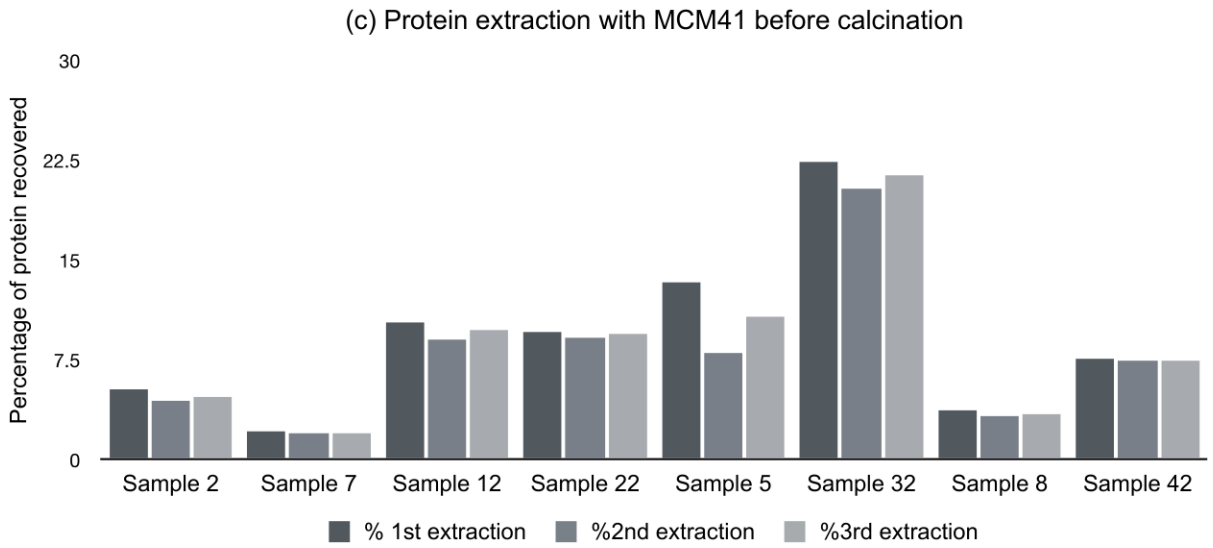

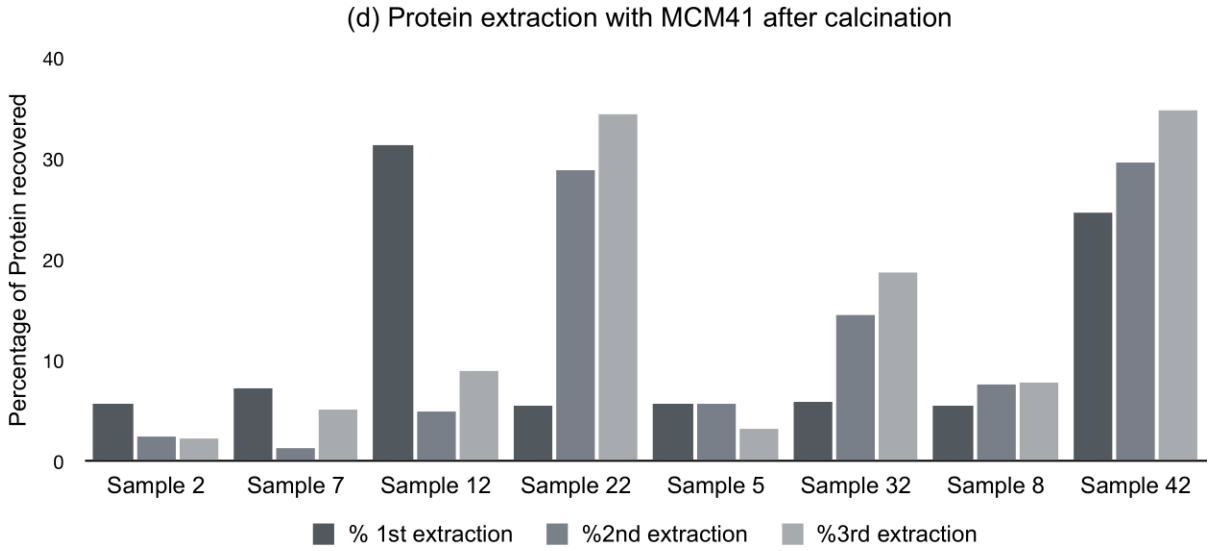

Figure 3.5 Percentage of Protein recovery for each extraction from Paint microsamples c) with MCM-41 before calcination d) with MCM-41 after calcination.

In Fig. 3.5c) the protein recovery is shown with MCM-41 before calcination and shows more or less the same general trend of increase-decrease-increase during the 1^{st}-2^{nd}-3^{rd} extractions in all paint models. Sample 2 and 7 have very low protein recovery in all extractions in comparison to the first two methods. Sample 12 also has a lower protein recovery than the previous two extraction techniques, but not as low in respect to sample 2 and 7. Sample 22 here has a higher protein recovery than the original technique, but lower protein recovery than with $NPSiO_2$. Sample 5 and 32, which are proteins of collagen have the highest protein recovery in comparison to the other two techniques and this increase is quite drastic. Sample 8 and 42, which are proteins of casein have the lowest protein recovery in comparison to the previous two methods.

In Fig 3.5d) the protein recovery is shown with MCM-41 after calcination and does not follow any particular trend among the paint models for the three extractions. Sample 2 has a low protein extraction, similar to the MCM-41 before calcination. Sample 7 has a higher protein recovery than MCM-41 before calcination, but still the protein values are very low indeed. Sample 12 in the first extraction has the highest protein values among all other techniques for this paint model. It recovers above 30% of the protein, although the other two extractions do not result in much output. Sample 22 has a low first extraction, but the 2^{nd} and 3^{rd} extractions are the highest among the other extraction techniques. This leads it to be the highest protein recovery technique for this paint model. Sample 5 has a low protein recovery than $NPSiO_2$

and MCM-41 uncalcined, but almost equivalent to the original procedure. Sample 32 has a step wise increase in protein recovery with each extraction. The third extraction almost retains 20% of the protein. Sample 8 has a low first extraction and an equivalent 2nd and 3rd extraction. Sample 42 has the highest protein recovery percentage among all paint models and other techniques while following a stepwise recovery trend.

Furthermore, the above results were combined to find the overall protein recovery. Figure 3.6 shows the total percentage of protein that was recovered from the paint models with each technique.

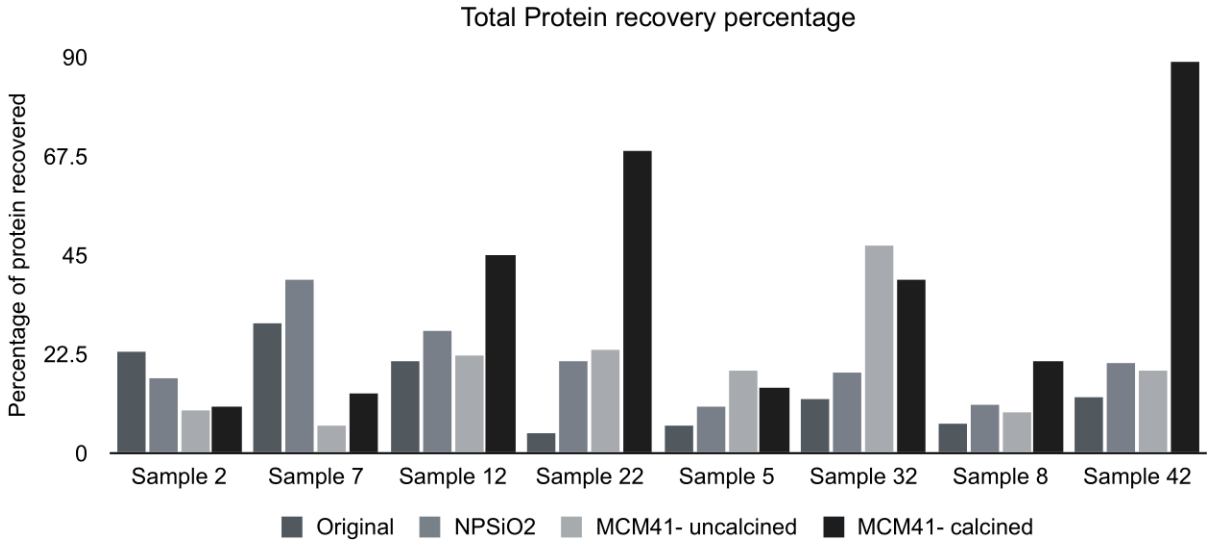

Figure 3.6 Total % of protein recovery from the Paint model samples

Except for the case of sample 2, all the other paint models had a larger amount of protein recovered with the use of the nanoparticles. In sample 7, the extraction with $NPSiO_2$ has the highest yield. In samples 12 and 22, which contain an ovalbumin binder and lead white pigment showed maximum protein recovery with the calcined MCM-41. For samples 5 and 32, which have a collagen binder, the uncalcined MCM-41 recovers the most protein, while the calcined MCM-41 follows next with just being a little bit lower. For samples 8 and 42, which have a casein binder, had maximum recovery with the calcined MCM-41. All the samples with the pigment lead white (12, 22, 32, 42) have a drastic increase in the overall protein recovered with MCM-41in comparison to the original procedure or $NPSiO_2$. In real paintings, the paint microsamples always contain pigments [160], therefore, this analysis holds importance for immunodetection with nanoparticles for real paint binders from real paintings.

In the samples with ovalbumin as the binder, the samples with pigments *i.e.,* sample12 and 22 recover more protein with MCM-41, whereas the samples without pigments *i.e.,* sample 2 and 7 prefer the original extraction procedure. Since ovalbumin is a globular protein, it is strongly affected by the pH of the system. In our case the phosphate buffer PBS has a pH= 7,4 which makes sure that ovalbumin is extracted from the paint samples but when the system contains silica nanoparticles, the globular proteins being small would easily adsorb and load on the surface of the silica nanoparticles while also changing the pH of the system. This intervention of silica nanoparticles traps ovalbumin making it very hard for them to escape into solution.

In case of the pigments being present, the pigment to binder ratio is high (3:1), therefore the pigments are strongly bounded to the binder. This makes it harder to recover proteins with the original extraction procedure. When the silica nanoparticles are present in the system, the proteins do still get partially adsorbed on the surface while still being unable to detach from the pigment. This forms a nanoparticle-protein-pigment complex, with both the nanoparticle and pigment competing to attract more protein within their vicinity. Eventually, the opposing forces cancel out each other to allow the protein to escape into the solution. This theory would hold true for the other paint models with pigments and collagen or casein binder *i.e.*, sample 32 and 42 where the protein recovery is almost 4 times that over their counterparts without pigments *i.e*., sample 5 and 8.

In the collagen paint models sample 5 and 32, the protein recovered in the uncalcined MCM-41 is slightly higher than the calcined MCM-41. This is largely due to the large size of collagen and the presence of the surfactant CTAB. The collagen proteins which after initially being attracted to adsorb on the surface of MCM-41 encounter CTAB which rapidly pushes the proteins right out into the solution whereas after calcination, CTAB is eliminated which allows the collagen proteins to be more tightly adhered on the surface of the MCM-41 than before calcination. Although due to its large size eventually it does fall out into solution, making it possible to fine tune the protein released.

Casein paint models i.e., sample 8 and 42 highly prefer the calcined MCM-41 extraction. This is because the uncalcined MCM-41 has the surfactant CTAB, and casein prefers to attach to it as they both are hydrophobic in nature. This causes the MCM-41 in its uncalcined state to finally get rid of surfactant loving casein with eventually cause a very large spike in protein recovery. The increase with $NPSiO_2$ and MCM-41 is due to their high protein loading capacity,

large pore size and easy encapsulation of the proteins on its surface which can then be fine-tuned for nanoparticle-based protein release and delivery [32-35]. This research shows how nanoparticles could help in the total protein extraction and quantification of paint microsamples by boosting the proteins through protein-nanoparticle surface interaction.

Finally, the protein recovery statistical analysis shows significant ($p< 0,05$) increase in protein recovery, above 1.3 times for $NPSiO_2$ and above 1.6 times for MCM-41. The statistical data supports the results obtained from the protein quantification and recovery.

3.8.3 Effect of silica nanoparticles on Immunoassays of paint models

The final objective of the silica nanoparticles is to observe how they affect the detection of proteins during immunodetection. The nanoparticles boost the protein recovery from the individual samples and therefore it is important to understand the efficacy for immunoassays such as immunodetection in combination with protein extracts from silica nanoparticles.

Table 3.4: Immunodetection activity with and without Nanoparticles

Sample	Without Nanoparticles (Uml^{-1})	With Calcined MCM-41 (Uml^{-1})
2- Egg white	10.65 ± 2.158	14.51 ± 0.342
7- Whole Egg	8.1 ± 0.723	8.178 ± 0.168
12- Egg white+ lead white	0.86 ± 3.496	2.098 ± 0.231
22- Whole Egg+ lead white	11.38 ± 1.865	16.865 ± 0.177
Commercial ovalbumin	19.32 ± 2.399	31.399 ± 0.894
5- Rabbit skin	7.9 ± 0.156	17.206 ± 0.334
32- Rabbit glue + lead white	0.7 ± 0.139	3.826 ± 0.203
Commercial collagen	1.785 ± 0.361	3.563 ± 0.943
8- casein cow's milk	1.69 ± 0.469	6.446 ± 0.265
42- casein cow's milk+ lead white	0.89 ± 0.222	6.214 ± 0.074
Commercial Casein	2.01 ± 0.252	9.33 ± 0.547

Table 3.4 demonstrates the change in activity in terms of Uml^{-1} for ELISA immunodetection with and without nanoparticles. As the calcined MCM-41 protein recovery demonstrated

immense potential among the silica nanoparticles (i.e. $NPSiO_2$, uncalcined MCM-41, calcined MCM-41) used for this investigation, we decided to assess the calcined MCM-41 as the right choice for comparison with the proteins from the paint models. From this table there is clear correlation between the increase in detection activity and the increase of protein recovery obtained with calcined MCM-41.

Therefore, in conclusion, a general trend of increase in protein concentration with the addition of silica particles was observed. The results of this research are a new dimension added to the investigation of protein binders from artworks. The above study shows that it is possible for silica nanoparticles to increase protein detection and extraction from paint binders, although further study of different pigments and different types on nanoparticles is required to understand the protein-nanoparticle dynamics and the effects on current immunodetection methodologies. The future works for expanding this study would be to produce paint models using a mixture of more pigments, protein binders, varnishes that simulate complex matrices which represent real paintings.

Chapter 4

Preparation of paint models with protein binders and their detection

4.1 Chromatograms and Mass Spectrums for Standards

Chromatography with Pyrolysis is a powerful tool to identify proteinaceous materials in cultural heritage artefacts. To begin with, from the literature review in the previous section, it was determined to obtain the Pyrolysis standards as given below by representation of the Chromatogram and Mass spectrum for each of the standards. The standards for Pyrolysis selected for our analysis were 1. Pyrrole and 2. 3-Pyrroline for the identification of collagen, 3. Maltol, 4. 2-Furanmethanal and for casein and 5. Indole and 6. 3-methyl Indole for egg albumin and yolk. The Table 4.6 below portrays the chromatograms and Mass spectra for the standards mentioned above and Table 4.7 which shows the retention time and m/z ratios.

Table 4.1 Chromatogram and Mass Spectrum Plots of the Standards

1	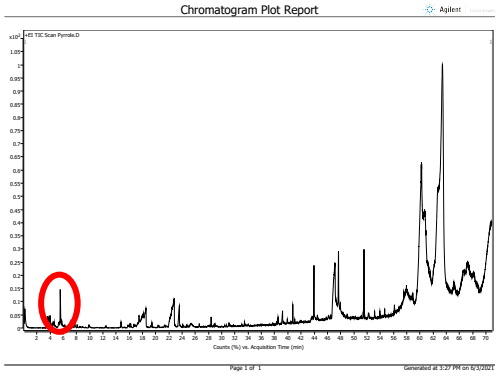	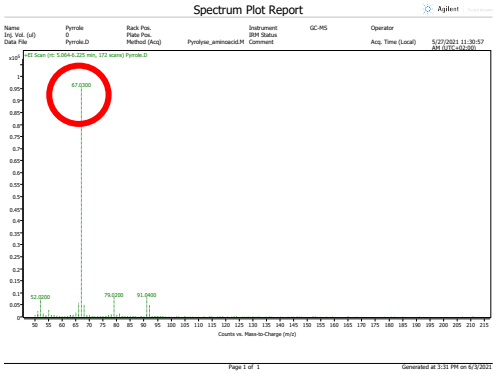

2

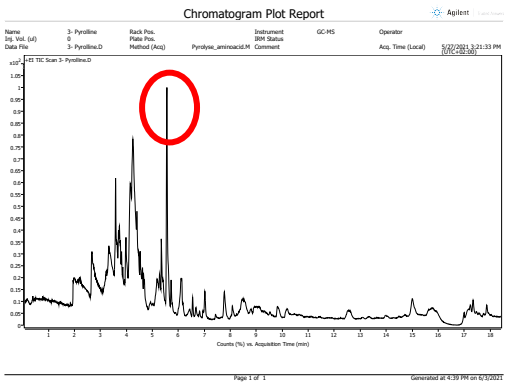
Chromatogram Plot Report
Agilent
Name 3- Pyrolline
Inj. Vol. (ul) 0
Data File 3- Pyrolline.D
Rack Pos.
Plate Pos.
Method (Acq)
Pyrolyse_aminoacid.M
Instrument
IRM Status
Comment
GC-MS
Operator
Acq. Time (Local) 5/27/2021 3:21:33 PM (UTC+02:00)
+EI TIC Scan 3- Pyrolline.D
Counts (%) vs. Acquisition Time (min)
Page 1 of 1
Generated at 4:39 PM on 6/3/2021

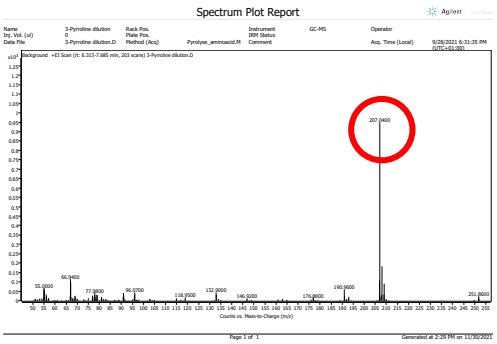
Spectrum Plot Report
Agilent
Name 3-Pyrroline dilution
Inj. Vol. (ul) 0
Data File 3-Pyrroline dilution.D
Rack Pos.
Plate Pos.
Method (Acq)
Pyrolyse_aminoacid.M
Instrument
IRM Status
Comment
GC-MS
Operator
Acq. Time (Local) 9/28/2021 6:31:35 PM (UTC+01:00)
Background +EI Scan (rt: 6.313-7.685 min, 203 scans) 3-Pyrroline dilution.D
207.0400
55.0000
66.0400
77.0800
96.0700
118.0900
132.0900
146.0200
176.0800
190.0600
250.0800
Counts vs. Mass-to-Charge (m/z)
Page 1 of 1
Generated at 2:29 PM on 11/30/2021

3

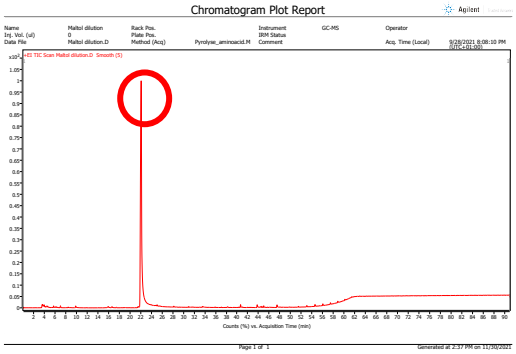
Chromatogram Plot Report
Agilent
Name Maltol dilution
Inj. Vol. (ul) 0
Data File Maltol dilution.D
Rack Pos.
Plate Pos.
Method (Acq)
Pyrolyse_aminoacid.M
Instrument
IRM Status
Comment
GC-MS
Operator
Acq. Time (Local) 9/28/2021 8:08:10 PM (UTC+01:00)
+EI TIC Scan Maltol dilution.D Smooth (5)
Counts (%) vs. Acquisition Time (min)
Page 1 of 1
Generated at 2:37 PM on 11/30/2021

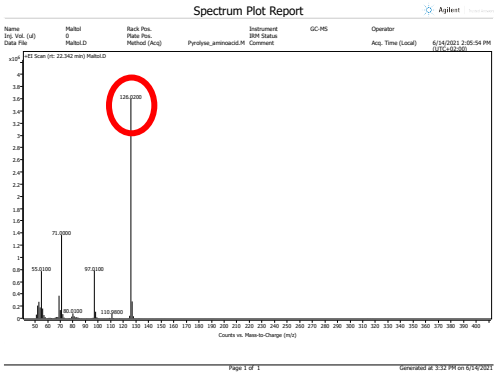
Spectrum Plot Report
Agilent
Name Maltol
Inj. Vol. (ul) 0
Data File Maltol.D
Rack Pos.
Plate Pos.
Method (Acq)
Pyrolyse_aminoacid.M
Instrument
IRM Status
Comment
GC-MS
Operator
Acq. Time (Local) 6/14/2021 2:05:54 PM (UTC+02:00)
+EI Scan (rt: 22.342 min) Maltol.D
126.0200
71.0000
55.0100
97.0100
90.0100
110.0800
Counts vs. Mass-to-Charge (m/z)
Page 1 of 1
Generated at 3:32 PM on 6/14/2021

4

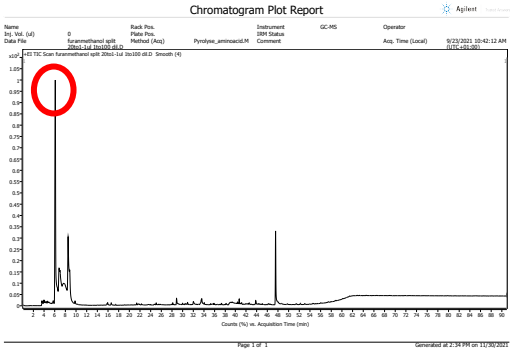
Chromatogram Plot Report
Agilent
Name
Inj. Vol. (ul) 0
Data File furanmethanol split 20to1-1ul 3to100 dil.D
Rack Pos.
Plate Pos.
Method (Acq)
Pyrolyse_aminoacid.M
Instrument
IRM Status
Comment
GC-MS
Operator
Acq. Time (Local) 9/23/2021 10:42:12 AM (UTC+01:00)
+EI TIC Scan furanmethanol split 20to1-1ul 3to100 dil.D Smooth (4)
Counts (%) vs. Acquisition Time (min)
Page 1 of 1
Generated at 2:34 PM on 11/30/2021

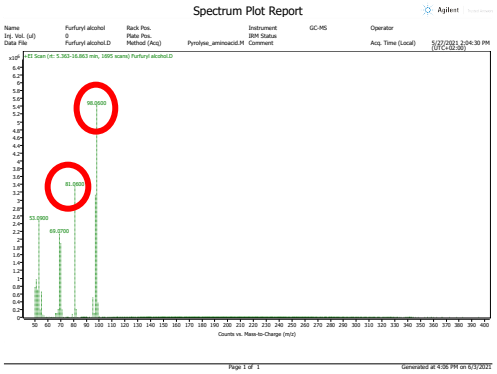
Spectrum Plot Report
Agilent
Name Furfuryl alcohol
Inj. Vol. (ul) 0
Data File Furfuryl alcohol.D
Rack Pos.
Plate Pos.
Method (Acq)
Pyrolyse_aminoacid.M
Instrument
IRM Status
Comment
GC-MS
Operator
Acq. Time (Local) 5/27/2021 2:04:30 PM (UTC+02:00)
+EI Scan (rt: 5.363-16.863 min, 1695 scans) Furfuryl alcohol.D
98.0600
81.0600
53.0900
69.0700
Counts vs. Mass-to-Charge (m/z)
Page 1 of 1
Generated at 4:06 PM on 6/3/2021

5

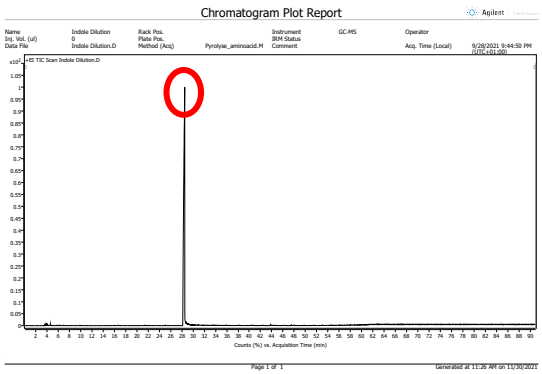
Chromatogram Plot Report
Agilent
Name Indole Dilution
Inj. Vol. (ul) 0
Data File Indole Dilution.D
Rack Pos.
Plate Pos.
Method (Acq)
Pyrolyse_aminoacid.M
Instrument
IRM Status
Comment
GC-MS
Operator
Acq. Time (Local) 9/28/2021 9:44:50 PM (UTC+01:00)
+EI TIC Scan Indole Dilution.D
Counts (%) vs. Acquisition Time (min)
Page 1 of 1
Generated at 11:26 AM on 11/30/2021

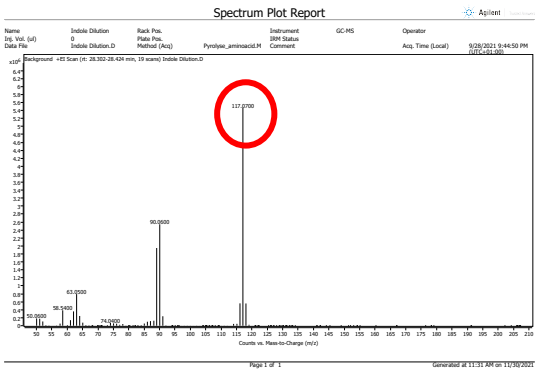
Spectrum Plot Report
Agilent
Name Indole Dilution
Inj. Vol. (ul) 0
Data File Indole Dilution.D
Rack Pos.
Plate Pos.
Method (Acq)
Pyrolyse_aminoacid.M
Instrument
IRM Status
Comment
GC-MS
Operator
Acq. Time (Local) 9/28/2021 9:44:50 PM (UTC+01:00)
Background +EI Scan (rt: 28.302-28.424 min, 19 scans) Indole Dilution.D
117.0700
90.0600
63.0500
58.5400
50.0600
74.0400
Counts vs. Mass-to-Charge (m/z)
Page 1 of 1
Generated at 11:31 AM on 11/30/2021

6

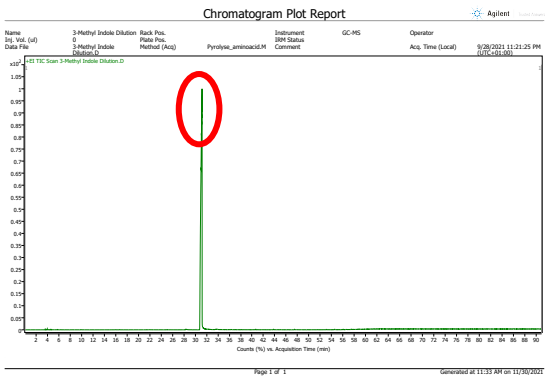

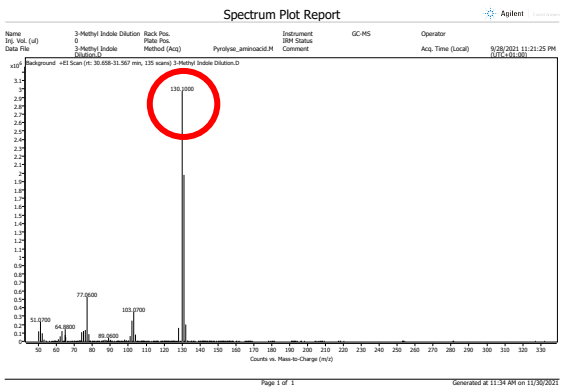

Table 4.2 m/z ratio & retention time and of standard compounds

Standard	m/z ratio	Retention time
Pyrrole	67	5-6 mins
3-Pyrroline	207	5-6 mins
2-Furanmethanol	81, 97	6-8 mins
Maltol	126	22-23 mins
Indole	117	28-29 mins
3-methyl Indole	130	31-33 mins

Paint models are reproductions of paintings and their respective layers with similar supports, binders, fillers, pigments, and varnishes. When paint models are subjected to external or artificial environments over an extended period of time, they appear to have the same chemical and physical characteristics to a microsample obtained from an aged painting [171]. As such, the binders consist of proteins such as collagen, casein and ovalbumin which need to be prepared from natural animal sources. Animal glues, which are made up of collagen, are popular in cultural heritage analysis and they can be from different species. The most common animal sources are from rabbit skin, bovine bones and gelatine from fishes [172]. For casein, milk is the primary source and for ovalbumin usually chicken eggs are an excellent source of this protein.

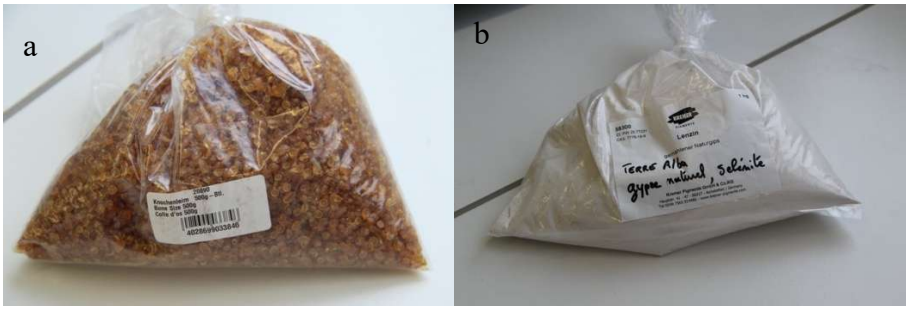

Figure 4.1 Materials used for the development of the paint model replicas: a- Bone glue, b- Gypsum sulphite, c- Calcium carbonate, d- Yellow ochre, e- Linseed Oil, f- overview of materials

Moreover, the preparation of animal glues, casein and ovalbumin are the starting point for the preparation of protein-based paint models. In figure 4.1 the different materials used for the development of the paint models have been presented.

4.2 Supports

The support is the area where the paint layers are deposited within a painting. Before the 17th century, thick pieces of wood were used as the supports. During the 17th century the wood paintings can only be found in the altarpiece present in churches. Petit Palais in Avignon is one important museum for wood paintings from the middle ages (13th-17th) century [171-173].

After the 17th century, most of the paintings are on canvas. This transformation took place with the addition of a small piece of canvas on top of the wood supports, which refers to as the joining of two pieces (calicot) of wood, and then slowly they started to realise that they don't need the wood and the canvas itself is sufficient. As the wood was expensive and heavy so only wood was used as a frame for the canvas. This is how the artists transited from wood to canvas for producing artworks [173, 174].

Figure 4.2 Supports for the proteinaceous paint models

4.3 The Layering in paintings based on the period

The layers in the painting are decided based on the support used. If the support is wood, the first layer is always a layer of animal glue or collagen sourced glue. This glue is applied all over the wood. The second layer is the ground layer which is always white in the painting. This layer is also known as the second support layer and contains either a filler such as $CaCO_3$ (carbonate), $CaSO_4$ (sulphate) or a layer of plaster $CaSO_4.2H_2O$ (gypsum sulphate). Each layer is flattened out after the application on wood. After the middle age (13^{th} – 17^{th} century), the ground is always dark or red due to red ochre and the addition of a thin layer of grey (17^{th}-19^{th} century). The reason for this colour change of the ground is owed to the fact that the painting is considered "hot" which corresponds to it being much easier to build the painting based on the coats [171,175]. During the 19^{th} century, the ground again becomes white again, because the canvas is already developed with a white ground layer already added. The animal glue was only used as the support layer on wood paintings [176]. After canvas replaced wood animal glue as a binder was only applied without a ground layer or without charge, but the switch is to oil instead of glue as the second layer. While layering, the layers applied need to be very thin otherwise there are a lot of cracks. Layer after layer is applied and repeated until the surface of the support has been completely covered [177]. After the ground has been prepared, now the pigment layers can be applied to develop the painting. While applying the pigment layer, it is important to check the pigment volume concentration so as to not have an gaps within the matter [171, 172, 178]. More pigment in the surface will give a matte (porous) finish, whereas less pigment will make the layer glass like or impermeable. In our recipes, a yellow ochre pigment was used for the paint models.

Figure 4.3 Developing different layers on the wooden supports

Figure 4.4 Initial layer of animal glue on the supports

4.4 Protocol for Preparation of Animal glues

Animal glues from rabbit skin and bovine bones is prepared usually in a concentration from 7-10% [171, 172, 175]. The gelatine glues prepared from fish such as sturgeon glue is prepared at a concentration of 2-4% [179]. The preparation of animal glues with rabbit skin, bovine bone, and fish have been discussed below.

The colour of the collagen defines the purity of collagen. The darker the colour of the collagen source, the lesser the purity of the collagen. The recipe for the preparation at 7% was used for bovine bone glue and rabbit skin glue [180].

Figure 4.5 Preparation of different animal glues

During the preparation of animal glues, a filler/ charge such as $CaCO_3$ or plaster/ $CasSO_4.2H_2O$ is added to the collagen-based glues to reduce the reflection of the pigment or increase the refractive index. The Tohe recipe that were prepared in our paint models are in a 4: 1 ratio, that means 4 times the of charge material was added to glue[171,172, 175,180]. Therefore, for 2,8g of glue we have around 12g of carbonate. In our recipe the amounts are multiplied by 4 for the glue with 100% charge, which is given in Table 1 showing the different types of paint models prepared from animal glues, the number of layers applied to each and the application of a final pigment layer on each of them.

4.5 Preparation of ovalbumin paint model

Only one paint model was prepared for ovalbumin. This paint model contains egg yolk and yellow ochre pigment. This paint model had a very high viscosity, therefore, only 1 layer was required for its preparation. The protocol involved 12g of yellow ochre for 1 egg yolk. The viscosity can be reduced by the addition of water [181].

Table 4.3 List of paint models for collagen and their preparation

No.	Name of the paint model	Layers	Preparation Protocol
1	Bone glue (7%) with 100% CaCO3	3	50 mL (7g of bovine bone collagen in 100mL of water swelling, heating at 40°C) + 46g of $CaCO_3$ (100%)
2	Bone glue (7%) with 25% CaCO3	12	50 mL (7g of bovine bone collagen in 100g of water)/2 + 12g of CaCO3 (25%)
3	Rabbit glue (7%) with 100% CaCO3	3	50 mL (7g of rabbit skin collagen in 100g of water)/2 + 46g of CaCO3 (100%)
4	Rabbit glue (7 %) with 25% CaCO3	12	50 mL (7g of rabbit skin collagen in 100g of water)/2 + 12g of CaCO3 (25%)
5	Linseed oil+ rabbit skin glue (10%) + yellow ochre in 10% of soap water + CaCO3	3	(10,1g rabbit skin in 100mL water (10%) heating at 40°C + 10g linseed oil) +25g CaCO3 + 25g of yellow ochre + 10g of soap
6	On Canvas + Bone glue (7%) + Oil+ Rabbit skin glue (10%) + yellow ochre in 10% of Soap Water + CaCO3	3+3	(10,1g rabbit skin (10%) + 10g oil) in 100mL water + 25g CaCO3 + 25g of yellow ochre + 10g of soap And Bone glue (7%)

The presence of more charge means that the paint will be more readily absorbed on the support and the easier it is for the surface to be soft.

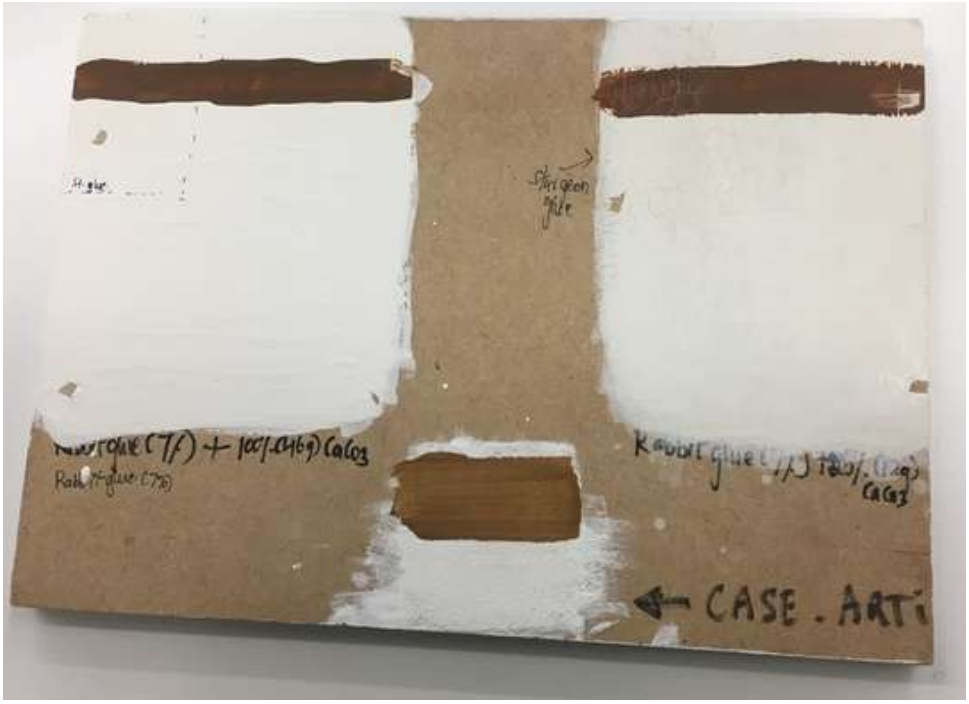

Figure 4.6 Paint models with Rabbit glue as binder and $CaCO_3$ as charge material

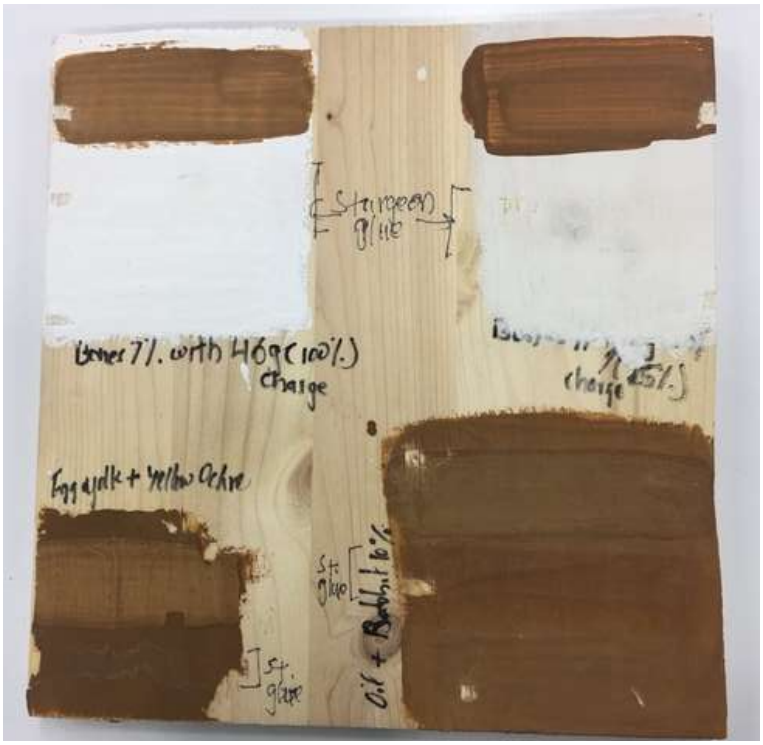

Figure 4.7 Representation of paint model replicas with bone glue, rabbit glue and egg yolk with different charge percentages (25-100%) and yellow ochre

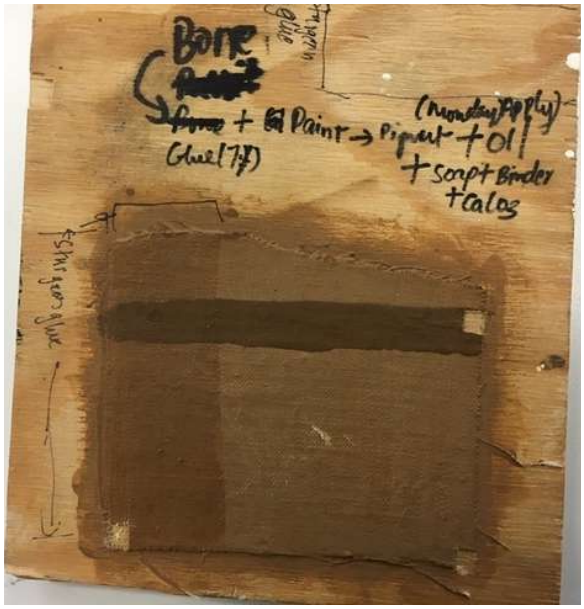

Figure 4.8 Paint model on canvas with Bone and rabbit skin glue and yellow ochre as charge

4.6 Chromatograms and Mass Spectrums Paint models of collagen

The paint model replicas for collagen were analyzed by Pyrolysis GC-MS in accordance with the procedures presented in [183, 184, 185]. The chromatograms and respective mass spectra for the paint model replicas mentioned are given below in Table 5.2

Table 4.4 Chromatogram and Mass Spectrum of 1. Bone glue with 100% $CaCO_3$, 2. Bone glue with 25% $CaCO_3$, 3. Rabbit glue with 100% $CaCO_3$, 4. Rabbit glue with 25% $CaCO_3$, 5. Linseed Oil+10% Rabbit glue+ yellow ochre+ $CaCO_3$, 6. Canvas+ yellow ochre + rabbit glue + bone glue

1

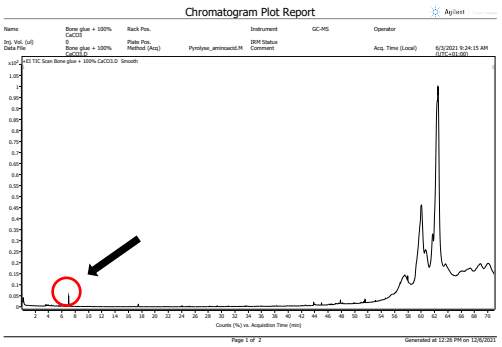

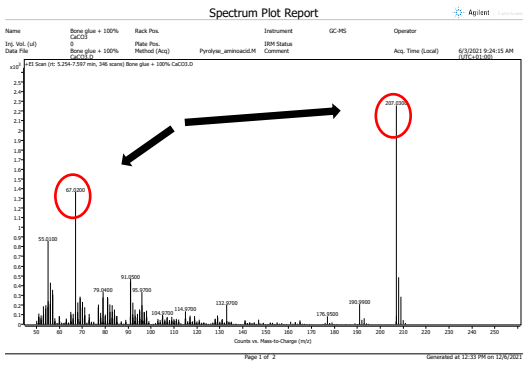

2

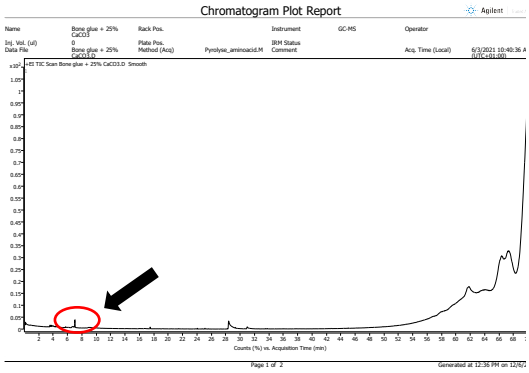

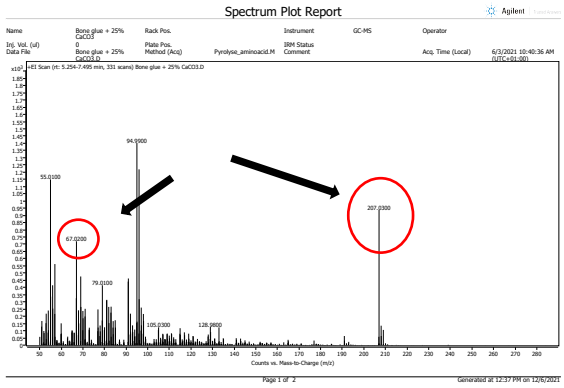

3

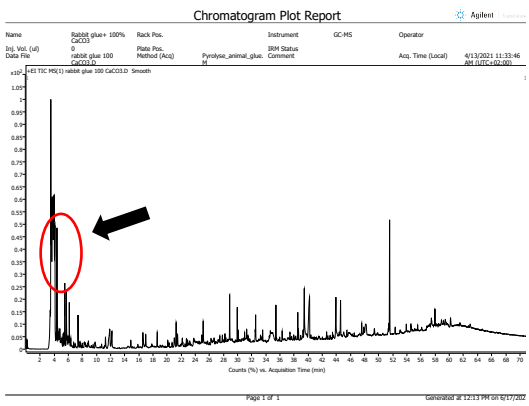

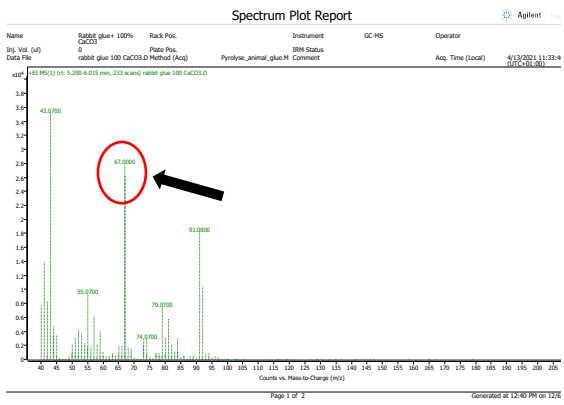

4

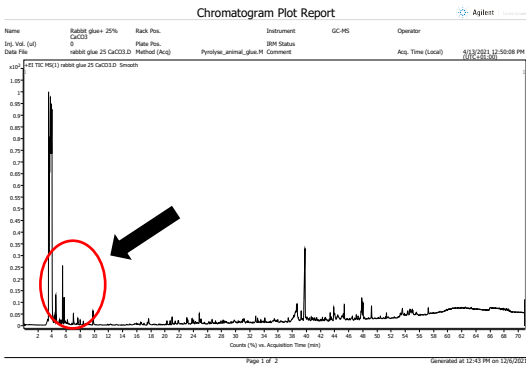

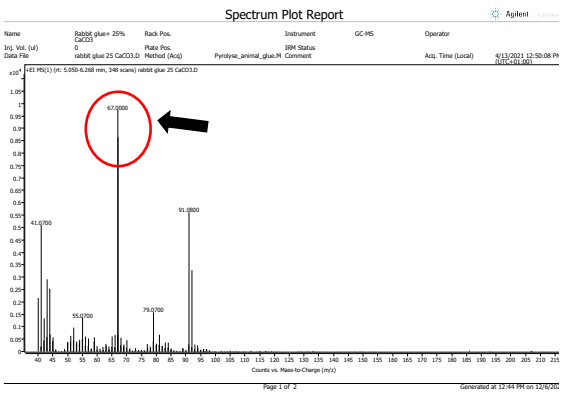

5

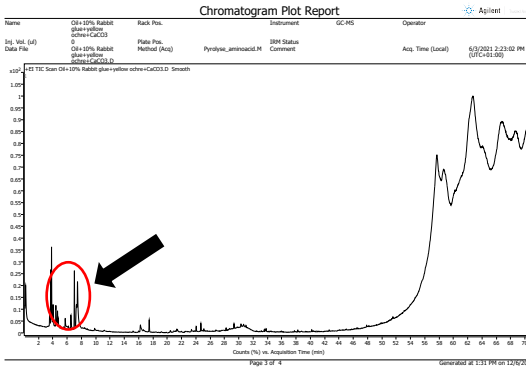

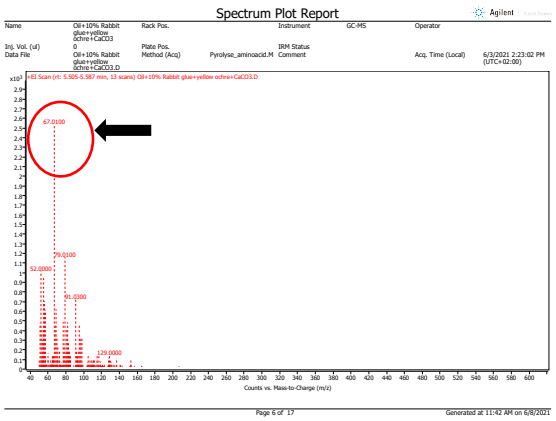

6

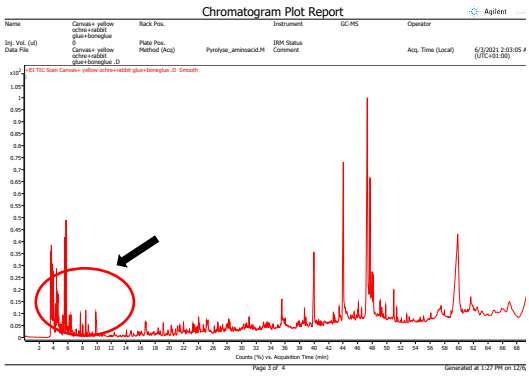

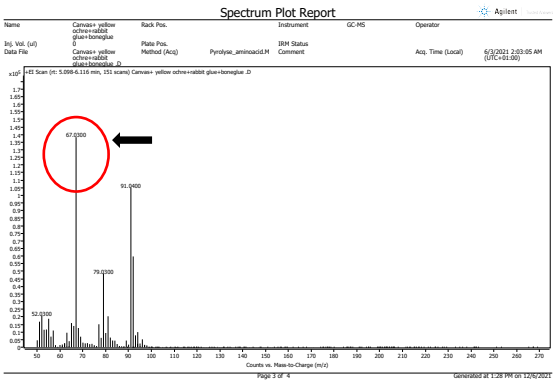

From Table 5.2 it can be noted that the chromatograms are shown on the left-hand side. From each of the chromatograms it was necessary to narrow out the region of retention at which the standard markers for collagen, i.e., Pyrrole (m/z= 67) and 2-Pyrroline (m/z= 207) were extracted in the form of the mass spectra on the right-hand side of the table. In the paint models that have Bone glue (1 & 2), it was possible to identify the two standard peaks for Pyrrole at 67 and Pyrroline at 207, whereas for the rest of the models that contained rabbit skin glue (3,4,5 & 6), it was only possible to identify the standard peak of Pyrrole at 67.

This fact is quite interesting, because the type of collagen present in the two glues are different from one another (Bone glue has collagen B and Rabbit skin glue collagen A) and the

difference in standard peaks is a key indicator of this feature. A lot of times it is difficult to identify the type of collagen present in an art sample that contains collagen as a proteinaceous binder. By identifying such trends with Pyrolysis GC-MS does provide a great insight into identifying the type of protein binder material used.

The main objective of this analysis was to identify the standard peaks from the paint models, but we can further identify the differences between different glues as well as shown and explained above. This indeed does make Pyrolysis along with chromatography an extremely useful tool while also providing complimentary analysis for immunoassays.

4.7 Preparation of casein

Casein was not used in most paintings and it is very rare to find it. After the World War II, in 1950 the artists wanted to find a new material for binders, therefore they found casein which is in fact a very old material. One of the paintings that has a casein binder present is by Victor Brauner called Atrapulation [182].

Casein was prepared with two different protocols:

The first protocol was obtained from [186].

1. Add 100mL of whole milk in a beaker and heat up to 40°C which stirring moderately.
2. Add acetic acid (100%) drop by drop until the pH is 4,6 (20mL of acid solution approx.)
3. Pour the mixture over a gauze and wring out the curd as much as possible. Now using the Buchner filter and coarse paper over a funnel and apply a vacuum over it.
4. Wring it again after changing the coarse paper.
5. Dry the casein by pressing it between absorbed papers, then place it in the open air in a ventilated area.
6.Yield obtained is around 17g of dry casein.

The second protocol is was obtained from [187]

1. Boil 5 minutes 1/2 litre of milk with 2 table spoon of alcohol vinegar
2. Using a fine filter, filter the mixture, then "curd" containing casein is obtained
3. Let the casein drain between one night at 24 hours: this produces about 100 g
4. Dilute a pinch of borax in water
5.Add the casein and mix
6. In another container, mix 150g of precipitated white chalk with 200ml of water
7. Mix the two pastes

After both the protocols were completed, the casein was dried in a hot air oven at 50°C. Once the casein powder dried, we prepared two recipes of casein that were the most common in paintings- a) Casein with Ammonia b) Casein with lime

a) Casein with Ammonia

1. Add 10g of dry casein powder in 35mL of water and keep it for 1h.
2. Prepare a solution of 2g of liquid ammonia (NH_3 35%) in 20mL of distilled water.
3. After 1h, add the ammonia solution drop by drop and also add 15mL of water later.
4. Wait for 30min and add 30mL of water again, which gives a honey like texture.

b) Casein with quicklime

1. Add 10g of dry casein powder to 35mL of water and wait for 1h.
2. Prepare 5g of quicklime (CaO) with 20mL of water.
3. Drop by drop add the lime solution to the casein mixture.
4. Wait for 30min and then add 45mL of water to this mixture.

After the casein recipes were prepared, a number of different paint models were developed as given below in Table 5.3.

Table 4.5 List of paint models for casein and their preparation

No.	Name of the paint model	Preparation Protocol
1	30mL casein ammonia + 100% CaCO3	30g casein ammonia + 30g of CaCO3
2	30g casein ammonia + 100% $CaSO_4.2H_2O$	30g casein ammonia + 30g $CaSO_4.2H_2O$
3	30g casein ammonia + 60% Yellow Ochre	30g casein ammonia + 18,5g yellow ochre
4	30g casein quicklime + 100% CaCO3	30g casein quicklime + 30g CaCO3
5	30g casein quicklime + 100% $CaSO_4.2H_2O$	30g casein quicklime+ 30g $CaSO_4.2H_2O$
6	30g casein quicklime + 60% Yellow Ochre	30g casein quicklime + 18,5g yellow ochre

An important point to note is that the casein paint models due to high viscosity only required a single layer for all developed paint models. Casein produces one of the strongest adhesives known and has been utilised by joiners and cabinetmakers for generations. Egyptian, Greek, Roman, and Chinese artisans are believed to have utilised it. Texts in the Hebrew language describe the use of curd (casein) in home painting and décor. It is reported that Michelangelo used a mixture of sour milk, oil, and pigments to create highlight effects on the walls. The substance employed in the ceiling paintings of upper Bavarian homes from the eighteenth century is quicklime. It is rarely employed as a painting medium by contemporary artists, with the exception of mural decorations. The casein paint models prepared as explained in Table 4.5 have been shown in Figure 4.9 below.

Figure 4.9 Representation of Paint models for casein and their preparation

From Figure 4.9, it can be observed that the casein paint models for quite thick and viscous layers which indeed shows why only a single layer is sufficient in most cases to provide an appealing effect. The same Pyrolysis GC-MS protocol mentioned in the section on collagen

was utilised to determine the chromatogram for each model and extract the assess the mass spectra to find the standard markers for casein. The standard markers for casein that were identified are 2-Furanmethanol/3-Furanmethanol which shows 2 peaks alternatively or together at m/z =81 and 97. Furthermore, the presence of a carbohydrate in the form of Maltol at m/z = 126 can also be identified to separate a casein binder from other proteins. As the casein models also have an initial layer of collagen based glue on the support, it was important to identify the standard peaks for collagen as well. The chromatograms and the respective mass spectra for the paint models have been described in Section 4.8 below.

4.8 Chromatograms and Mass Spectra of the Paint models of Casein

The chromatograms and mass spectra of the paint models of casein have been show below in sequence of Table 4.5.

Table 4.6.1. Chromatogram and Mass spectrum of Casein ammonia+ 100% gysum sulphite

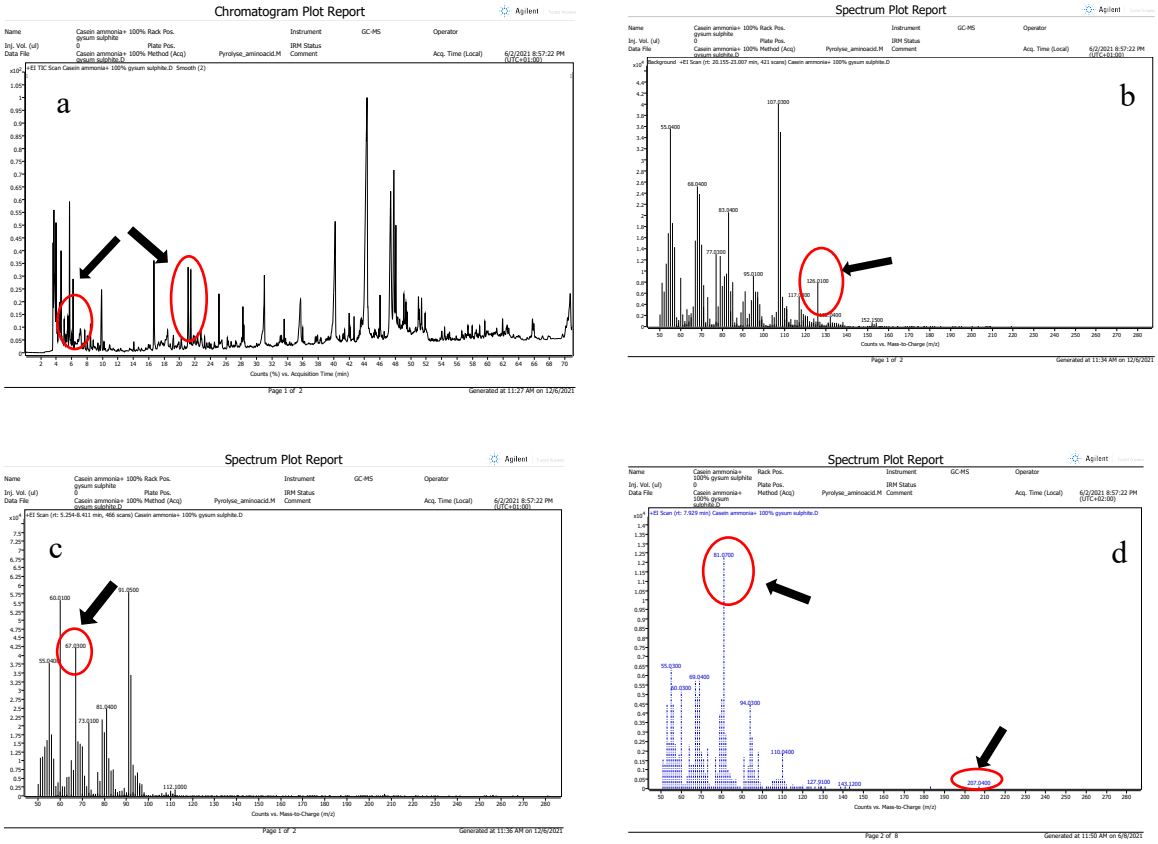

In the casein paint model, it was possible to identify the standard markers of maltol in b, pyrrole in c and 2-Furanmethanol and 3-pyrroline in d as show in mass spectra above.

Table 4.6.2. Chromatogram and Mass spectrum of Casein ammonia+ 100% $CaCO_3$

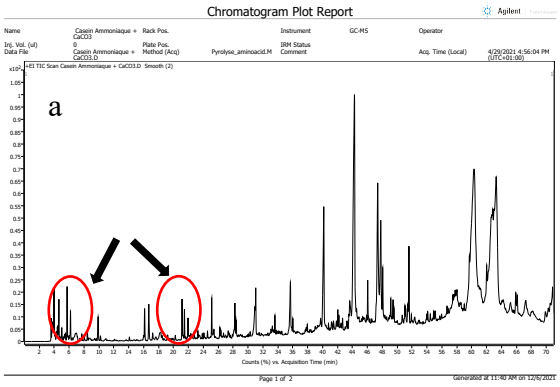

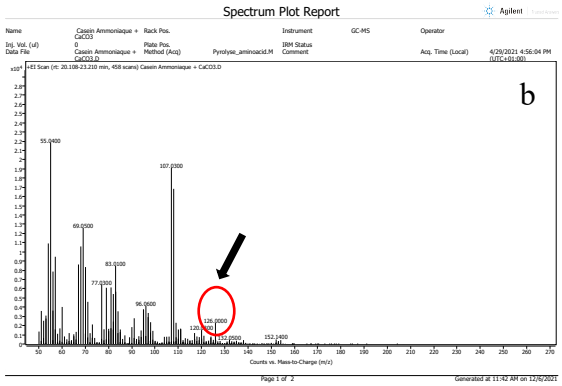

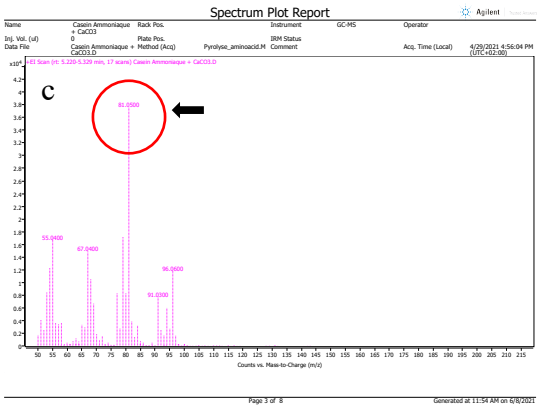

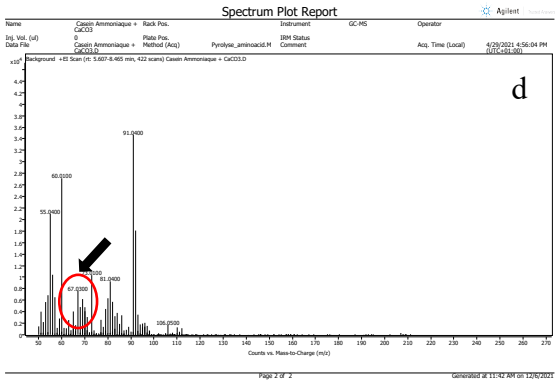

Here in the 2nd paint model, it was possible to identify the peaks of maltol in b and 2-furanmethanol in c, but we observe that there is a bit of a difference in the peak of the pyrrole in d which is comparitively smaller. The difference might be due to the filler which here is $CaCO_3$ and gypsum sulphite in the first one.

Table 4.6.3. Chromatogram and Mass spectrum of Casein Ammonia + 60% Yellow Ochre

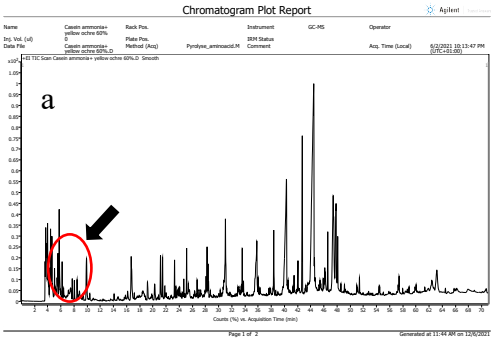

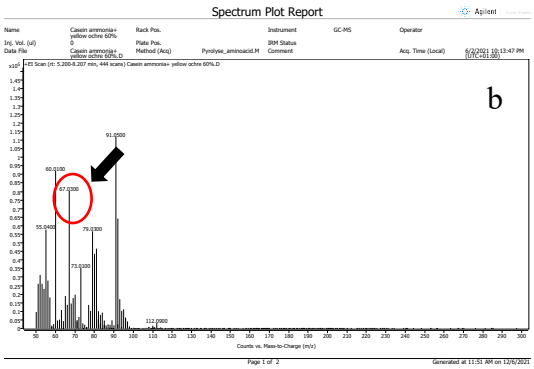

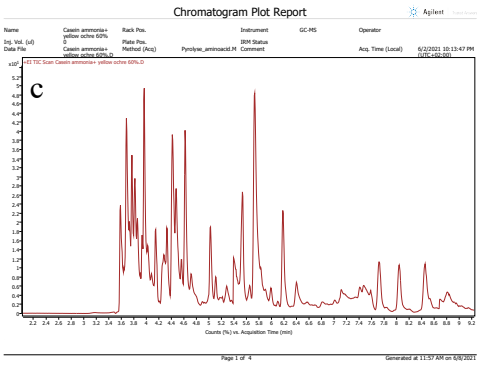

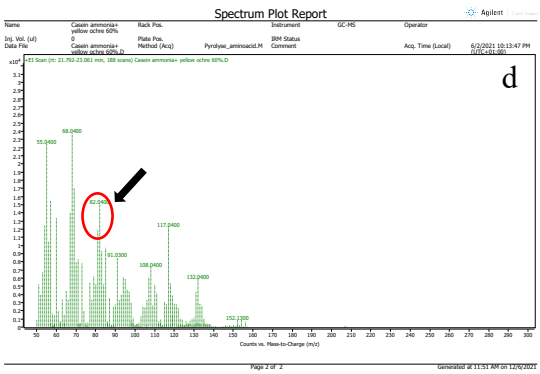

In paint model 3, it was possible to identify the peak of only 2-furanmethanol in d and the presence of collagen was identified in b.

Table 4.6.4. Chromatogram and Mass spectrum of Casein quick lime+ 100% Gypsum Sulphite

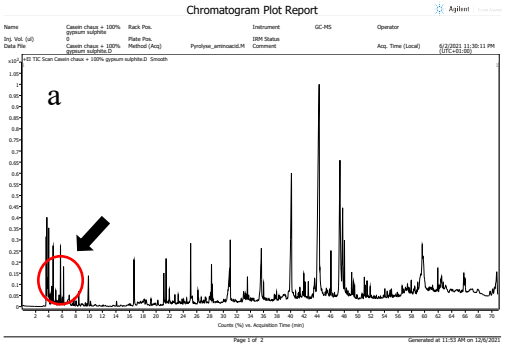

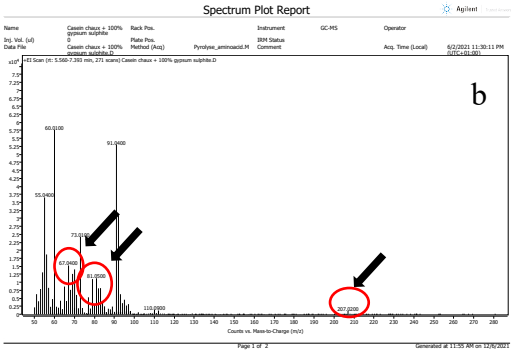

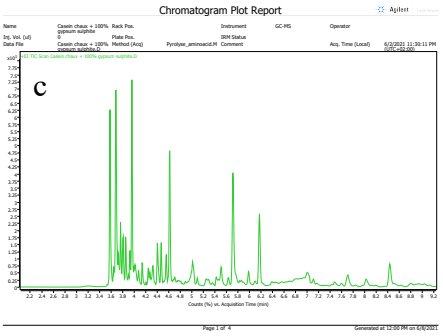

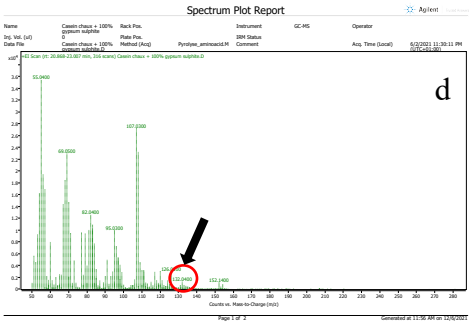

In paint model 4 we observe that it was possible to identify the peaks of 2-furanmethanol, pyrrole and 3-pyrroline in b, and the presence of maltol in d.

Table 4.6.5. Chromatogram and Mass spectrum of Casein quick lime + 100% $CaCO_3$

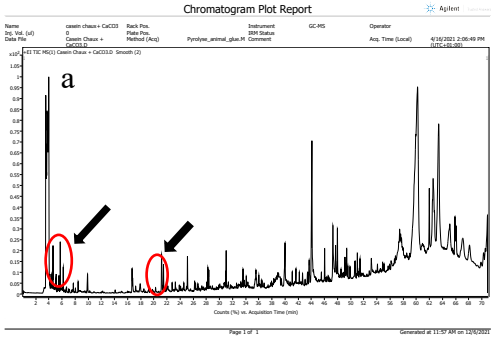

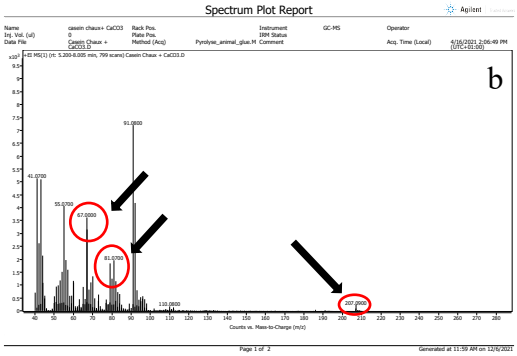

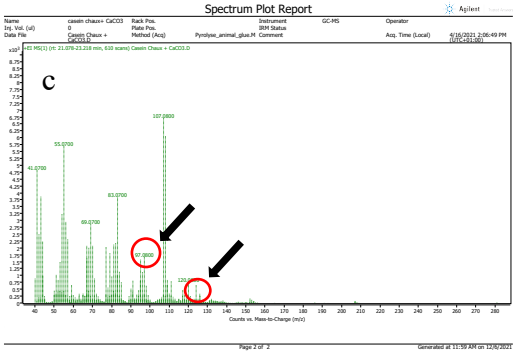

In paint model 5 it can be noted that the same peaks observed in paint model 4 was observed in b, whereas in c, maltol and 3-furanmethanol were identified for casein detection.

Table 4.6.6. Chromatogram and Mass spectrum of Casein quick lime+ 60% Y. Ochre

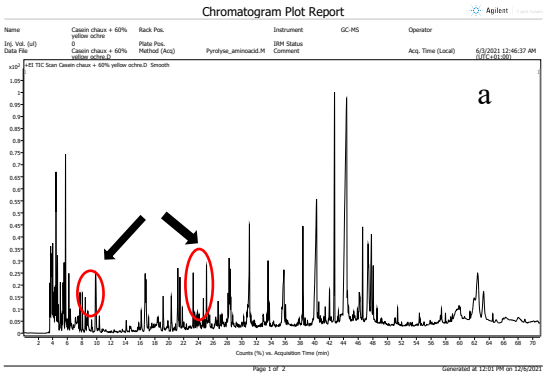

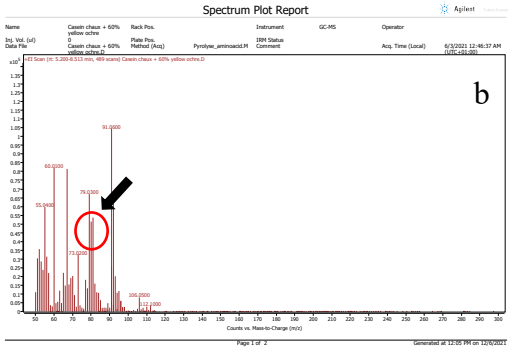

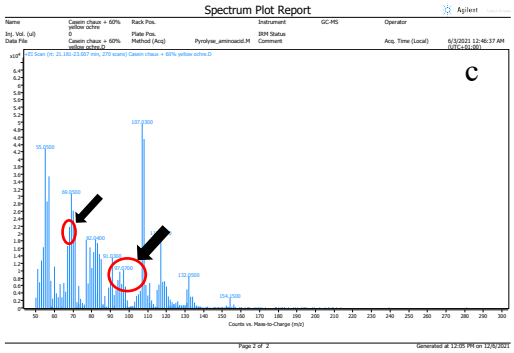

Paint model 6 of casein has a similar spectrum as with the yellow ochre paint model 3. They both show a peak of 2-furanmethanol in b and then pyrrole and 3-furanmethanol in c.

The standard markers for casein were identified in all paint models and this is a good indicator of the detection of casein with Pyrolysis GC-MS.

Therefore, with Pyrolysis, even though we have several standard markers to identify the presence of casein, it provides uniform results within developed paint models. Furthermore, the presence of a collagen binder present makes it a good technique to identify different proteins within the same sample.

To summarize, casein-based paint models were possible to characterize with the Pyrolysis GC-MS quite effectively.

4.9 Chromatogram and Mass spectrum for Egg yolk + Yellow ochre

There was just one paint model used for ovalbumin paint binders. The figure below demonstrates the chromatogram and the mass spectrum for this egg yolk-based paint model.

Table 4.7 Chromatogram and Mass spectrum for Egg yolk + Yellow ochre

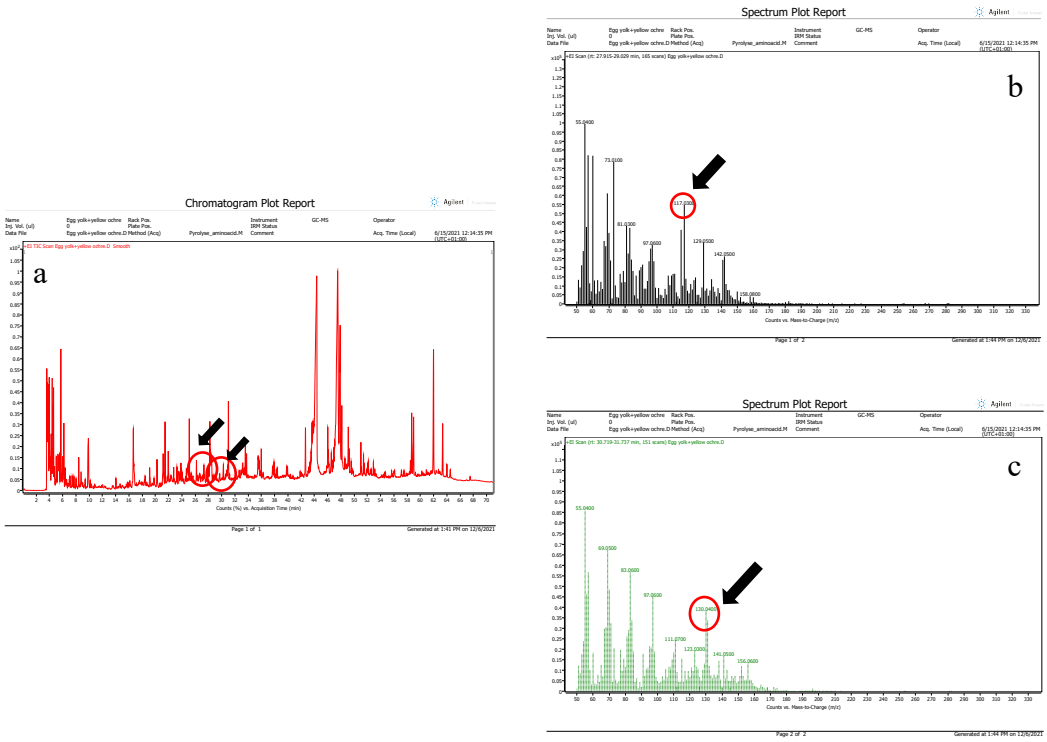

Finally, from the above chromatogram and mass spectra it was possible to observe the standard markers for Indole at m/z=117 in b and 3-methyl indole at m/z=130 in c which detect the presence of egg albumin. In conclusion, it was possible to identify the collagen, casein and ovalbumin protein binders that were developed with the help of the standard molecular markers presented in Table 4.2

4.10 Immunodetection of Realized Paint models

After the confirmation by Pyrolysis GC-MS of the presence of the different proteins in the specimens these were all identified by ELISA in the table 4.8 below with the procedure previously optimized, showing once again the validity of the immuno-design methodology and its use applied to painting, as a more accessible method, without the need for such expensive equipment.

Table 4.8: Immunodetection activity with and without Nanoparticles

S. No.	Sample	Without Nano particles (Uml^{-1})	With Nanoparticles (Uml^{-1})
1	**Bone glue with 100% $CaCO_3$,**	15.85 ± 0.354	18.09 ± 0.698
2	**Bone glue with 25% $CaCO_3$**	3.97 ± 0.945	5.88 ± 0.395
3	**Rabbit glue with 100% $CaCO_3$**	17.54 ± 1.083	21.54 ± 0.756
4	**Rabbit glue with 25% $CaCO_3$**	6.86 ± 2.245	8.14± 0.978
5	**Linseed Oil+10% Rabbit glue+ yellow ochre+ $CaCO_3$**	7.68± 0.427	10.89± 2.986
6	**Canvas+ yellow ochre + rabbit glue + bone glue**	14.69± 0.226	15.83± 0.431
7	**Casein ammonia+ 100% gypsum sulphite**	9.01 ± 2.399	11.3 ± 0.898
8	**Casein ammonia+ 100% $CaCO_3$**	7.49 ± 0.152	17.12 ± 0.334
9	**Casein Ammonia + 60% Yellow Ochre**	6.71 ± 0.742	13.82 ± 0.938
10	**Casein quick lime+ 100% Gypsum Sulphite**	3.45 ± 0.361	3.59 ± 0.943
11	**Casein quick lime + 100% $CaCO_3$**	1.54 ± 0.103	2.06 ± 0.165
12	**Casein quick lime+ 60% Y. Ochre**	1.04 ± 0.268	1.21 ± 0.094
13	**Egg yolk + Yellow ochre**	19.73 ± 1.843	23.33 ± 3.387

Chapter 5

Case studies

This chapter illustrates several case studies for the identification of proteinaceous binders from various sampled artefacts from the Perpignan Museum in Perpignan, France. The detection of the proteinaceous binders were characterized by Pyrolysis GC-MS and ELISA immunoassays evidencing the possibility of Immunodetection of Paint Binders as an efficient and easy methodology .

Four different artefacts were selected for this study

Table 5.1.

Table 5.1 Case Studies of the artefacts used for the identification of proteinaceous binders

Case No.	Description
1	Villeneuve Altarpiece of St. Julian & St. Baselisse
2	Rivesaltes Altarpiece of Christ, 1710
3	Conseil Departmental, Altarpiece of the Annunciation, 1714
4	Statue of the Virgin of Hope

A further overview of the microsamples used for analysis has been shown in Figure 5.1

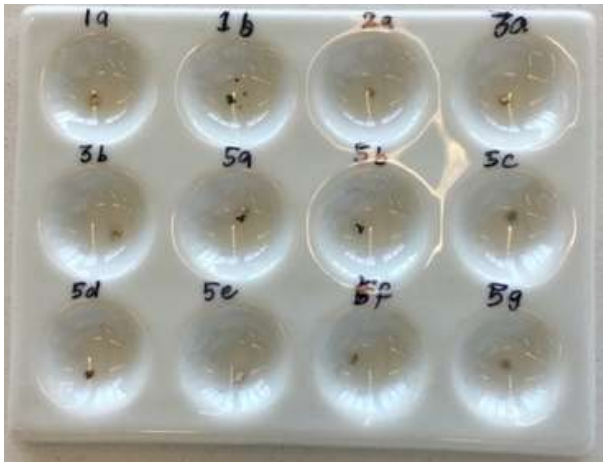

Figure 5.1 Overview of microsamples used for analysis in a pallet.

5.1 Villeneuve Altarpiece of St. Julian & St. Baselisse

This work was executed around 1690 at the School of Jean-Jacques Mélair, sculptor from Carcassonne (CCRP attribution).

Bruno Tollon attributes the altarpiece to the sculptor Louis Ribera. According to him, this altarpiece is made in the same way as that of Saint Eulalie d'Alénya and that of Saint Gaudérique de Baixas. However, he adds that "the figures retain here [in Villeneuve], with their oval faces and their chins too strong, the somewhat heavy style of the statues of Notre-Dame de la Pave and the Rosaire de la Réal" which are attributed to him.

The entire original base with altar table and side doors has been replaced by a masonry base. A late 19th - early 20th century altar, in white marble, which stood in front of the altarpiece has been removed and placed in a side chapel.

This altarpiece has a base, two main registers and a pediment with 3 bays and four twisted columns in the 1st register. This has a beautiful decoration carved with fruits, flowers, and foliage.

It consists of seven statues: 1st register in the center, in a double niche, Saint Julien and Baselisse, on each side, Saint Peter and Saint Paul, 2nd register, Saint Teresa of Avila in the center and two plaster statues (unprotected) on each side. A high relief of God the Father serves as a crown. Also, two busts with the predella of the 2nd register and heads of cherubs as consoles.

Technical description

Support: the altarpiece is 82cm from the wall on the left and 28cm on the right. It rests on a masonry bench at the back, 160 cm high. It is fixed to the wall by numerous wooden beams. It is essentially made of softwood, with mortise and tenon joints and wrought iron nails.

Polychromy: the polychromy has been entirely resumed in matt green for the structure and the gilding is also taken over by a second gilding. The sgraffiti of the costumes of the statues, undoubtedly original, are covered with varnish. The skin tones are repainted and the gilding re-gilded.

Note: the statues of Saint Peter, the nun, and God the Father appear to be of a different style. The plaster statues are later (the niches around are also modified).

Two samples were taken from the altarpiece, one from the golden decorations incorporated within the altarpiece, and the other from the green structure composing the altarpiece (Fig. 5.2)

Figure 5.2 Villeneuve Altarpiece of St. Julian & St. Baselisse

Table 5.2 Villeneuve Altarpiece samples used for analysis

Sample Nº	Name of Place, Time	Area of Sampling
1a	**Villeneuve**	Altarpiece of Christ
1b	**Villeneuve**	Altarpiece of Christ

5.1.1 Villeneuve- Sample 1a

The sample **1a** was extracted from the golden decorations from the Altarpiece St. Julian & St. Baselisse. Below in Table 5.3 the characterization of this sample has been shown.

Table 5.3 Characterization of sample 1a with a-Stratigraphy, b-Chromatogram, d e, f, - Mass spectra

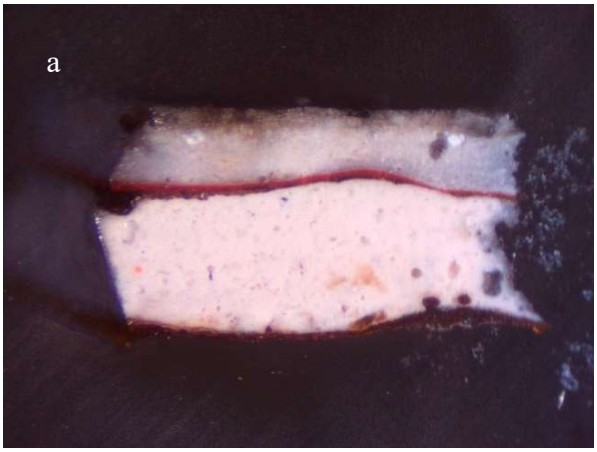

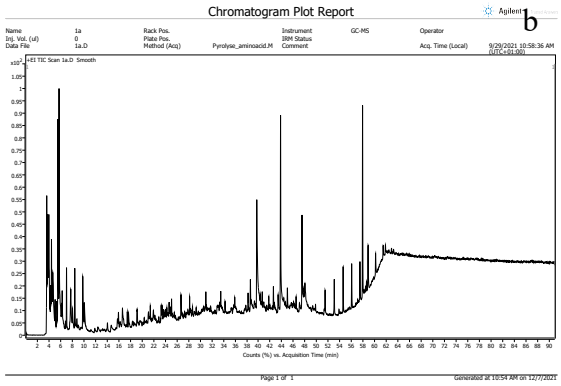

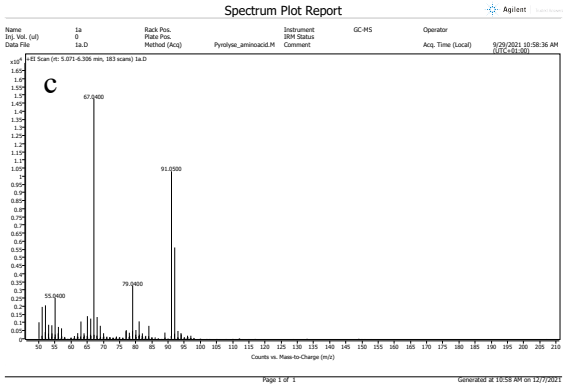

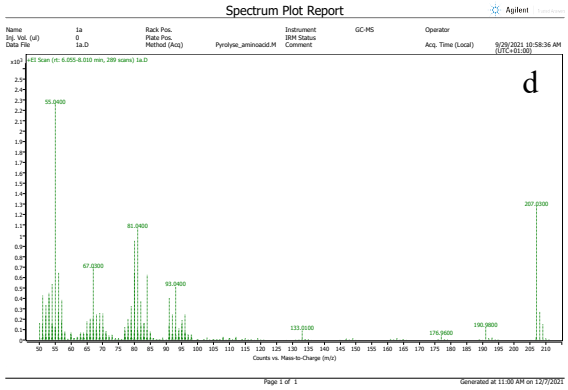

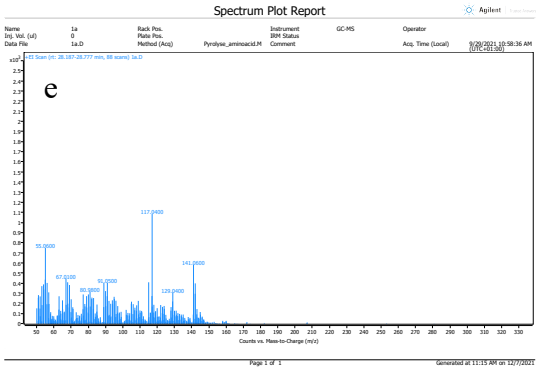

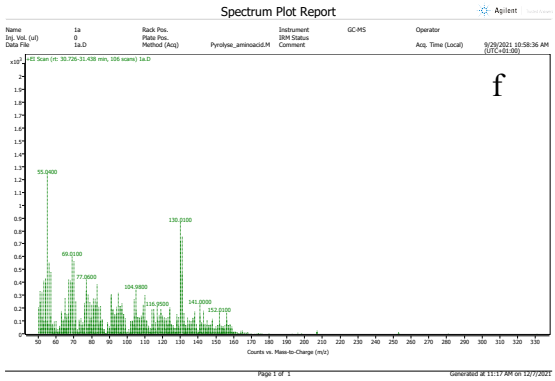

5.1.2 Villeneuve- Sample 1b

Sample **1b** was extracted from the altarpiece where there was a coating of green. The characterization of sample **1b** has been shown below in Table 5.4.

Table 5.4 Characterization of sample 1b with a-Stratigraphy, b-Chromatogram, c, d, e, f, g- Mass spectra


a

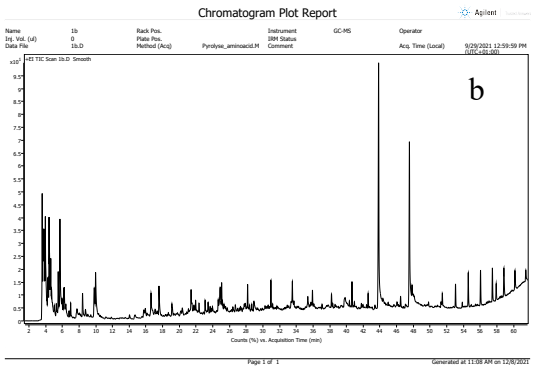
Chromatogram Plot Report
b

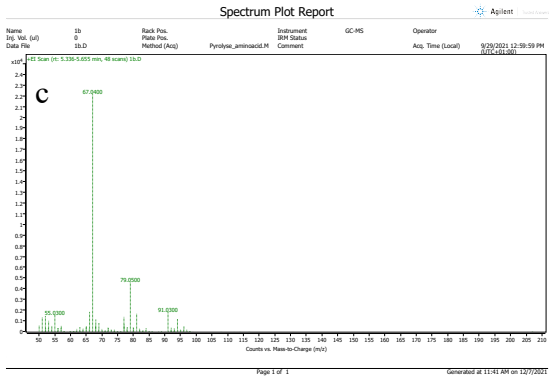
Spectrum Plot Report
c
67.0400
79.0500
55.0300
91.0300

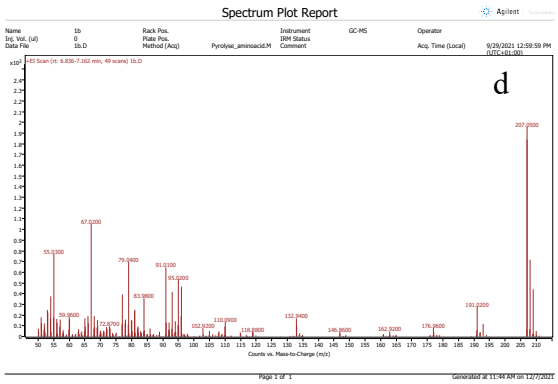
Spectrum Plot Report
d
207.0500
67.0200
55.0300
79.0400
91.0100
95.0200
83.9800
132.0400
191.0200

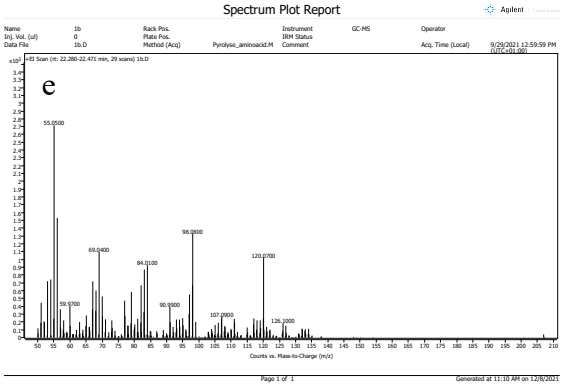
Spectrum Plot Report
e
55.0500
69.0400
84.0100
98.0800
120.0700
59.9700
90.0900
107.0900
136.1000

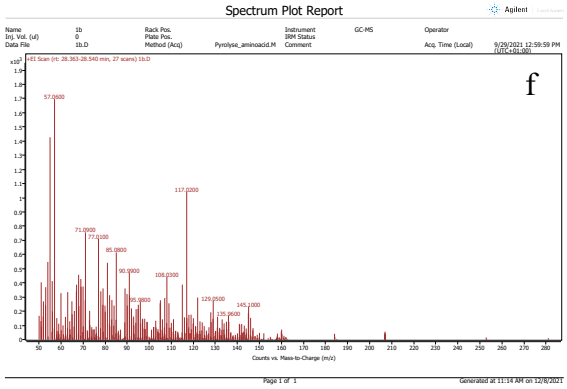
Spectrum Plot Report
f
57.0600
117.0200
71.0900
77.0100
85.0800
90.9900
108.0300
129.0500
145.1000

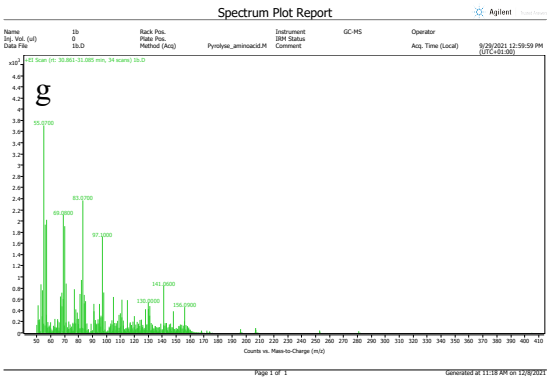
Spectrum Plot Report
g
55.0700
83.0700
69.0800
97.1000
141.0600
130.0000
156.0900

5.2 Rivesaltes Altarpiece of Christ, 1710

The 1707 altarpiece of traditional composition in the brotherhood of the Sanch is of exceptional quality, executed by Miquel Anglade, sculptor; the acanthus metamorphoses into female heads, the angels multiply: the concern for figuration takes precedence over architectural concern, a great fantasy.

The register of the brotherhood of the Sanch of the church mentions the payment of sculpture work to Anglada, which received in 1706, 110 livres, then in 1707, 211 livres and 13 sols, and in 1708, 266 livres 7 sols, in the total 587 pounds and 20 sols. This same register records payments for gilding work in the chapel and altarpiece of the Sanch between 1709 and 1722 to Joan Escribà, Félix Escribà and Joan Casadevall.

In 1709, the brotherhood remunerated "Joan Escribà per compta del rataula", to the tune of 257 pounds, last 18 and 11 cents. Despite the death of Joan Escribà on September 20, 1710, work continued since his widow received four payments between 1711 and 1713. These payments testify to the maintenance of Joan Escribà's workshop, a workshop run by his widow and where his nephew , Félix Escribà, heir to his uncle's profession, continues the gilding of the Sanch altarpiece. In 1715, Félix Escribà, who had become a master gilder, intervened in his own name in Rivesaltes since the brotherhood paid him the sum of 200 pounds, supplemented in 1716 by 11 pounds.

The details of the work are not specified, but they may correspond to the gilding of the frames of the four paintings of the Passion, painted by Antoni Guerra menor, whose brotherhood wanted in 1710 to entrust the gilding to Joan Escribà. As the ornamental work on the chapel of La Sanch continued, Félix Escribà received other payments in 1719, 1720 and 1721, for a total sum of 471 pounds 13 sous and 10 deniers. The extension of the work over several years probably explains the dustiness of the altarpiece and the need for dusting ("espolsar") in 1721 before resuming any gilding work. After 1721, Félix Escribà disappeared from the account book of the brotherhood of Sanch, and it was Joan Casadavall who received a final payment in 1722: "Tenim donat al Senyor Casadebal adorador per lo rest del deuta de dorar las garnisas y pintar la capella tot comptat ly anem donat the sum of zixanta y seven francs treza under y onsa diners ". Julien Lugand specifies that the gilder Joan Casadevall was paid in 1720 for the gilding of the crown of the altarpiece. The floor of the church was redone in 1990.

The altarpiece consists of a central niche with a flat bottom housing a sculpted Calvary group: a large crucifix between the Virgin and Saint John. It rests on 4 steps (removable central part) and is surmounted by a canopy; the uprights which accost the niche and the canopy are two-thirds interrupted by an entablature. On each side are placed 2 full-length angels holding the emblems of the Passion. The decor is very rich with many leaves, cherubs holding the instruments of the Passion and allegorical figures. At the coronation emerges a half-length God the Father sketching the sign of blessing. The altar table is framed by 2 small columns and decorated with a central medallion with "IHS". Support: altar in white limestone; plaster baseboards; central stone and brick base; no access to the back of the altarpiece except by the removable steps; fixing to the wall by joists and metal brackets.

Polychromy: generalized repainting probably from the 19th century: grainy skin tones in oil, flat black (sensitive to alcohol) and blue, aqueous gilding (orange plate and intermediate preparation) and with a mixture (or bronzine?), Silver plating, eraser lacquer (?), metallic stars. Original with aqueous gilding (dark red plate), patterns engraved in the preparation, sgraffitos, colored lacquers on gold, smooth and clear skin tones in oil.

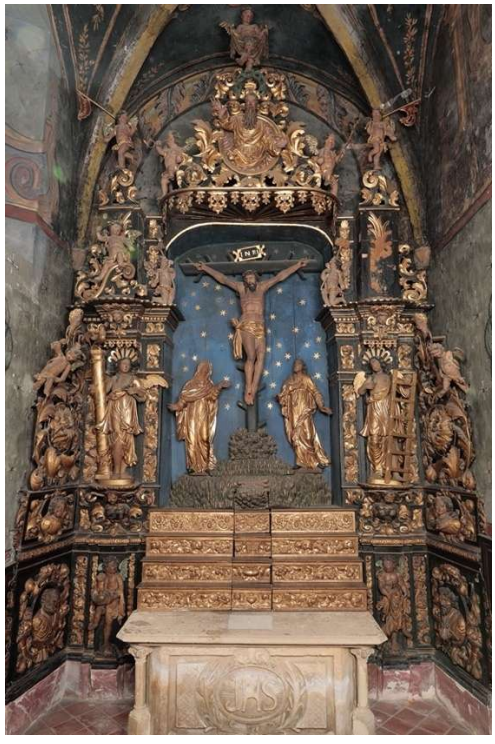

Figure 5.3 Rivesaltes , Altarpiece of Christ, 1710

Table 5.5 Rivesaltes samples used for analysis

Sample Nº	Name of Place, Time	Area of Sampling
2a	Rivesaltes, 1710	Altarpiece of Christ
2c	Rivesaltes, 1710	Altarpiece of Christ

5.2.1 Rivesaltes- Sample 2a

The Sample **2a** was extracted from the Rivesaltes altarpiece and the characterization was carried out as given below in Table 5.6.

Table 5.6 Characterization of sample 2a with a-Stratigraphy, b- Chromatogram, c &d-Mass spectra

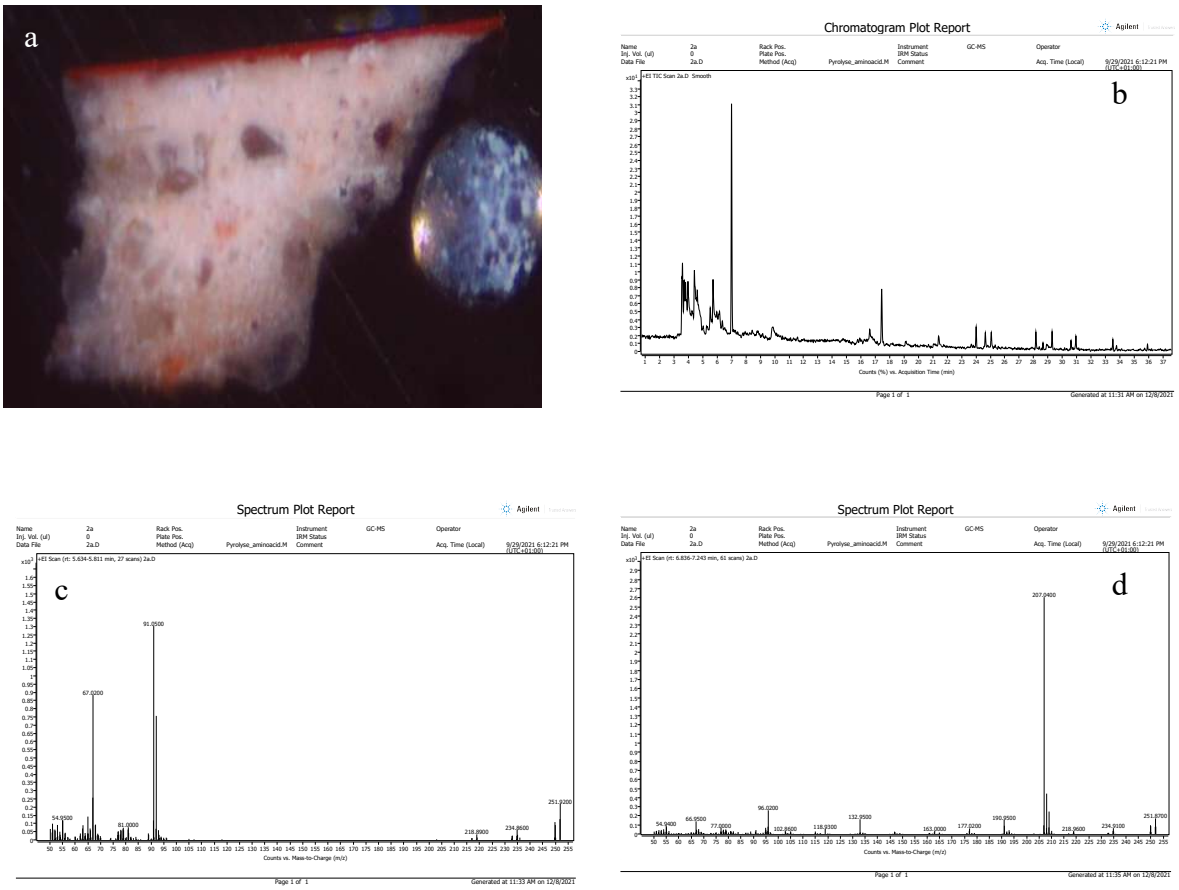

5.2.2 Rivesaltes- Sample 2c

The Sample **2c** was also extracted from the Rivesaltes altarpiece and the characterization was carried out as given below in Table 5.7.

Table 5.7 Characterization of sample 2c with a-Stratigraphy, b- Chromatogram, c, d ,e & f- Mass spectra

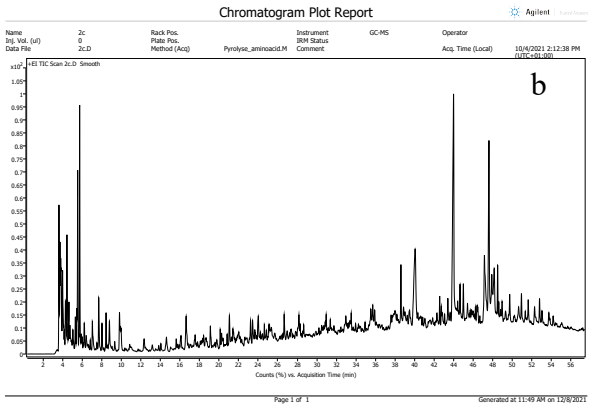

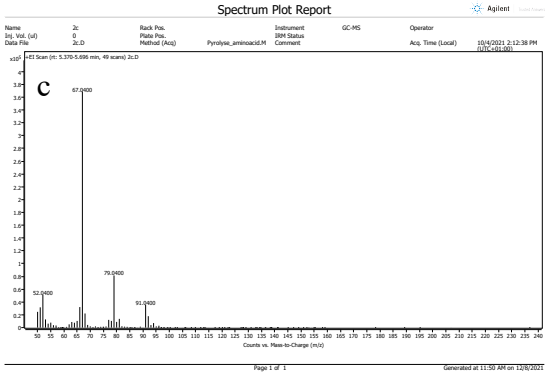

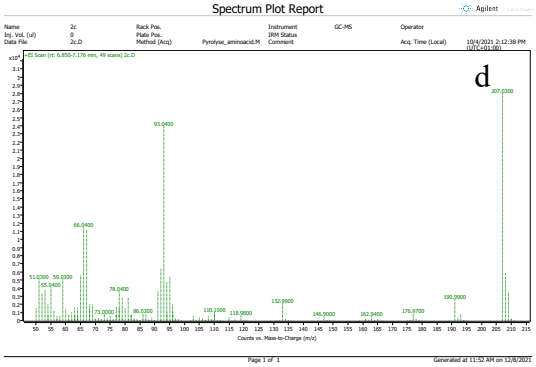

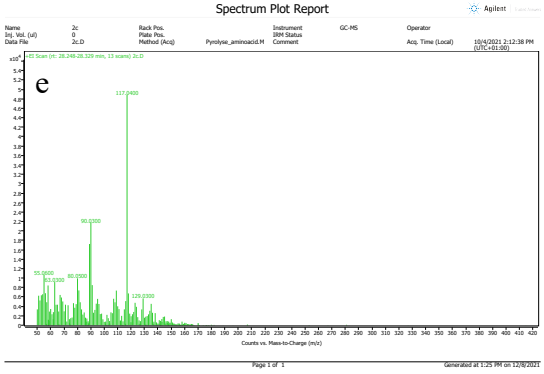

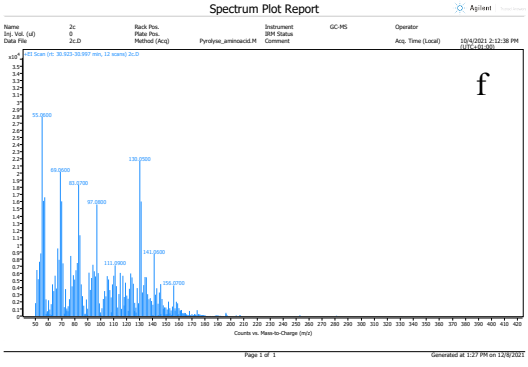

5.3 Conseil Departmental, Altarpiece of the Annunciation, 1714

The altarpiece of the Annunciation, until 1940, adorned the high altar of the private chapel of Mas Girvès de Llo, in Cerdanya. This farmhouse, formerly farmhouse Oliba, entered the heritage of Salvador Girvès in 1667, a farmer (agricola) in Err where he lives. He then initiated reconstruction and expansion work on the farmhouse, which was continued by his descendants. His son, Gabriel Girvès, settled there in 1680, and it is certainly to him that we owe the construction of the chapel between the end of the 17th century and the beginning of the 18th century. Several elements point in this direction. On the one hand, the gate of the farmhouse, placed in line with the door of the chapel, was completed in 1710. On the other hand, in the will of the son of Gabriel Girvès, Sauveur Girvès, drawn up on July 8, 1732, he asks that his heir and his family "be held and obliged to keep the chapel erected and built joining his house with all decency and to maintain it with all the ornaments necessary for the celebration of the Holy Sacrifice of the Mass so that the legate made by my late father [Gabriel Girvès] in the same way continues to be observed perpetually ". Finally, it is important to note that the owner of the chapel of the farmhouse is none other than the Archangel Saint Gabriel, or his own patron saint... unless it is a question of honoring the memory. of his grandfather, also named Gabriel. Whoever the initiator, the erection of this chapel and the importance of the farmhouse testify to the power of this family, which established its power in Cerdanya from the second half of the 17th century and for nearly two and a half centuries.

Once the chapel was built, Gabriel Girvès and his wife, Teresa Rocafort, commission an altarpiece to adorn the choir. To recall their names, the sculptor places, above the central panel, a sculpted medallion surmounted a crown, featuring the initials of the sponsors and their respective arms. This shield, which is said to be quartered because of its division into four equal sections, can be described as follows: 1st, gold, the letter T of azure [for Teresa]; 2nd, azure, three stars of gold [for Rocafort]; 3rd, Gules, the letter G d´or [for Gabriel]; 4th, gold, to a tree with sinople leaves [for Girvès]. These same weapons were carved on the facade of the farmhouse.

Neither the contract for the sculpture of the altarpiece, nor that for the gilding and polychromy have been found in the archives. They were probably taken between 1700 and 1714 at Rafael Beringo, a notary of Saillagouse, whose deeds have unfortunately not reached us. However, despite the lack of documentation, art historians stylistically attribute the sculpture of the altarpiece to Josep Sunyer, installed in Prades, and the gilding of the work to Félix Escribà.

The choice of Josep Sunyer is not due to chance. Above all else, he is certainly the best sculptor of the moment: it is quite likely that a wealthy family will be willing to bring in the most popular sculptor of his time to magnify the ornamentation of his private chapel. In addition, at the beginning of the 18th century, Josep Sunyer regularly intervenes in Cerdanya, where he is responsible for numerous companies in Llívia (1700-1704), Font-Romeu (1704-1707), Osséja (1709), Puigcerdà (1711 -1712), Ur, Clerà, Latour-de-Carol. Also, it is probably during this same time interval that the Annunciation altarpiece is produced.

Figure 5.4 Conseil Departmental Altarpiece of the Annunciation

Altarpiece with two registers and three bays with an altar table. Altarpiece comprising a main register, with two side niches, housing two statues of Saint Anthony of Padua on the left, Saint Isidore on the right, and in the centre a bas relief representing the Annunciation. The different bays are separated by twisted columns decorated with vine branches and birds, decorated with cherubs' heads, bay leaves, oak, acanthus leaves. The entablature has in the centre a crowned coat of arms surmounted in the upper register by a statue of Saint Teresa in a niche. The upper part is decorated with fine garlands of flowers (poppy, sunflowers, roses), fruits.

The steps are decorated with heads of cherubs as well as the tops of columns. The altar front in the form of a rectangular frame is composed of a moulded border carved with laurel leaves (which appears to have been modified). Plant interlacing of flowers and open and closed sunflowers, half-heads of cherubs spitting foliage, adorn the background; the oxidation of the original silver leaf is reminiscent of leather. In the centre, a medallion takes up the theme of

the Immaculate Conception on clouds. All the backgrounds are saturated with guilloche patterns and punches.

Altarpiece in softwood, and statues in hardwood on the back not hollowed out. The assembly is done using tenons and mortises. Accessibility to the back is possible. The polychromy is original. The funds are engraved in the preparation, with guilloche motifs, and at the level of the floral interlacing niches, floral arrangements in vases. The gilding is polished and matte tempera; small decorative elements (pearls) are highlighted by a technique of "lacquer" on gold of red or green color. Graffiti adorns the clothes, the plumage of the birds, the bottom of the bas-relief of the Annunciation. The quality of the polychromy and the style are reminiscent of Escriba's work. The silver leaf is very oxidized at the front of the altar. The altarpiece has been reassembled.

Table 5.8 Conseil Departmental samples used for analysis

Sample Nº	Name of Place, Time	Area of Sampling
3a	**Conseil Departmental, 1714**	**Altarpiece of the Annunciation**
3b	**Conseil Departmental, 1714**	**Altarpiece of the Annunciation**

5.3.1 Conseil Departmental- Sample 3a

The Sample **3a** was also extracted from the altarpiece of the Annunciation of Conseil Departmental and the characterization was carried out as given below in Table 5.9.

Table 5.9 Characterization of sample 3a with a-Stratigraphy, b- Chromatogram, c, d, e, & f- Mass spectra

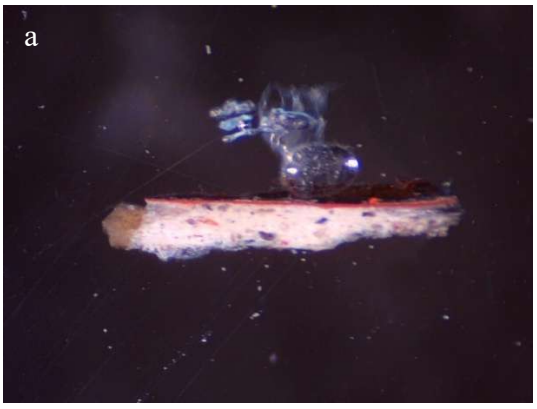

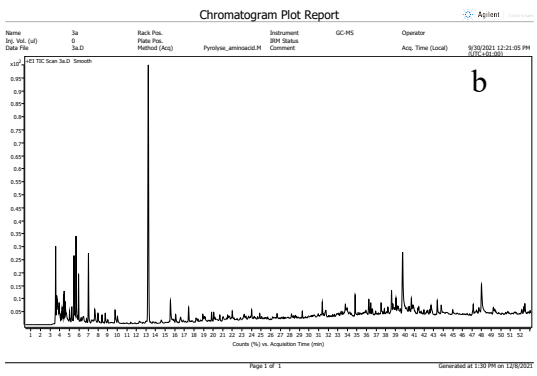

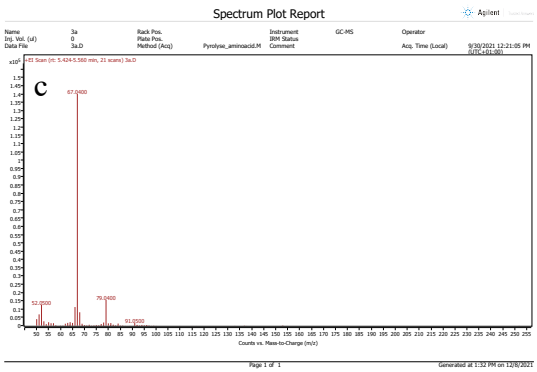

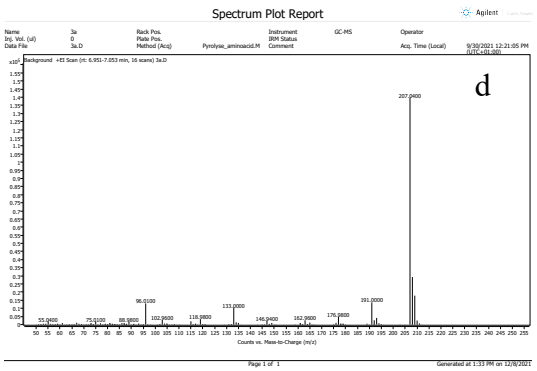

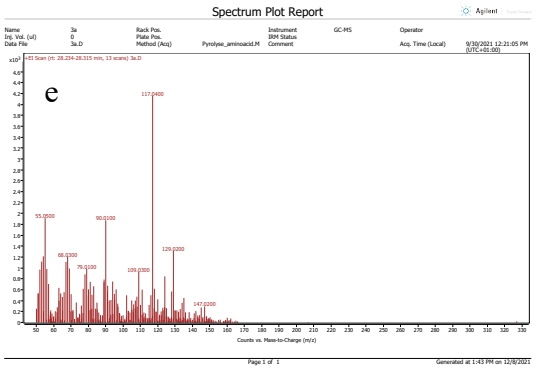

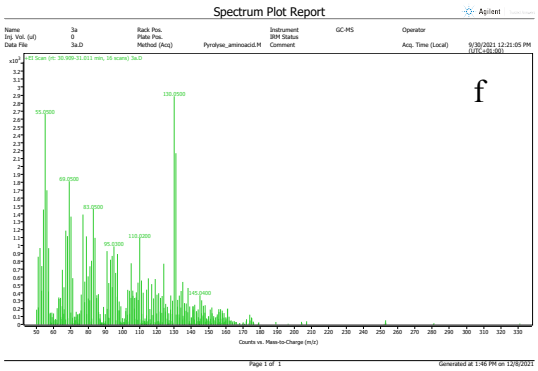

5.3.2 Conseil Departmental- Sample 3b

The Sample **3b** was also extracted from the altarpiece of the Annunciation of Conseil Departmental and the characterization was carried out as given below in Table 5.10.

Table 5.10 Characterization of sample 3b with a-Stratigraphy, b- Chromatogram, c, d, e, f, g & h- Mass spectra

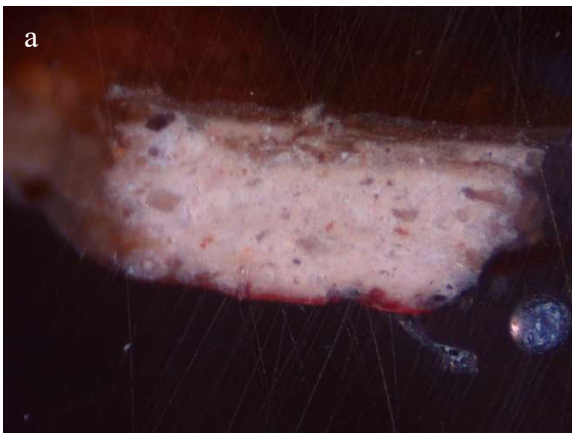

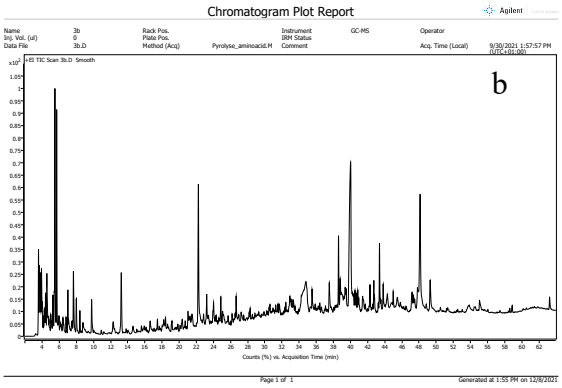

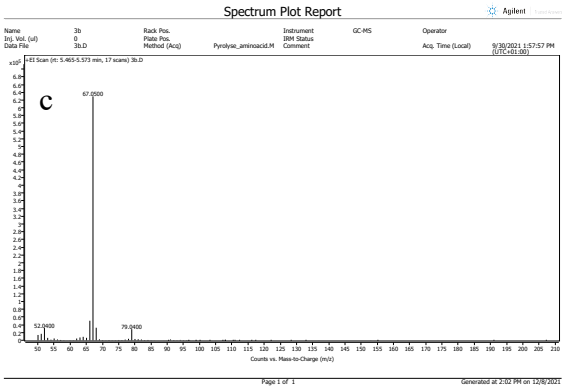
Spectrum Plot Report
Agilent
Name 3b
Inj. Vol. (ul) 0
Data File 3b.D
Rack Pos.
Plate Pos.
Method (Acq)
Pyrolyse_aminoacid.M
Instrument
IRM Status
Comment
GC-MS
Operator
Acq. Time (Local)
9/30/2021 1:57:57 PM (UTC+01:00)
+EI Scan (rt: 5.465-5.573 min, 17 scans) 3b.D
c
67.0500
52.0400
79.0400
Counts vs. Mass-to-Charge (m/z)
Page 1 of 1
Generated at 2:02 PM on 12/8/2021

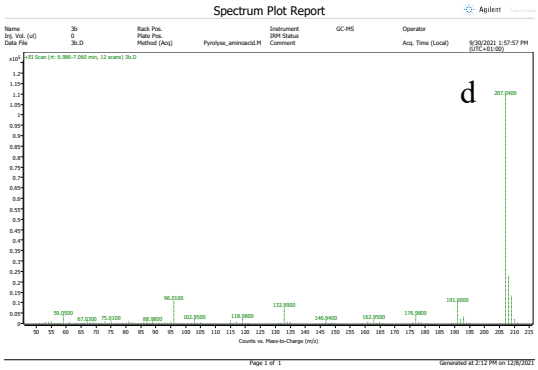
Spectrum Plot Report
Agilent
Name 3b
Inj. Vol. (ul) 0
Data File 3b.D
Rack Pos.
Plate Pos.
Method (Acq)
Pyrolyse_aminoacid.M
Instrument
IRM Status
Comment
GC-MS
Operator
Acq. Time (Local)
9/30/2021 1:57:57 PM (UTC+01:00)
+EI Scan (rt: 6.986-7.060 min, 12 scans) 3b.D
d
207.0400
96.0100
59.0500
67.0300
75.0300
88.9800
102.9500
118.9800
132.9900
146.9400
162.9500
176.9800
191.0000
Counts vs. Mass-to-Charge (m/z)
Page 1 of 1
Generated at 2:12 PM on 12/8/2021

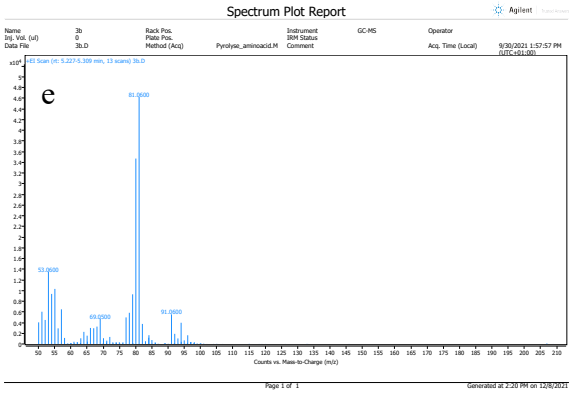
Spectrum Plot Report
Agilent
Name 3b
Inj. Vol. (ul) 0
Data File 3b.D
Rack Pos.
Plate Pos.
Method (Acq)
Pyrolyse_aminoacid.M
Instrument
IRM Status
Comment
GC-MS
Operator
Acq. Time (Local)
9/30/2021 1:57:57 PM (UTC+01:00)
+EI Scan (rt: 5.227-5.309 min, 13 scans) 3b.D
e
81.0500
53.0500
69.0500
91.0600
Counts vs. Mass-to-Charge (m/z)
Page 1 of 1
Generated at 2:20 PM on 12/8/2021

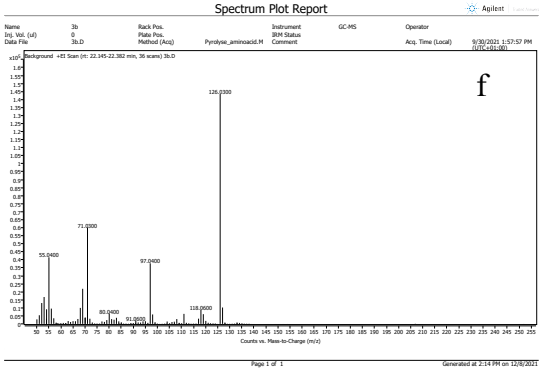
Spectrum Plot Report
Agilent
Name 3b
Inj. Vol. (ul) 0
Data File 3b.D
Rack Pos.
Plate Pos.
Method (Acq)
Pyrolyse_aminoacid.M
Instrument
IRM Status
Comment
GC-MS
Operator
Acq. Time (Local)
9/30/2021 1:57:57 PM (UTC+01:00)
Background +EI Scan (rt: 22.145-22.382 min, 36 scans) 3b.D
f
126.0300
71.0300
55.0400
97.0400
80.0400
91.0600
118.0600
Counts vs. Mass-to-Charge (m/z)
Page 1 of 1
Generated at 2:14 PM on 12/8/2021

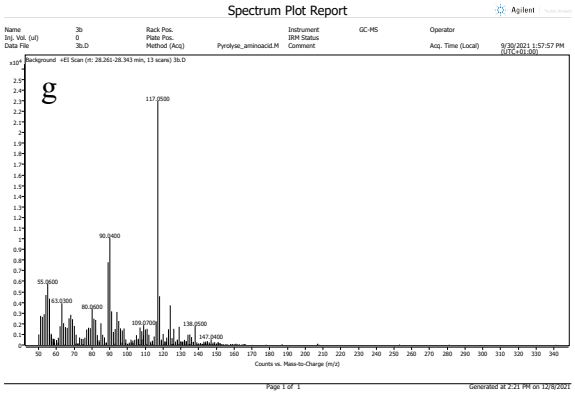
Spectrum Plot Report
Agilent
Name 3b
Inj. Vol. (ul) 0
Data File 3b.D
Rack Pos.
Plate Pos.
Method (Acq)
Pyrolyse_aminoacid.M
Instrument
IRM Status
Comment
GC-MS
Operator
Acq. Time (Local)
9/30/2021 1:57:57 PM (UTC+01:00)
Background +EI Scan (rt: 28.261-28.343 min, 13 scans) 3b.D
g
117.0500
90.0400
55.0600
63.0300
80.0600
105.0700
138.0500
147.0400
Counts vs. Mass-to-Charge (m/z)
Page 1 of 1
Generated at 2:21 PM on 12/8/2021

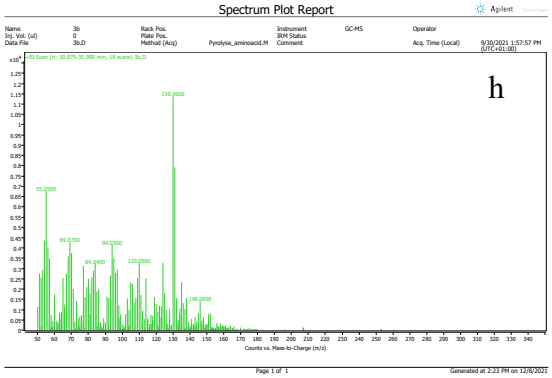
Spectrum Plot Report
Agilent
Name 3b
Inj. Vol. (ul) 0
Data File 3b.D
Rack Pos.
Plate Pos.
Method (Acq)
Pyrolyse_aminoacid.M
Instrument
IRM Status
Comment
GC-MS
Operator
Acq. Time (Local)
9/30/2021 1:57:57 PM (UTC+01:00)
+EI Scan (rt: 30.875-30.990 min, 18 scans) 3b.D
h
130.0600
55.0500
69.0700
94.0300
84.0400
110.0500
146.0600
Counts vs. Mass-to-Charge (m/z)
Page 1 of 1
Generated at 2:23 PM on 12/8/2021

5.4 Case Study of the Statue of the Virgin of Hope

This statue is one of the latest polychrome wood productions, while standard polychrome plaster and terracotta products already exist.

Figure 5.5 Statue of Virgin of Hope with Baby Christ in the Left Hand

The Virgin is standing, holding the Child on her left arm, and a sea anchor in her right hand (the latter has been added). She is dressed in a long dress, and draped in a coat with abundant pleats. The Child is concealed by a long tunic. He blesses with his right hand, and carries a cruciferous orb with his left hand. The Virgin is veiled and crowned; a crown in golden metallic leaves has been added around the wooden crown. It is placed on a very high wall console.

The support is carved from a trunk hollowed out on the back and closed by a shutter; assemblies on the sides and for the hands; anchor attached and attached by hand by a string (open hook not used at the top of the anchor); piton closed in the back allowing the statue to be fixed. This is a polychromic original with satin colours, gilding with the mixture or golden paint, lapel simply covered with preparation, anchor with polished aqueous gilding.

Table 5.11 Virgin Marry Statue samples used for analysis

Sample Nº	Name of Place, Time	Area of Sampling
5a	Molitg les Bains, 19th century	Red dress (Purple)
5b	Molitg les Bains, 19th century	Blue coat (blue & gold)

5c	Molitg les Bains, 19th century	Base of the sculpture (grey)
5d	Molitg les Bains, 19th century	Hair of Baby Christ (Brownish white)
5e	Molitg les Bains, 19th century	Clothes of baby Christ (purple with gold)
5f	Molitg les Bains, 19th century	Crown of Virgin Mary (gold)
5g	Molitg les Bains, 19th century	Beige Coat Inside(Beige with gold)

5.4.1 Molitg les Bains - Sample 5a

The Sample **5a** was also extracted from Red dress of **Statue of Virgin of Hope** of the Molitg les Bains and the characterization was carried out as given below in Table 5.12.

Table 5.12 Characterization of sample 5a with a-Stratigraphy, b-Chromatogram, c, d, e- Mass spectra

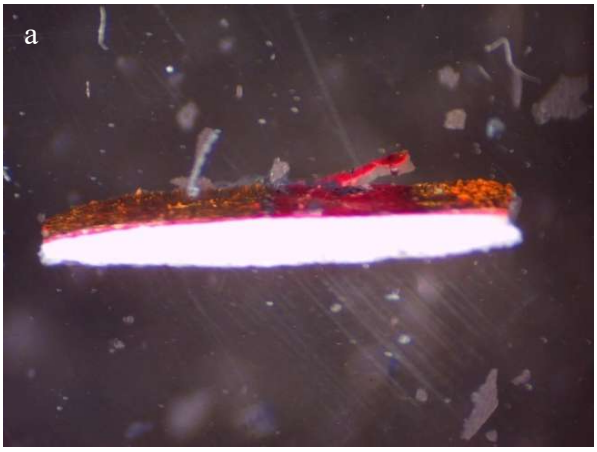

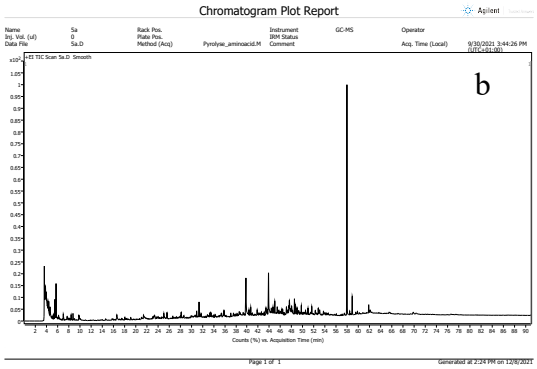

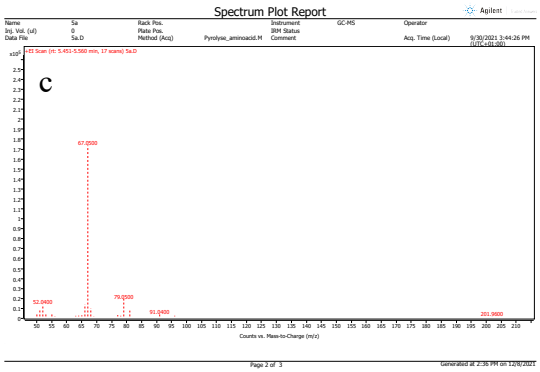

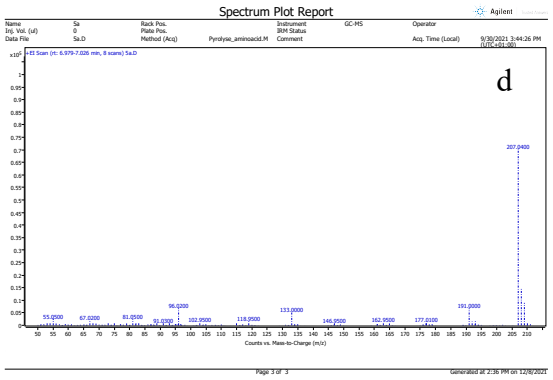

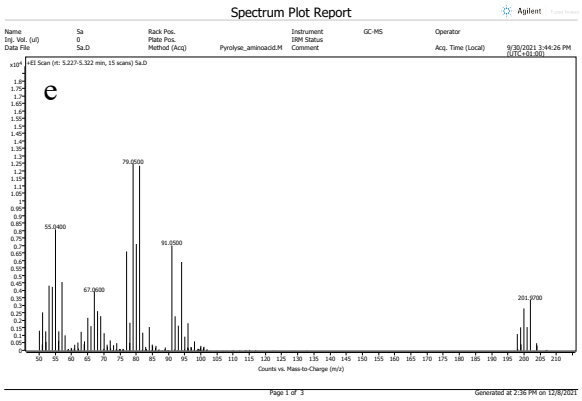

5.4.2 Molitg les Bains - Sample 5b

The Sample **5b** was also extracted from Blue coat of **Statue of Virgin of Hope** of the Molitg les Bains and the characterization was carried out as given below in Table 5.13.

Table 5.13 Characterization of sample 5b with a-Stratigraphy, b-Chromatogram, c, d, e- Mass spectra

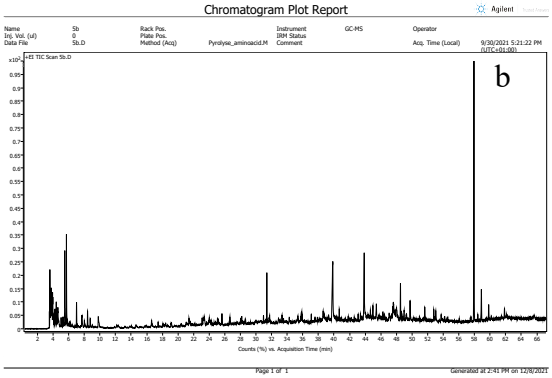

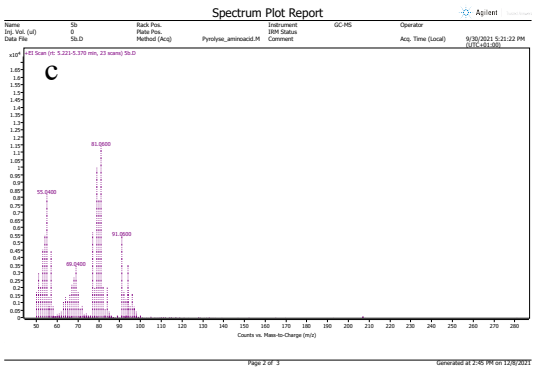

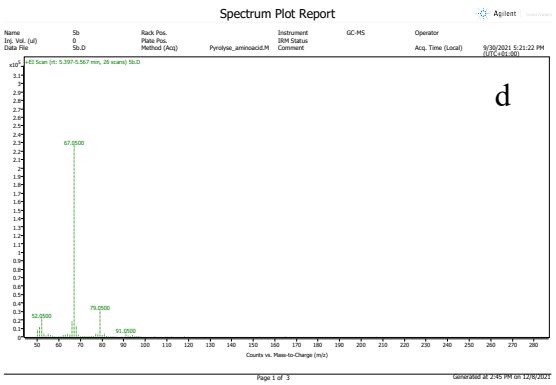

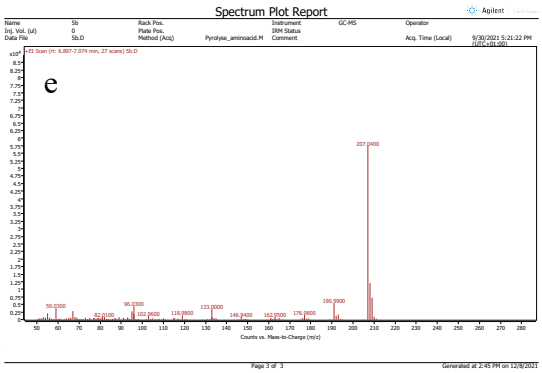

5.4.3 Molitg les Bains - Sample 5c

The Sample **5c** was also extracted from Base of the sculpture of **Statue of Virgin of Hope** of the Molitg les Bains and the characterization was carried out as given below in Table 5.14.

Table 5.14 Characterization of sample 5c with a-Stratigraphy, b-Chromatogram, c & d-Mass spectra

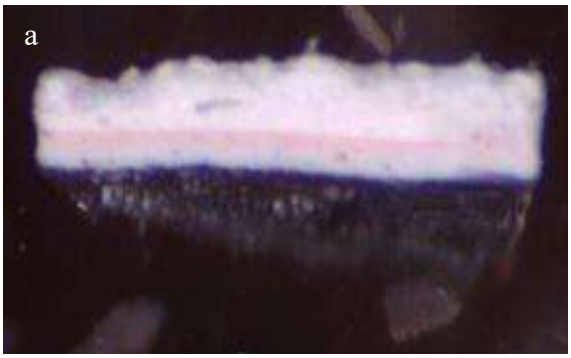

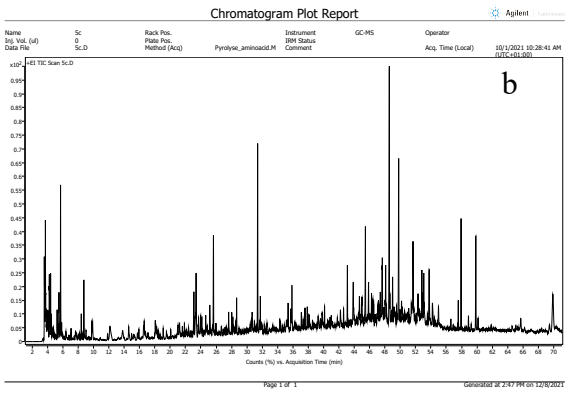

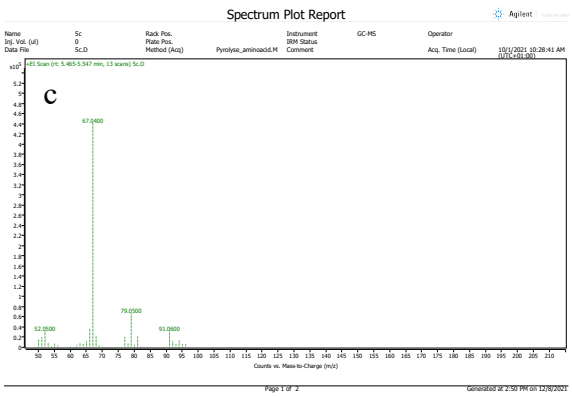

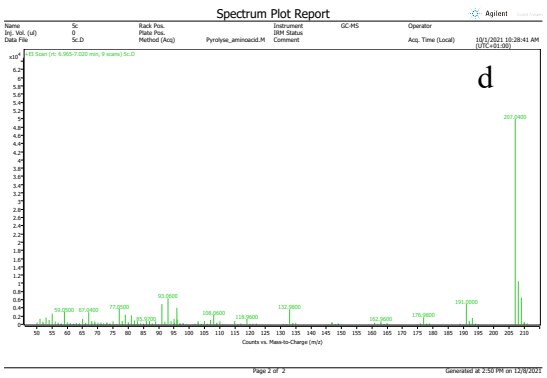

5.4.4 Molitg les Bains - Sample 5d

The Sample **5d** was also extracted from Hair of Baby Christ of **Statue of Virgin of Hope** of the Molitg les Bains and the characterization was carried out as given below in Table 5.15.

Table 5.15 Characterization of sample 5d with a-Stratigraphy, b- Chromatogram, c, d, e & f-Mass spectra

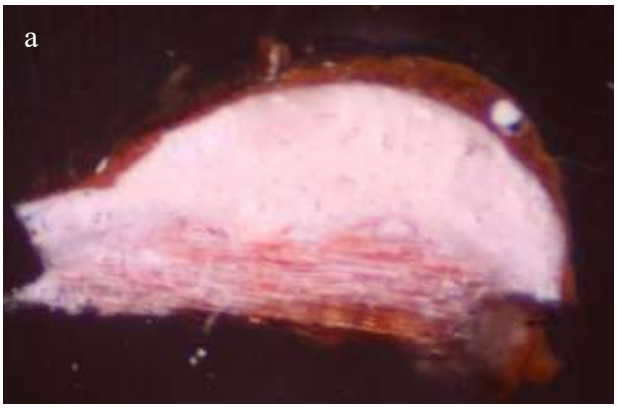

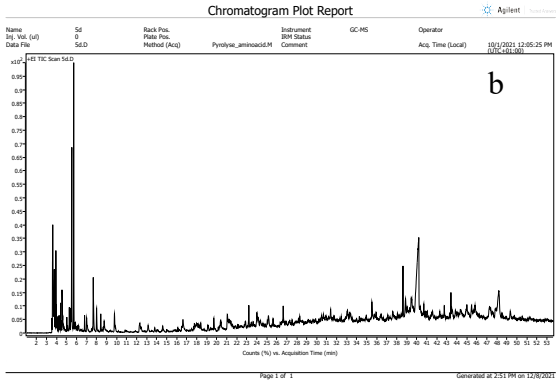

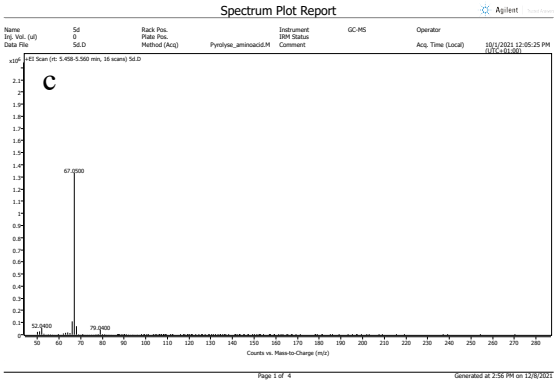

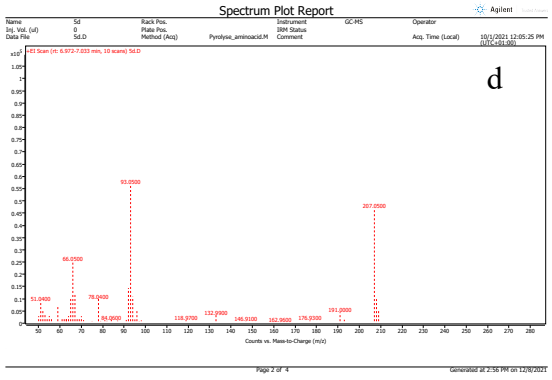

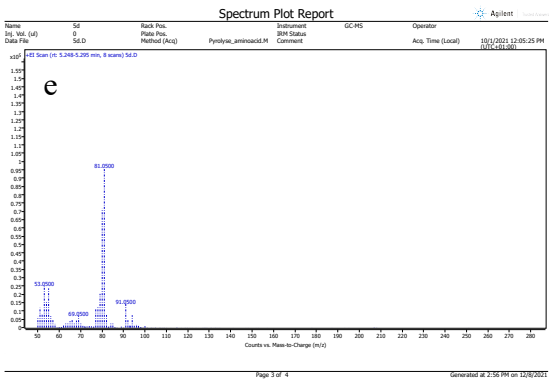

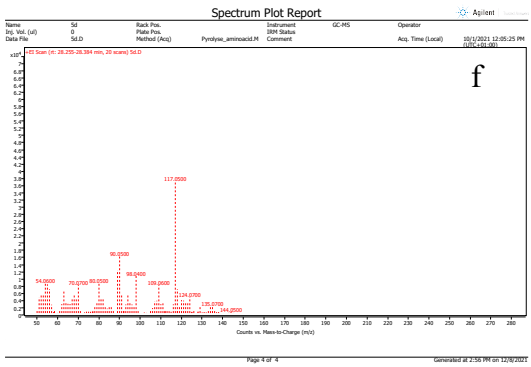

5.4.5 Molitg les Bains - Sample 5e

The Sample **5e** was also extracted from Clothes of Baby Christ from the **statue of Virgin of Hope** of the Molitg les Bains and the characterization was carried out as given below in Table 5.16.

Table 5.16 Characterization of sample 5e with a-Stratigraphy, b- Chromatogram, c, d, e-Mass spectra

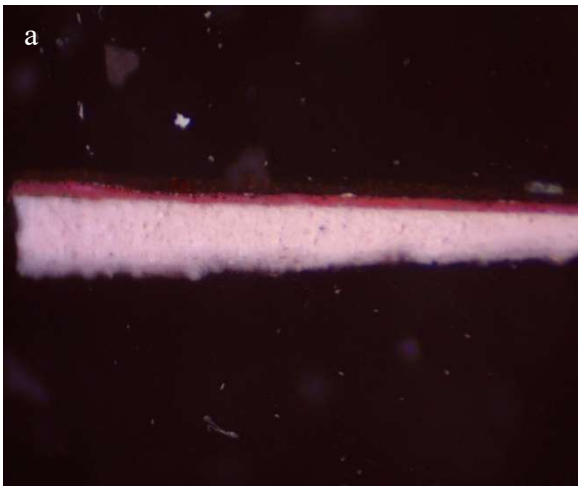

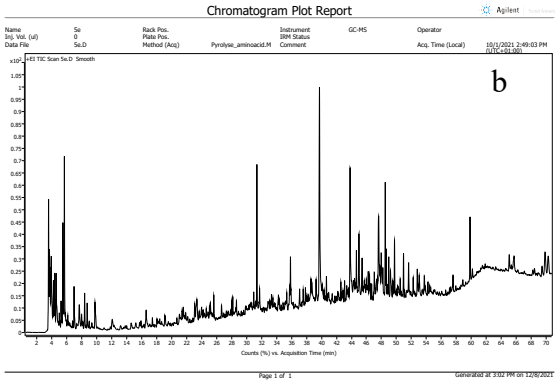

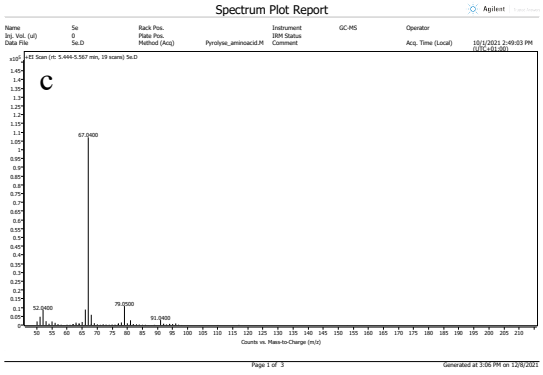

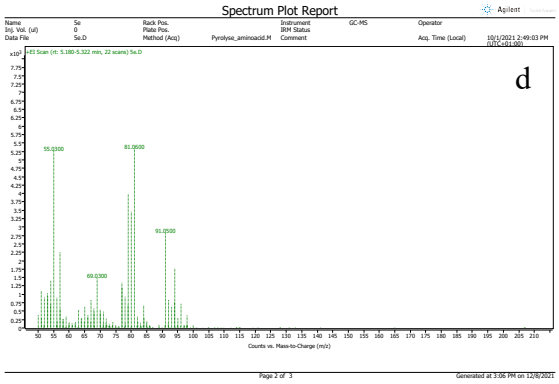

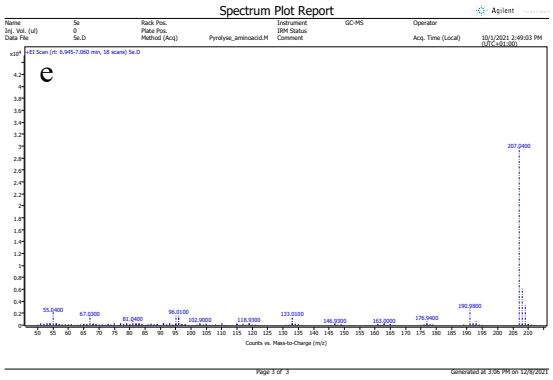

5.4.6 Molitg les Bains - Sample 5f

The Sample **5f** was also extracted from Crown of Virgin Mary of **Statue of Virgin of Hope** of the Molitg les Bains and the characterization was carried out as given below in Table 5.17.

Table 5.17 Characterization of sample 5f with a-Stratigraphy, b- Chromatogram, c, d, e & f-Mass spectra

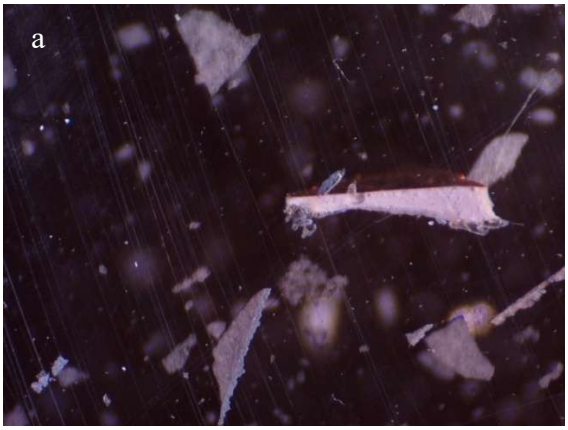

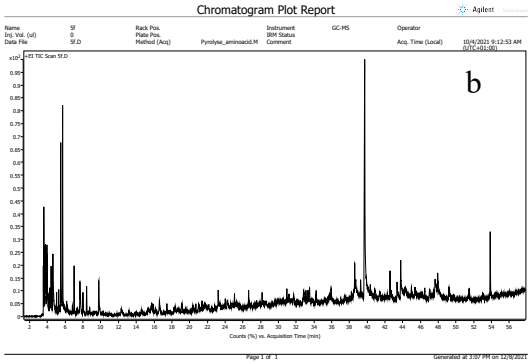

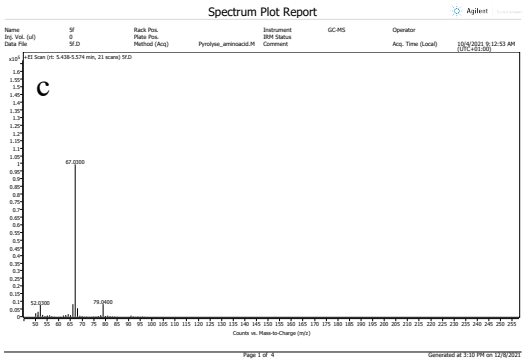

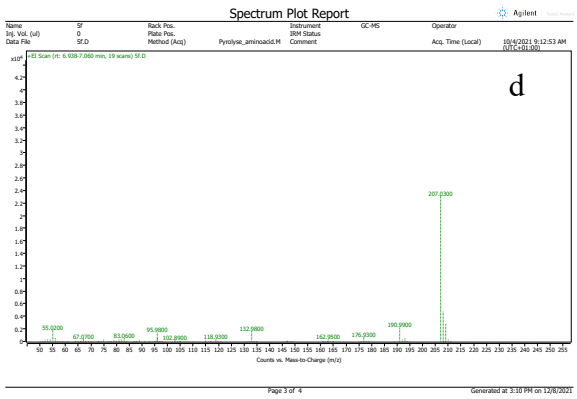

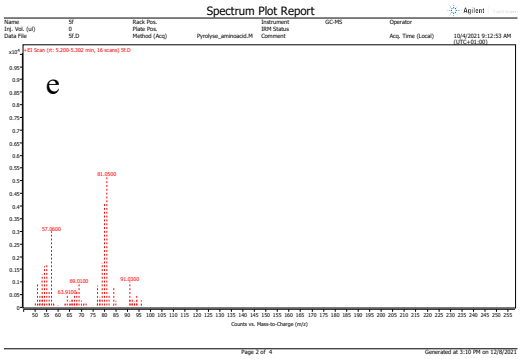

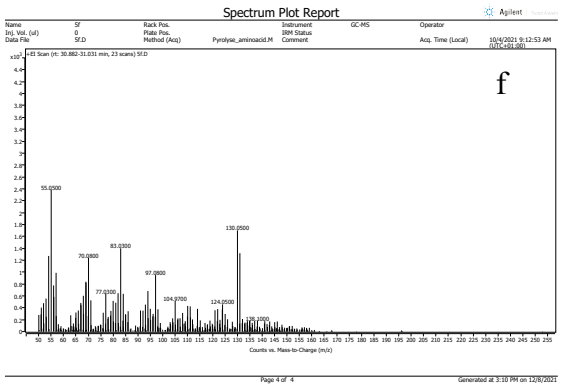

5.4.7 Molitg les Bains - Sample 5g

The Sample **5g** was also extracted from Beige Coat Inside of **Statue of Virgin of Hope** of the Molitg les Bains and the characterization was carried out as given below in Table 5.18.

Table 5.18 Characterization of sample 5g with a-Stratigraphy, b-Chromatogram, c & d-Mass spectra

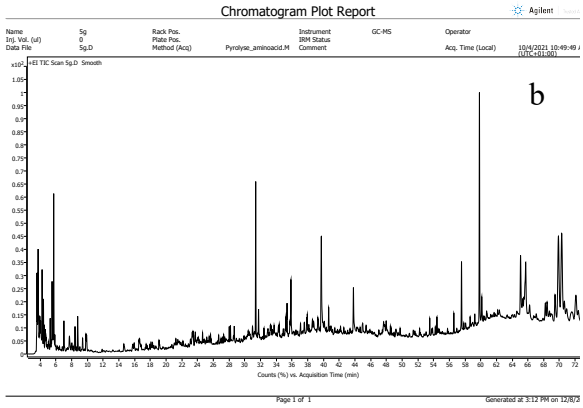

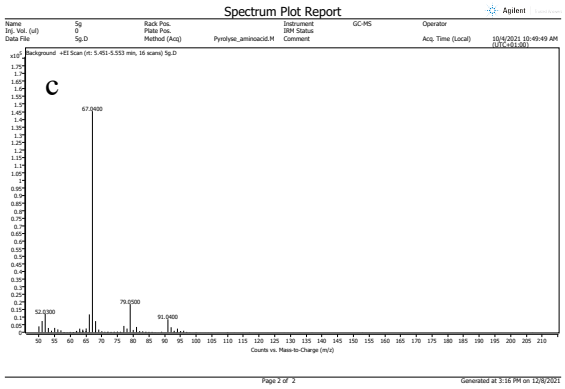

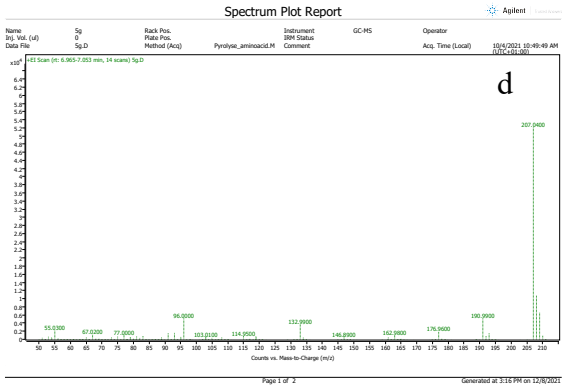

5.5 Results comparison Py-GC-MS vs ELISA

In section 5.1, 5.2, 5.3 and 5.4 the characterization of the four case studies from the Perpignan museum have been examined. The stratigraphy illustrated the different layers present in each sample. The final analysis was that of Pyrolysis GC-MS from which the chromatograms were obtained which further allowed to interpolate the mass spectra for fingerprinting the molecular markers of collagen, casein and ovalbumin. The Table 5.19 gives an overview into the results for the Pyrolysis GC-MS.

Table 5.19 Detection and intensity of proteins with Pyrolysis GC-MS

	Py-GC-MS	Py-GC-MS	Py-GC-MS
Sample No.	**Ovalbumin**	**Casein**	**Collagen**
1a	**	Inconclusive	**
1b	Inconclusive	**	*
2a	NA	NA	*
2c	NA	**	NA
3a	****	Inconclusive	****
3b	****	****	****
5a	NA	Inconclusive	***
5b	NA	*	***
5c	NA	NA	****
5d	Inconclusive	**	**
5e	NA	**	****
5f	**	**	****
5g	NA	NA	****

*	Possible presence
**	Confirmed presence
***	Good presence
****	Strong presence
NA	No presence

As can be observed from this Table, the presence of collagen is quite evident in almost all samples whereas casein in present in some samples and ovalbumin is present only in a selected few samples. In some samples it was not possible to confirm whether the protein is present as only one of the markers were present and this is a drawback of chromatography because it can lead to inconclusive results at times. Furthermore, as the sensitivity of Py-GC-MS is quite high, it can sometimes provide contradicting evidence of a false positive or false negative.

Finally, the same samples analysed in the previous sections were characterised with ELISA to see the comparison with the chromatography research shown in Table 5.19.

Table 5.20 shows the detection and intensity of proteins with ELISA below.

Table 5.20 Detection and intensity of proteins with ELISA

	Bradford	ELISA	ELISA	ELISA
Sample No.	**Protein (ug/m**	**Ovalbumin**	**Casein**	**Collagen**
1a	5.9	**	NA	**
1b	18.0	NA	**	*
2a	27.4	NA	*	*
2c	7.6	NA	**	NA
3a	1.5	NA	*	NA
3b	28.2	****	**	NA
5a	43.3	**	**	NA
5b	30.3	*	**	**
5c	48.0	****	*	*
5d	60.0	NA	**	NA
5e	67.5	**	**	*
5f	7.3	**	**	NA

*	Possible presence
**	Confirmed presence
***	Good presence
****	Strong presence
NA	No presence

After comparing Table 5.20 and 5.19 it can be seen that the somewhat similar protein detection shows up with both methods. With Pyrolysis-GC-MS it can be seen that the detection of collagen is quite impressive whereas with ELISA it lacks the detection due to the type of collagen antibody used for this research and the presence of different types of collagen rather makes it hard to correctly identify all types of collagen. On the other hand, ELISA provides correspondingly accurate results for the samples where in Pyrolysis-GC-MS the result might be inconclusive. In conclusion it can be inferred that both methods provide excellent sensitivity and complement each other.

Conclusions

In this study, a great emphasis on protein detection in cultural heritage artefacts specifically artworks such as paintings and sculptures was carried out over an extended period. Initially, paint models of ovalbumin, casein and collagen were utilised in immunodetection of the proteins with Indirect ELISA. The proteins were extracted with several developed protocols and an extensive analysis on the protein concentration was achieved. Furthermore, with ELISA based immunodetection it was possible to detect each set of protein individually and with substantial accuracy. The limit of detection for each paint model under analysis was determined with a series of serial dilutions and a selectivity study provided confirmation of distinctly being able to assess the proteins. To further optimise the accuracy of ELISA, silica based nanoparticles were synthesised, characterised and tested to increase the protein extraction levels for each protein. This study was one of the first attempt made in cultural heritage artworks to use nanobiotechnology for optimisation of immunodetection of proteinaceous materials. A new set of replica paint mock-ups were developed and characterisation was performed with ELISA as well as the introduction of Pyrolysis GC-MS by using standard markers to identify each protein separately. In the end, four different case studies from the Perpignan Museum in France were characterised by first obtaining the stratigraphy of the samples and characterising each of the samples with Pyrolysis GC-MS and ELISA. Finally the results of Pyrolysis GC-MS and ELISA were compared to see whether the two methods could serve as complimentary methods for protein analysis. In conclusion, the ELISA and Pyrolysis results were summed up to be complimentary while providing excellent data to support future studies on proteinaceous materials. As always, a deeper analysis is required on other artefacts that contain proteins to further provide more relevance to this study.

ANNEX I

Steps for the sample preparation in stratigraphy

1. Preparing/selecting the mould and gluing the samples
2. Using a resin and catalyser solution to entrap the sample
3. Polishing the dried resin

Figure 1.1 Selection of the moulds and the Resin used for the sample preparation

To start the protocol, it is important to select the moulds for preparing the samples. Once the moulds are selected as shown in Fig. 1.1, the samples that need to be investigated are glued to the bottom of a mould in a vertical upright position and numbered/labelled.

After the samples are placed in the moulds, the resin + catalyser solution is prepared with 1 part resin + 2-4% catalyser. This mixture needs to be stirred so as to provide a uniform solution before it is poured into the moulds. While stirring it is important to not remove the stirrer because there is a possibility of formation of air bubbles in the drops.

Once the resin solution is ready, it is immediately poured into each mould with the direction of flow being the same as the direction of the sample in the vertical position. This is due to the fact that if the resin solution flows in the opposite direction, the samples place in the vertical upright position my tumble at the bottom or fall over and ruin the entire stratigraphic analysis.

Once each mould is filled with the resin solution, it is allowed to sit overnight for the resins to dry. On the following day, the dried resins in the moulds, need to be removed and placed on a paper with sample numbers written at the edge of each resin sample as shown in Fig. 1.2 below.

Figure 1.2 Dried resin samples with labelled numbers

Furthermore, the resins prepared now need to undergo polishing to smoothen the surface and obtain more clarity to the layers under a bifocal microscope.

For polishing, different grain sizes were used. These were P1200, P600, P240 and P120 respectively. P120 is the initial grain size used for all samples, following P240, P600 and P1200. The P1200 is the last one used for all samples. P600 & P1200 are used for samples with a smaller size. As with the increase in grain size, the resins get finer. In the end an aluminium solution is used to give the final polish clarity on the surface of the resins.

Now that the samples are ready, the next step is to take the pictures under the bifocal microscope and determine the number of layers present in each sample while also imaging them with a camera head attached to the bifocal microscope. The images taken show the stratigraphy of each sample. An example of an image taken with stratigraphic layers is shown below in Fig. 1.3.

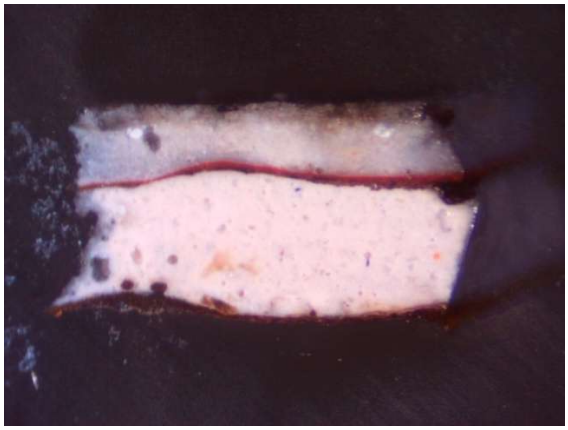

Figure 1.3 Stratigraphy of a paint sample

Naphthol Blue Black (Amido Black)

Initially, the Naphthol blue solution was synthesized in laboratory conditions, while the resins in the microsample were put into tubes using a syringe based method. According to the staining intensity obtained from solutions named NA_1, NA_2 and NA_3 the preparation of which is shown in Table 4.2, the protein can be identified (animal glue, egg, casein). This setup was allowed to dry off overnight, and the following morning the Amido Black Assay was performed.

Table 1.2: Preparation of the three solutions used for the Amido Black Assay in Proteic binders

Solution	pH	Reactants used
NA_1	2,0	0.1 g Amido Black 10B 450 mL AcOH glacial 450 mL AcONa 0.1 N 100 mL glycerol
NA_2	3,6	0.1 g Amido Black 10B 450 mL AcOH glacial 450 mL AcONa 0.1 N 30 mL Na_2HPO_4 70 mL glycerol
NA_3	7,0	0.1 g Amido Black 10B 900 mL Distilled Water 100 mL glycerol

After the preparation of the three solutions, they are applied to each sample individually to the samples that are present inside tubes that have resin. Once the samples have been soaked in the solutions, they are washed with a vinegar solutions to remove the extra dye colour. After the rising is completed the samples are kept on a thin glass lamina and put under study with a

bifocal microscope. In Fig. 4.4, is an example of a sample after the Amido black reaction has been done and ready to assess it under a microscope.

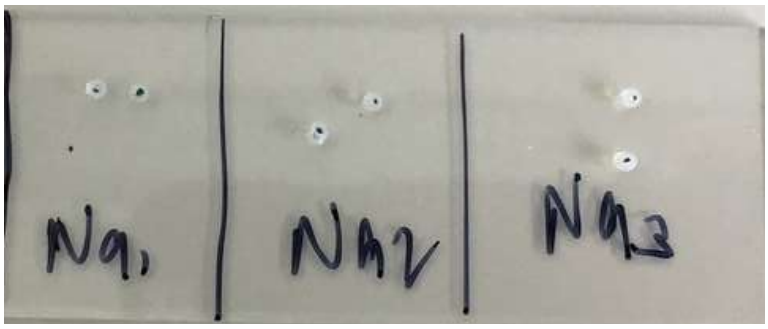

Figure 1.4 Sample after the reaction with three solutions NA_1, NA_2 and NA_3 of amido black

Finally, the results from the intensity translates to the darker the bluish colour of each sample for each of the Amido black solutions are compared with the Table 4.3 below to qualitatively have an estimate of the type of protein present in the samples.

Table 4.3 Identification Table with Amido Black 10B solutions NA_1, NA_2, NA_3

Protein Binder	**NA_1 (pH=2)**	**NA_2 (pH= 3,6)**	**NA_3 (pH= 7)**
Gelatin	+	++	+++
Casein	++	+++	++
Egg whole (yolk + white)	++	++	+
Egg white	++	+++	+
Egg yolk	+++	+++	+

The main drawback of this method is that it is only possible to detect one protein at a time and since proteinaceous binders are quite often in a combination of one or more proteins, and, mainly, the amido black test is difficult to interpret and can be inconclusive.

ANNEX II

Materials

The following reagents were used for sample preparation and ELISA experiments:
Phosphate-buffered saline solution (PBS, 137 mM NaCl, 10 mM phosphate (10.1 mM Na2HPO4, 1.8 mM KH2PO4), 2.7 mM KCl, pH 7.4) was used to dilute antigens and for washing step after the antigen incubation. PBS with Tween-20 (Sigma®), 0.05% solution (PBS-T) was used for the washing step after the incubation with primary and secondary antibodies.

Bovine serum albumin 1% (BSA, Acros Organics™) in PBS was used as a blocking solution, and solutions of BSA 0.1% in PBS and BSA 0.1% in PBS-T were used to dilute the primary and secondary antibodies, respectively.

Commercial standards of ovalbumin (albumin from chicken egg white, A5378, Sigma-Aldrich), commercial collagen from rabbit skin (Type I, Sigma-Aldrich), collagen from bovine Achilles tendon (C9879, Sigma-Aldrich) and casein (C3400, Sigma-Aldrich) were used as specific controls for the primary antibodies.

Coomassie blue dye G-250 (Acros Organics™) [0.6% (m/v) in Hydrochloric acid 0.6 M (HCl)] was used for protein quantification.

The primary antibodies of Monoclonal Anti-chicken Egg Albumin (Ovalbumin) antibody produced in mouse (Reference A6075, Sigma-Aldrich), Monoclonal Anti-Collagen antibody Type I produced in mouse (Reference C2456, Sigma-Aldrich), Polyclonal Anti-Casein Kinase II antibody produced in rabbit (Reference SAB4500514, Sigma-Aldrich) were used after the addition of the antigens.

The secondary antibodies of Monoclonal Anti-mouse IgG (whole molecule)-Alkaline Phosphatase antibody produced in rabbit (Reference A2418, Sigma-Aldrich), Polyclonal Anti-Rabbit IgG (whole molecule)-Alkaline Phosphatase antibody produced in goat (Reference A3687, Sigma-Aldrich) were used to link the with the first antibodies.

Glycine buffer solution (0.1 M, pH 10.4, with 1 mM MgCl2 and 1 mM ZnCl2) was used to dilute the substrate p-NPP (1 mg mL-1) and for washing step immediately before the substrate addition.

4-Nitrophenyl phosphate disodium salt hexahydrate (p-nPP, Sigma-Aldrich) was the substrate that produces an optical signal for detection after the antigen-antibody interactions. All reagents were used and diluted in de-ionized Millipore water.

Apparatus

The following apparatus was used to perform ELISA and related experiments:

96-well Microtiter plates (maximum volume 500µl) from Nunc^{TM}, 96-well Microtiter plates (maximum volume 150µl) were used for performing the ELISA and Bradford experiments. Micropipettes (100-1000µl, 10-100µl, 0.5-10µl), Microchannel (20-200µl), Standard Microtips (10µl, 200µl, 1000µl), Eppendorf tubes (1.5mL), 90mm disc plates, falcon tubes (50mL, 15mL), were the analytical tools used to perform ELISA in the microtiter plates.

Microplate reader (Thermo Scientific, Model Multiskan Go) was used to read the ELISA plates after the experiment was completed. An incubator (Memmert, Model IN110) was used for accelerating the ELISA experimental procedure (at 37° C).

The curve is linear (R^2= 0.9953) and we obtain an equation (y= 0.0095x + 0.0025). The absorbance values obtained from unknown protein extracts of paint models is substituted into this equation as y and the final value of x gives the amount of protein in solution (µg/ml).

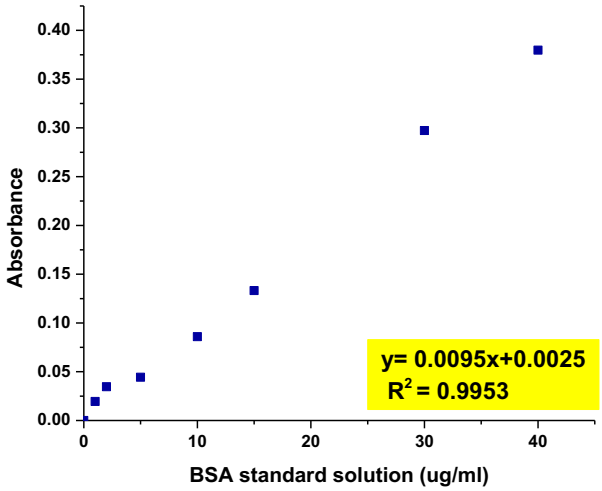

Figure 2.1 BSA Standard Curve (BSA (in ug/ml) vs Absorbance) with Coomassie Blue (Bradford Assay)

ANNEX III

Appendix A

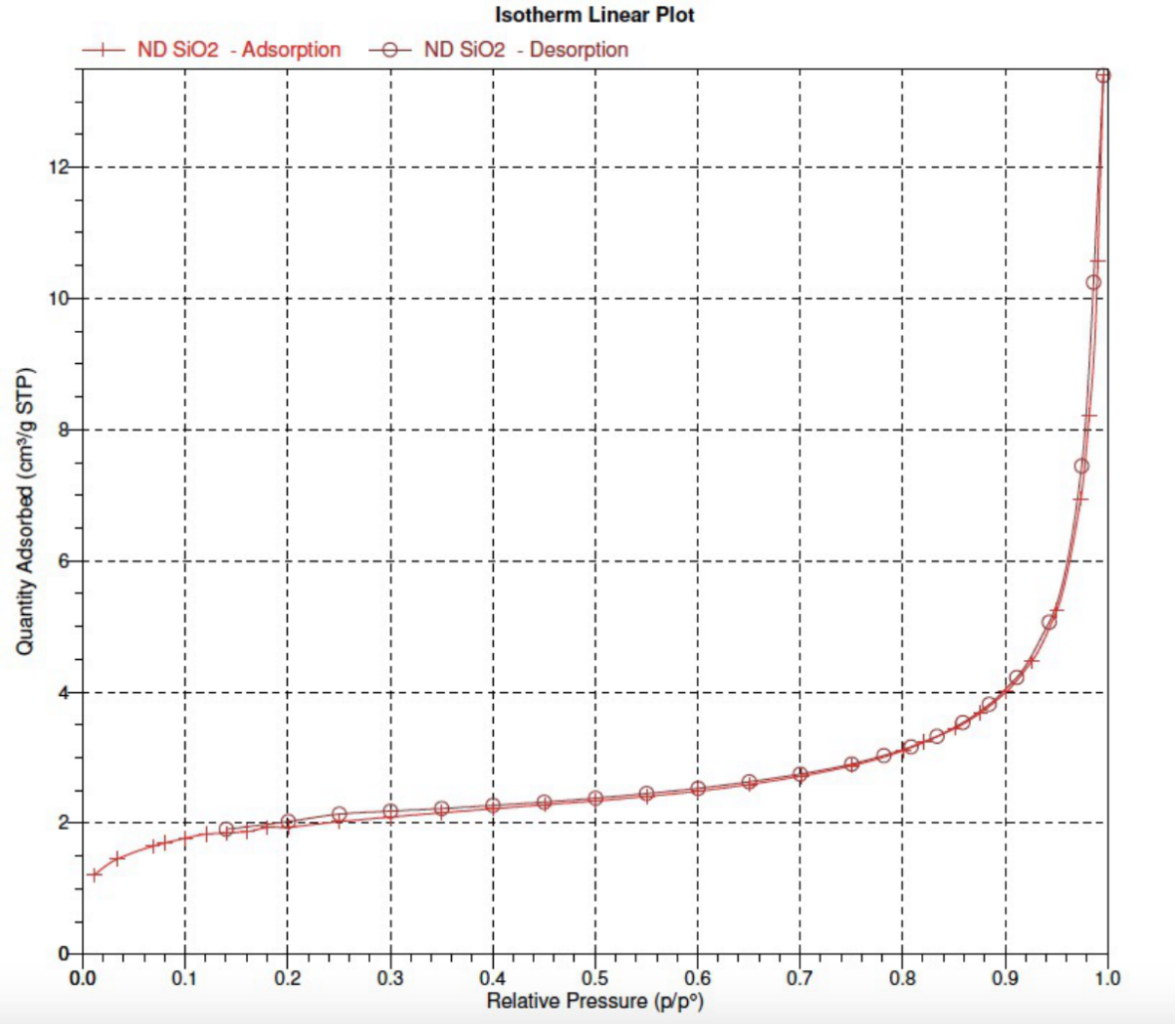

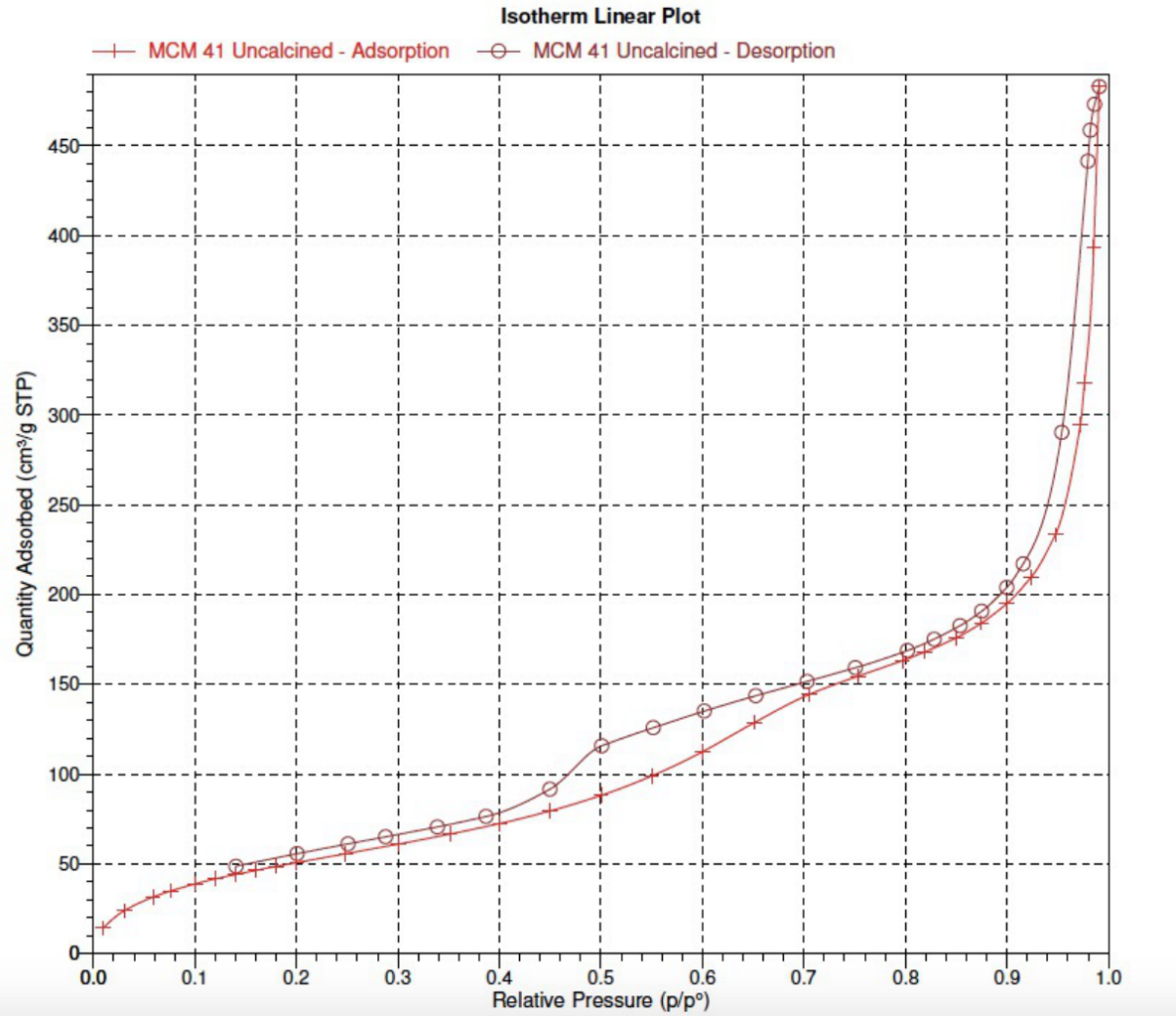
Isotherm Linear Plot
MCM 41 Uncalcined - Adsorption
MCM 41 Uncalcined - Desorption
Quantity Adsorbed (cm³/g STP)
Relative Pressure (p/p°)
0
50
100
150
200
250
300
350
400
450
0.0
0.1
0.2
0.3
0.4
0.5
0.6
0.7
0.8
0.9
1.0

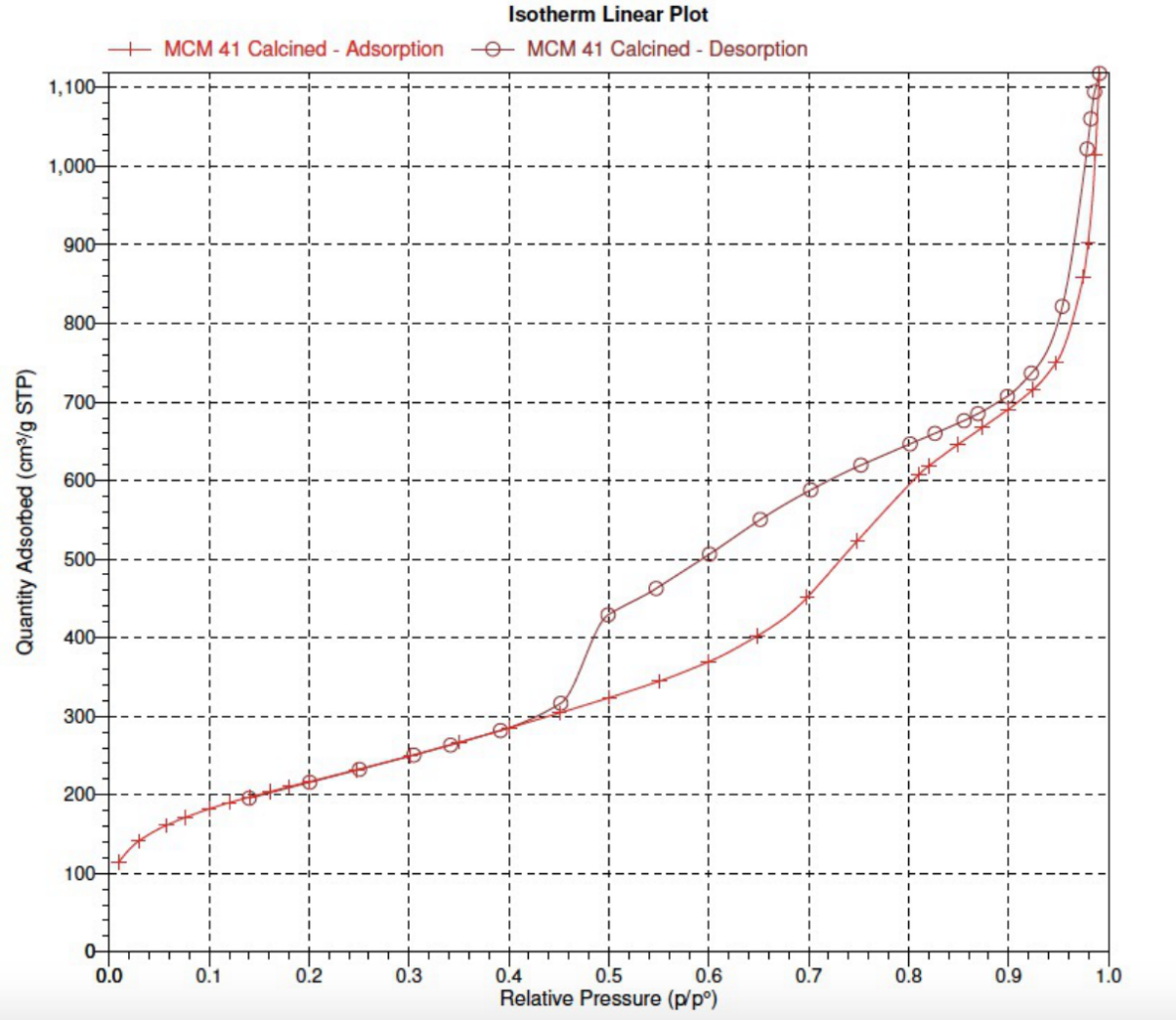

Fig 3.6: Isotherms of Nitrogen Porosimetry of a)NPSiO_2 b) MCM-41 uncalcined c)MCM-41 calcined

References

1. Brumann, C. (2015). Cultural heritage. In *International encyclopedia of the social and behavioral sciences* (pp. 414-419). Elsevier.

2. Vecco, M. (2010). A definition of cultural heritage: From the tangible to the intangible. *Journal of cultural heritage*, *11*(3), 321-324.

3. Pavlidis, G. (2019). Recommender systems, cultural heritage applications, and the way forward. *Journal of Cultural Heritage*, *35*, 183-196.

4. Turk, J., Pranjić, A. M., Hursthouse, A., Turner, R., & Hughes, J. J. (2019). Decision support criteria and the development of a decision support tool for the selection of conservation materials for the built cultural heritage. *Journal of Cultural Heritage*, *37*, 44-53.

5. Teza, G., Trevisani, S., & Pesci, A. (2019). The role of geoenvironmental sciences in Cultural Heritage preservation: the case of 1000 year old leaning bell tower of Caorle (Venice). *Journal of Cultural Heritage*, *39*, 270-277.

6. Trigger, B. G. (1989). *A history of archaeological thought*. Cambridge university press.

7. Prott, L., & O'Keefe, P. (1984). Law and the Cultural Heritage: Vol. I-Discovery and Excavation.

8. Blake, J. (2000). On defining the cultural heritage. *International & Comparative Law Quarterly*, *49*(1), 61-85.

9. Bowitz, E., & Ibenholt, K. (2009). Economic impacts of cultural heritage–Research and perspectives. *Journal of cultural heritage*, *10*(1), 1-8.

10. Timothy, D. J., & Nyaupane, G. P. (Eds.). (2009). *Cultural heritage and tourism in the developing world: A regional perspective*. Routledge.

11. De la Torre, M. (2013). Values and heritage conservation. *Heritage & Society*, *6*(2), 155-166.

12. Richards, G. (2018). Cultural tourism: A review of recent research and trends. *Journal of Hospitality and Tourism Management*, *36*, 12-21.

13. Liritzis, I., Laskaris, N., Vafiadou, A., Karapanagiotis, I., Volonakis, P., Papageorgopoulou, C., & Bratitsi, M. (2020). ARCHAEOMETRY: AN OVERVIEW. *Scientific Culture*, *6*(1).

14. Giuffrida, M. G., Mazzoli, R., & Pessione, E. (2018). Back to the past: deciphering cultural heritage secrets by protein identification. *Applied microbiology and biotechnology*, *102*, 5445-5455.

15. Dong, J., Locquet, A., Melis, M., & Citrin, D. S. (2017). Global mapping of stratigraphy of an old-master painting using sparsity-based terahertz reflectometry. *Scientific reports*, *7*(1), 15098.

16. Barberis, E., Baiocco, S., Conte, E., Gosetti, F., Rava, A., Zilberstein, G., ... & Manfredi, M. (2018). Towards the non-invasive proteomic analysis of cultural heritage objects. *Microchemical Journal*, *139*, 450-457.

17. Manuel Madariaga, J., & Romano, F. P. (2019). Non-destructive and microanalytical techniques in art and cultural heritage. *MICROCHEMICAL JOURNAL*, *145*, 1070-1070.

18. Salvador, C., Silva, M., Rosado, T., Vaz Freire, R., Bordalo, R., Candeias, A., & Caldeira, A. T. (2016). Biodeterioration of easel paintings: development of new mitigation strategies.

19. Kuckova, S., Hynek, R., & Kodicek, M. (2007). Identification of proteinaceous binders used in artworks by MALDI-TOF mass spectrometry. *Analytical and Bioanalytical Chemistry*, *388*, 201-206.

20. Teule, R., Scholten, H., Van den Brink, O. F., Heeren, R. M., Zafiropulos, V., Hesterman, R., ... & Albuquerque, M. B. (2003). Controlled UV laser cleaning of painted artworks: a systematic effect study on egg tempera paint samples. *Journal of Cultural Heritage*, *4*, 209-215.

21. Pollard, A. M. (2007). *Analytical chemistry in archaeology*. Cambridge University Press.

22. Evershed, R. P. (1993). Biomolecular archaeology and lipids. *World archaeology*, *25*(1), 74-93.

23. Colombini, M. P., & Modugno, F. (Eds.). (2009). *Organic mass spectrometry in art and archaeology*. John Wiley & Sons.

24. Mills, J. S., & White, R. (1977). Natural resins of art and archaeology their sources, chemistry, and identification. *Studies in conservation*, 22(1), 12-31.

25. Hahn, O. (2012). Analytical techniques in art, archaeology and conservation science. *Analytical and bioanalytical chemistry*, 402(4), 1411-1411.

26. Beneš, M., Zitová, B., Hradilová, J., & Hradil, D. (2008, January). Image processing in material analyses of artworks. In *International Conference on Computer Vision Theory and Applications* (Vol. 2, pp. 521-524). SCITEPRESS.

27. Botteon, A., Colombo, C., Realini, M., Castiglioni, C., Piccirillo, A., Matousek, P., & Conti, C. (2020). Non-invasive and in situ investigation of layers sequence in panel

paintings by portable micro-spatially offset Raman spectroscopy. *Journal of Raman Spectroscopy*, *51*(10), 2016-2021.

28. Branden, C. I., & Tooze, J. (2012). *Introduction to protein structure*. Garland Science.

29. Scheraga, H. A. (2014). *Protein structure*. Academic Press.

30. Schulz, G. E., & Schirmer, R. H. (2013). *Principles of protein structure*. Springer Science & Business Media.

31. Cartechini, L., Vagnini, M., Palmieri, M., Pitzurra, L., Mello, T., Mazurek, J., & Chiari, G. (2010). Immunodetection of proteins in ancient paint media. *Accounts of chemical research*, *43*(6), 867-876.

32. Liu, Y., Li, Y., Chang, R., Zheng, H., Li, M., Hu, Z., ... & Wang, B. (2016). Identification of proteinaceous binders in ancient tripitaka by the use of an enzyme-linked immunosorbent assay. *Analytical Sciences*, *32*(7), 735-740.

33. Salvador, C., Branco, A., Candeias, A., & Caldeira, A. T. (2017). Innovative approaches for immunodetection of proteic binders in art.

34. White, R. (1984). The characterization of proteinaceous binders in art objects. *National Gallery Technical Bulletin*, *8*, 5-14.

35. Salvador, C., Branco, A., Fialho, A., Semedo, M., Martins, S., Candeias, M. F., ... & Karmali, A. (2014). Detection of proteic binders in easel paintings using monoclonal antibodies. *Science, Technology and Cultural Heritage*, 329-334.

36. Ranalli, G., Zanardini, E., & Sorlini, C. (2009). Biodeterioration–including cultural heritage. In *Encyclopedia of microbiology* (pp. 191-205). Elsevier.

37. Falkiewicz-Dulik, M., Janda, K., & Wypych, G. (2015). *Handbook of material biodegradation, biodeterioration, and biostablization*. Elsevier.

38. Ager, F. J., Respaldiza, M. A., Scrivano, S., Ortega-Feliu, I., Kriznar, A., & Gomez-Tubio, B. (2020). Cultural heritage science at CNA (seville, Spain): Applications of XRF and IBA techniques to art and archaeological objects. *Radiation Physics and Chemistry*, *167*, 108324.

39. Arslanoglu, J., Schultz, J., Loike, J., & Peterson, K. (2010). Immunology and art: using antibody-based techniques to identify proteins and gums in artworks. *Journal of biosciences*, *35*(1), 3.

40. Palmieri, M., Vagnini, M., Pitzurra, L., Rocchi, P., Brunetti, B. G., Sgamellotti, A., & Cartechini, L. (2011). Development of an analytical protocol for a fast, sensitive and specific protein recognition in paintings by enzyme-linked immunosorbent assay (ELISA). *Analytical and bioanalytical chemistry*, *399*, 3011-3023.

41. Jiang, L., He, L., & Fountoulakis, M. (2004). Comparison of protein precipitation methods for sample preparation prior to proteomic analysis. *Journal of Chromatography A*, *1023*(2), 317-320.

42. Tokarski, C., Martin, E., Rolando, C., & Cren-Olivé, C. (2006). Identification of proteins in renaissance paintings by proteomics. *Analytical chemistry*, *78*(5), 1494-1502.

43. Sciutto, G., Zangheri, M., Prati, S., Guardigli, M., Mirasoli, M., Mazzeo, R., & Roda, A. (2017). Immunochemical micro imaging analyses for the detection of proteins in artworks. *Analytical Chemistry for Cultural Heritage*, 213-240.

44. Hu, W., Zhang, H., & Zhang, B. (2015). Identification of organic binders in ancient Chinese paintings by immunological techniques. *Microscopy and Microanalysis*, *21*(5), 1278-1287.

45. Matthew, D. (2009). Shoulders and Ronald T. *Collagen Structure and Stability Raines Annu. Rev. Biochem*, *78*, 929-958.

46. Ramshaw, J. A., Shah, N. K., & Brodsky, B. (1998). Gly-XY tripeptide frequencies in collagen: a context for host–guest triple-helical peptides. *Journal of structural biology*, *122*(1-2), 86-91.

47. Varelis, P., Melton, L., & Shahidi, F. (2018). *Encyclopedia of food chemistry*. Elsevier.

48. Strixner, T., & Kulozik, U. (2011). Egg proteins. In *Handbook of food proteins* (pp. 150-209). Woodhead publishing.

49. Mine, Y. (2015). Egg Proteins. In "Applied Food Protein Chemistry," ed. by Z. Ustunol.

50. Fox, P. F., & Mulvihill, D. M. (1990). Casein. In *Food gels* (pp. 121-173). Dordrecht: Springer Netherlands.

51. Cartechini, L., Vagnini, M., Palmieri, M., Pitzurra, L., Mello, T., Mazurek, J., & Chiari, G. (2010). Immunodetection of proteins in ancient paint media. *Accounts of chemical research*, *43*(6), 867-876.

52. Liu, Y., Li, Y., Chang, R., Zheng, H., Li, M., Hu, Z., ... & Wang, B. (2016). Identification of proteinaceous binders in ancient tripitaka by the use of an enzyme-linked immunosorbent assay. *Analytical Sciences*, *32*(7), 735-740.

53. Salvador, C., Branco, A., Candeias, A., & Caldeira, A. T. (2017). Innovative approaches for immunodetection of proteic binders in art.

54. White, R. (1984). The characterization of proteinaceous binders in art objects. *National Gallery Technical Bulletin*, *8*, 5-14.

55. Castro, R. Mateo, M. T. Dome, V. Peris Marti, JV Gimeno Adelantado, and F. Bosch Reig. "Study of binding media in works of art by gas chromatographic analysis of amino acids and fatty acids derivatized with ethyl chloroformate." *Journal of Chromatography A* 778, no. 1-2 (1997): 373-381.

56. Townsend, J. H., & Keune, K. (2006). Microscopical techniques applied to traditional paintings. *Infocus Magazine*, *41*(1), 54.

57. Creagh, D. C., & Bradley, D. A. (2000). *Radiation in art and archeometry*. Elsevier.

58. Di Gianvincenzo, F., Peggie, D., Mackie, M., Granzotto, C., Higgitt, C., & Cappellini, E. (2022). Palaeoproteomics guidelines to identify proteinaceous binders in artworks following the study of a 15th-century painting by Sandro Botticelli's workshop. *Scientific Reports*, *12*(1), 10638.

59. Picollo, M., Aceto, M., & Vitorino, T. (2018). UV-Vis spectroscopy. *Physical sciences reviews*, *4*(4), 20180008.

60. Rosi, F., Miliani, C., Clementi, C., Kahrim, K., Presciutti, F., Vagnini, M., ... & Sgamellotti, A. (2010). An integrated spectroscopic approach for the non-invasive study of modern art materials and techniques. *Applied Physics A*, *100*, 613-624.

61. Chércoles Asensio, R., San Andrés Moya, M., De la Roja, J. M., & Gómez, M. (2009). Analytical characterization of polymers used in conservation and restoration by ATR-FTIR spectroscopy. *Analytical and bioanalytical chemistry*, *395*, 2081-2096.

62. Marinach, C., Papillon, M. C., & Pepe, C. (2004). Identification of binding media in works of art by gas chromatography–mass spectrometry. *Journal of Cultural Heritage*, *5*(2), 231-240.

63. Milovanović, G. A., Ristić-Šolajic, M., & Janjić, T. J. (1982). Separation and identification of synthetic organic pigments in artists' paints by thin-layer chromatography. *Journal of Chromatography A*, *249*(1), 149-154.

64. Vallance, S. L., Singer, B. W., Hitchen, S. M., & Townsend, J. H. (1998). The development and initial application of a gas chromatographic method for the characterization of gum media. *Journal of the American Institute for Conservation*, *37*(3), 294-311.

65. Niessen, W. M. A. (1999). State-of-the-art in liquid chromatography–mass spectrometry. *Journal of Chromatography A*, *856*(1-2), 179-197.

66. Vallance, S. L. (1997). Critical review: Applications of chromatography in art conservation: Techniques used for the analysis and identification of proteinaceous and gum binding media. *Analyst*, *122*(6), 75R-81R.

67. Casoli, A., Mirti, P., & Palla, G. (1995). Characterization of medieval proteinaceous painting media using gas chromatography and gas chromatography—mass spectrometry. *Fresenius' journal of analytical chemistry*, *352*, 372-379.

68. Acikara, Ö. B. (2013). Ion-exchange chromatography and its applications. *Column chromatography*, *10*, 55744.

69. Russell, J., Singer, B. W., Perry, J. J., & Bacon, A. (2011). The identification of synthetic organic pigments in modern paints and modern paintings using pyrolysis-gas chromatography–mass spectrometry. *Analytical and Bioanalytical Chemistry*, *400*, 1473-1491.

70. Salvador, C., Branco, A., Fialho, A., Semedo, M., Martins, S., Candeias, M. F., ... & Karmali, A. (2014). Detection of proteic binders in easel paintings using monoclonal antibodies. *Science, Technology and Cultural Heritage*, 329-334.

71. Ranalli, G., Zanardini, E., & Sorlini, C. (2009). Biodeterioration–including cultural heritage. In *Encyclopedia of microbiology* (pp. 191-205). Elsevier.

72. Dulik, M. F., Janda, K., & Wypych, G. (2015). Handbook of Material Biodegradation, Biodeterioration, and Biostablization.

73. Ager, F. J., Respaldiza, M. A., Scrivano, S., Ortega-Feliu, I., Kriznar, A., & Gomez-Tubio, B. (2020). Cultural heritage science at CNA (seville, Spain): Applications of XRF and IBA techniques to art and archaeological objects. *Radiation Physics and Chemistry*, *167*, 108324.

74. Arslanoglu, J., & Schultz, J. (2009). Immunology and Art: Using antibody-based techniques to identify proteins and gums in binding Media and adhesives. *The Metropolitan Museum of Art Bulletin*, *67*(1), 40-45.

75. Palmieri, M., Vagnini, M., Pitzurra, L., Rocchi, P., Brunetti, B. G., Sgamellotti, A., & Cartechini, L. (2011). Development of an analytical protocol for a fast, sensitive and specific protein recognition in paintings by enzyme-linked immunosorbent assay (ELISA). *Analytical and bioanalytical chemistry*, *399*, 3011-3023.

76. Serefidou, M., Bracci, S., Tapete, D., Andreotti, A., Biondi, L., Colombini, M. P., ... & Parenti, D. (2016). Microchemical and microscopic characterization of the pictorial quality of egg-tempera polyptych, late 14th century, Florence, Italy. *Microchemical Journal*, *127*, 187-198.

77. Bakiler, M., Kırmızı, B., Öztürk, Ö. O., Hanyalı, Ö. B., Dağ, E., Çağlar, E., & Köroğlu, G. (2016). Material characterization of the Late Roman wall painting samples from Sinop Balatlar Church Complex in the black sea region of Turkey. *Microchemical Journal*, *126*, 263-273.

78. Gebremariam, K. F., Kvittingen, L., & Banica, F. G. (2016). Physico-Chemical Characterization of Pigments and Binders of Murals in a Church in Ethiopia. *Archaeometry*, *58*(2), 271-283.

79. Stanzani, E., Bersani, D., Lottici, P. P., & Colomban, P. (2016). Analysis of artist's palette on a 16th century wood panel painting by portable and laboratory Raman instruments. *Vibrational Spectroscopy*, *85*, 62-70.

80. Valadas, S., Candeias, A., Mirao, J., Tavares, D., Coroado, J., Simon, R. & Carvalho, M. L. (2011). Study of mural paintings using in situ XRF, confocal synchrotron-μ-XRF, μ-XRD, optical microscopy, and SEM-EDS—the case of the frescoes from Misericordia Church of Odemira. *Microscopy and Microanalysis*, *17*(5), 702-709.

81. Mathe, C., & Vieillescazes, C. (2002). Comprehension des mecanismes de coloration des liants proteiques picturaux a l'aide du Noir Amide 10B. *Actualite Chimique*, (7), 11-14.

82. Wilson, C. M. (1979). Studies and critique of Amido Black 10B, Coomassie Blue R, and Fast Green FCF as stains for proteins after polyacrylamide gel electrophoresis. *Analytical biochemistry*, *96*(2), 263-278.

83. Cotte, M., Susini, J., Solé, V. A., Taniguchi, Y., Chillida, J., Checroun, E., & Walter, P. (2008). Applications of synchrotron-based micro-imaging techniques to the chemical analysis of ancient paintings. *Journal of analytical atomic spectrometry*, *23*(6), 820-828.

84. Cotte, M., Welcomme, E., Solé, V. A., Salomé, M., Menu, M., Walter, P., & Susini, J. (2007). Synchrotron-based X-ray spectromicroscopy used for the study of an atypical micrometric pigment in 16th century paintings. *Analytical chemistry*, *79*(18), 6988-6994.

85. Henderson, J. (2013). *The science and archaeology of materials: an investigation of inorganic materials*. Routledge.

86. Van Grieken, R., & Janssens, K. (Eds.). (2004). *Cultural heritage conservation and environmental impact assessment by non-destructive testing and micro-analysis*. CRC Press.

87. Dallongeville, S., Garnier, N., Rolando, C., & Tokarski, C. (2016). Proteins in art, archaeology, and paleontology: from detection to identification. *Chemical reviews*, *116*(1), 2-79.

88. Mills, J., & White, R. (2012). *Organic chemistry of museum objects*. Routledge.

89. Kazarian, S. G., & Chan, K. L. A. (2006). Applications of ATR-FTIR spectroscopic imaging to biomedical samples. *Biochimica et Biophysica Acta (BBA)-Biomembranes*, *1758*(7), 858-867.

90. Della Ventura, G., Bellatreccia, F., Marcelli, A., Cestelli Guidi, M., Piccinini, M., Cavallo, A., & Piochi, M. (2010). Application of micro-FTIR imaging in the Earth sciences. *Analytical and Bioanalytical Chemistry*, *397*, 2039-2049.

91. Kazarian, S. G., & Chan, K. A. (2004). FTIR imaging of polymeric materials under high-pressure carbon dioxide. *Macromolecules*, *37*(2), 579-584.

92. Glassford, S. E., Byrne, B., & Kazarian, S. G. (2013). Recent applications of ATR FTIR spectroscopy and imaging to proteins. *Biochimica et Biophysica Acta (BBA)-Proteins and Proteomics*, *1834*(12), 2849-2858.

93. Scalarone, D., Chiantore, O., & Riedo, C. (2008). Gas chromatographic/mass spectrometric analysis of on-line pyrolysis–silylation products of monosaccharides. *Journal of Analytical and Applied Pyrolysis*, *83*(2), 157-164.

94. Perkiömäki, K. Developing Applications of Ion Chromatography for Aqueous Conservation Treatments of Cultural Heritage Artifacts.

95. Manhita, Ana, Vanda Santos, Helena Vargas, Antonio Candeias, Teresa Ferreira, and Cristina Barrocas Dias. "Ageing of brazilwood dye in wool–a chromatographic and spectrometric study." *Journal of cultural heritage* 14, no. 6 (2013): 471-479.

96. Poulin, J., Kearney, M., & Veall, M. A. (2022). Direct Inlet Py-GC-MS analysis of cultural heritage materials. *Journal of Analytical and Applied Pyrolysis*, *164*, 105506.Degano, I., & La Nasa, J. (2017). Trends in high performance liquid chromatography for cultural heritage. *Analytical chemistry for cultural heritage*, 263-290.

97. Pirok, B. W., den Uijl, M. J., Moro, G., Berbers, S. V., Croes, C. J., van Bommel, M. R., & Schoenmakers, P. J. (2019). Characterization of dye extracts from historical cultural-heritage objects using state-of-the-art comprehensive two-dimensional liquid chromatography and mass spectrometry with active modulation and optimized shifting gradients. *Analytical chemistry*, *91*(4), 3062-3069.

98. Reeves, T., Popelka-Filcoff, R. S., & Lenehan, C. E. (2013). Towards identification of traditional European and indigenous Australian paint binders using pyrolysis gas chromatography mass spectrometry. *Analytica Chimica Acta*, *803*, 194-203.

99. Han, J., Wanrooij, J., van Bommel, M., & Quye, A. (2017). Characterisation of chemical components for identifying historical Chinese textile dyes by ultra high performance liquid chromatography–photodiode array–electrospray ionisation mass spectrometer. *Journal of Chromatography A*, *1479*, 87-96.

100. Kusch, P. (2019). *Pyrolysis–gas chromatography: mass spectrometry of polymeric materials*.

101. Peris-Vicente, J., Adelantado, J. G., Carbó, M. D., Castro, R. M., & Reig, F. B. (2006). Characterization of waxes used in pictorial artworks according to their relative amount of fatty acids and hydrocarbons by gas chromatography. *Journal of chromatography A*, *1101*(1-2), 254-260.

102. La Nasa, J., Modugno, F., & Degano, I. (2021). Liquid chromatography and mass spectrometry for the analysis of acylglycerols in art and archeology. *Mass Spectrometry Reviews*, *40*(4), 381-407.

103. Karadag, R. (2014, November). Some non-destructive and micro-analytical methods for the conservation on textiles from cultural heritage. In *Proceedings of the 19th International Conference on Cultural Heritage and New Technologies* (pp. 1-12).

104. Badea, E. (2019). Chemistry for cultural heritage: Connecting past and future. *Heritage Science*, *7*(1), 1-4.

105. Chiantore, O., Riedo, C., & Scalarone, D. (2009). Gas chromatography–mass spectrometric analysis of products from on-line pyrolysis/silylation of plant gums used as binding media. *International Journal of Mass Spectrometry*, *284*(1-3), 35-41.

106. Cuoco, G., Mathe, C., Archier, P., & Vieillescazes, C. (2011). Characterization of madder and garancine in historic French red materials by liquid chromatography-photodiode array detection. *Journal of cultural heritage*, *12*(1), 98-104.

107. Han, B., Daheur, G., & Sablier, M. (2016). Py-GCxGC/MS in cultural heritage studies: An illustration through analytical characterization of traditional East Asian handmade papers. *Journal of analytical and applied pyrolysis*, *122*, 458-467.

108. Germinario, G., Rigante, E. C., van der Werf, I. D., & Sabbatini, L. (2017). Pyrolysis gas chromatography–mass spectrometry of triarylmethane dyes. *Journal of analytical and applied pyrolysis*, *127*, 229-239.

109. Peris-Vicente, J., Adelantado, J. G., Carbó, M. D., Castro, R. M., & Reig, F. B. (2006). Characterization of proteinaceous glues in old paintings by separation of the o-phtalaldehyde derivatives of their amino acids by liquid chromatography with fluorescence detection. *Talanta*, *68*(5), 1648-1654.

110. No, A. M. C. T. B., & Analytical Methods Committee. (2018). Analytical pyrolysis in cultural heritage. *Analytical Methods*, *10*(46), 5463-5467.

111. Karapanagiotis, I., Lakka, A., Valianou, L., & Chryssoulakis, Y. (2008). High-performance liquid chromatographic determination of colouring matters in historical garments from the Holy Mountain of Athos. *Microchimica Acta*, *160*, 477-483.

112. Bongiorno, D., Caponetti, E., & Ceraulo, L. (2009). Mass spectrometry coupled to chromatography systems and cultural heritage: a case study on the content of an ancient jar. In *CHEMISTRY AND CONSERVATION SCIENCE 2ND RESIDENTIAL SUMMER SCHOOL PALERMO (ITALY), 20TH-27TH JULY 2008 PROCEEDINGS* (pp. 27-45). EA Varella and E. Caponetti.

113. Chieli, A., Sanyova, J., Doherty, B., Brunetti, B. G., & Miliani, C. (2016). Chromatographic and spectroscopic identification and recognition of ammoniacal cochineal dyes and pigments. *Spectrochimica Acta Part A: Molecular and Biomolecular Spectroscopy*, *162*, 86-92.

114. Petroviciu, I., Berghe, I. V., Cretu, I., Albu, F., & Medvedovici, A. (2012). Identification of natural dyes in historical textiles from Romanian collections by LC-DAD and LC-MS (single stage and tandem MS). *Journal of Cultural Heritage*, *13*(1), 89-97.

115. Frade, J. C., Ribeiro, M. I., Graça, J., & Rodrigues, J. (2009). Applying pyrolysis-gas chromatography/mass spectrometry to the identification of oriental lacquers: study of two lacquered shields. *Analytical and bioanalytical chemistry*, *395*, 2167-2174.

116. Silva, M., Rosado, T., Teixeira, D., Candeias, A., & Caldeira, A. T. (2015). PRODUCTION OF GREEN BIOCIDES FOR CULTURAL HERITAGE. NOVEL BIOTECHNOLOGICAL SOLUTIONS. *International Journal of Conservation Science*, *6*..

117. Reber, E. A. (2020). Gas chromatography-mass spectrometry (GC-MS): applications in archaeology. *In Encyclopedia of Global Archaeology* (pp. 4441-4457). Cham: Springer International Publishing.

118. Heron, C., & Stacey, R. (2000). Archaeology: uses of chromatography in. *Encyclopedia of Separation Science*, 2083-2089.

119. Shedrinsky, A. M., Wampler, T. P., & Baer, N. S. (1991). Pyrolysis gas chromatography (PyGC) applied to the study of natural waxes in art and archaeology. In *Science, Technology and European Cultural Heritage* (pp. 553-558). Butterworth-Heinemann.

120. Fremout, W., Dhaenens, M., Saverwyns, S., Sanyova, J., Vandenabeele, P., Deforce, D., & Moens, L. (2010). Tryptic peptide analysis of protein binders in works of art by liquid chromatography–tandem mass spectrometry. *Analytica chimica acta*, 658(2), 156-162.

121. Colombini, M. P., & Modugno, F. (2004). Characterisation of proteinaceous binders in artistic paintings by chromatographic techniques. *Journal of Separation Science*, 27(3), 147-160.

122. Fremout, W., Sanyova, J., Saverwyns, S., Vandenabeele, P., & Moens, L. (2009). Identification of protein binders in works of art by high-performance liquid chromatography–diode array detector analysis of their tryptic digests. *Analytical and bioanalytical chemistry*, 393(8), 1991-1999.

123. Colombini, M. P., Modugno, F., Giacomelli, M., & Francesconi, S. (1999). Characterisation of proteinaceous binders and drying oils in wall painting samples by gas chromatography–mass spectrometry. *Journal of Chromatography A*, 846(1-2), 113-124.

124. Chiavari, G., Gandini, N., Russo, P., & Fabbri, D. (1998). Characterisation of standard tempera painting layers containing proteinaceous binders by pyrolysis (/methylation)-gas chromatography-mass spectrometry. *Chromatographia*, 47(7), 420-426.

125. Witkowski, B., Biesaga, M., & Gierczak, T. (2012). Proteinaceous binders identification in the works of art using ion-pairing free reversed-phase liquid chromatography coupled with tandem mass spectrometry. *Analytical Methods*, 4(5), 1221-1228.

126. Carbini, M., Stevanato, R., Rovea, M., Traldi, P., & Favretto, D. (1996). Curie-point Pyrolysis-Gas Chromatography/Mass Spectrometry in the Art Field. 2—The Characterization of Proteinaceous Binders. *Rapid communications in mass spectrometry*, 10(10), 1240-1242.

127. Bonaduce, I., & Andreotti, A. (2009). Py-GC/MS of organic paint binders. *Organic mass spectrometry in art and archaeology*, 304-326.

128. Chiavari, G., Fabbri, D., Galletti, G. C., & Mazzeo, R. (1995). Use of analytical pyrolysis to characterize Egyptian painting layers. *Chromatographia*, 40(9), 594-600.

129. Degano, I., Modugno, F., Bonaduce, I., Ribechini, E., & Colombini, M. P. (2018). Recent advances in analytical pyrolysis to investigate organic materials in heritage science. *Angewandte Chemie International Edition*, 57(25), 7313-7323.

130. Hu, W., Zhang, H., & Zhang, B. (2015). Identification of organic binders in ancient Chinese paintings by immunological techniques. *Microscopy and Microanalysis*, *21*(5), 1278-1287.

131. Wu, S. H., Mou, C. Y., & Lin, H. P. (2013). Synthesis of mesoporous silica nanoparticles. *Chemical Society Reviews*, *42*(9), 3862-3875.

132. Sun, Y., Kang, C., Zhang, A., Liu, F., Hu, J., Zhong, X., & Xie, J. (2016). Co-delivery of dual-drugs with nanoparticle to overcome multidrug resistance. *European Journal of BioMedical Research*, *2*(2), 12-18.

133. Baglioni, P., Carretti, E., & Chelazzi, D. (2015). Nanomaterials in art conservation. *Nature Nanotechnology*, *10*(4), 287-290.

134. Hagens, W. I., Oomen, A. G., de Jong, W. H., Cassee, F. R., & Sips, A. J. (2007). What do we (need to) know about the kinetic properties of nanoparticles in the body?. *Regulatory toxicology and pharmacology*, *49*(3), 217-229

135. Rajput, N. (2015). Methods of preparation of nanoparticles-a review. *International Journal of Advances in Engineering & Technology*, *7*(6), 1806.

136. Pal, S. L., Jana, U., Manna, P. K., Mohanta, G. P., & Manavalan, R. (2011). Nanoparticle: An overview of preparation and characterization. *Journal of applied pharmaceutical science*, (Issue), 228-234.

137. Wang, S. (2009). Ordered mesoporous materials for drug delivery. *Microporous and mesoporous materials*, *117*(1-2), 1-9.

138. Lin, C. X. C., Qiao, S. Z., Yu, C. Z., Ismadji, S., & Lu, G. Q. M. (2009). Periodic mesoporous silica and organosilica with controlled morphologies as carriers for drug release. *Microporous and Mesoporous Materials*, *117*(1-2), 213-219.

139. Izquierdo-Barba, I., Martinez, Á., Doadrio, A. L., Pérez-Pariente, J., & Vallet-Regí, M. (2005). Release evaluation of drugs from ordered three-dimensional silica structures. *European Journal of Pharmaceutical Sciences*, *26*(5), 365-373.

140. Maria, G., Berger, D., Nastase, S., & Luta, I. (2012). Kinetic studies on the irinotecan release based on structural properties of functionalized mesoporous-silica supports. *Microporous and mesoporous materials*, *149*(1), 25-35.

141. ALOthman, Z. A. (2012). A review: fundamental aspects of silicate mesoporous materials. *Materials*, *5*(12), 2874-2902.

142. Tan, W., Wang, K., He, X., Zhao, X. J., Drake, T., Wang, L., & Bagwe, R. P. (2004). Bionanotechnology based on silica nanoparticles. *Medicinal research reviews*, *24*(5), 621-638.

143. Rao, K. S., El-Hami, K., Kodaki, T., Matsushige, K., & Makino, K. (2005). A novel method for synthesis of silica nanoparticles. *Journal of colloid and interface science*, 289(1), 125-131.

144. Song, S. W., Hidajat, K., & Kawi, S. (2005). Functionalized SBA-15 materials as carriers for controlled drug delivery: Influence of surface properties on matrix− drug interactions. *Langmuir*, *21*(21), 9568-9575.

145. Song, S. W., Hidajat, K., & Kawi, S. (2005). Functionalized SBA-15 materials as carriers for controlled drug delivery: Influence of surface properties on matrix− drug interactions. *Langmuir*, *21*(21), 9568-9575.

146. Maria, G., Stoica, A. I., Luta, I., Stirbet, D., & Radu, G. L. (2012). Cephalosporin release from functionalized MCM-41 supports interpreted by various models. *Microporous and Mesoporous Materials*, *162*, 80-90.

147. Kresge, A. C., Leonowicz, M. E., Roth, W. J., Vartuli, J. C., & Beck, J. S. (1992). Ordered mesoporous molecular sieves synthesized by a liquid-crystal template mechanism. *nature*, *359*(6397),710-712.

148. Monnier, A., Schuth, F., Huo, Q., Kumar, D., & Margolese, D. (1993). RS 45 Maxwell, GD Stucky, M. Krishnamurty, P. Petroff and et al. *Science*, *261*, 1299-1303.

149. Karakassides, M. A., Bourlinos, A., Petridis, D., Coche-Guerènte, L., & Labbè, P. (2000). Synthesis and characterization of copper containing mesoporous silicas. *Journal of Materials Chemistry*, *10*(2), 403-408.

150. Hoffmann, F., Cornelius, M., Morell, J., & Fröba, M. (2006). Silica-based mesoporous organic–inorganic hybrid materials. *Angewandte Chemie International Edition*, *45*(20), 3216-3251.

151. Cao, N., Zhao, Y., Sang, B., Wang, Z., Cao, L., Sun, L., & Zou, X. (2016). Fabrication of autofluorescent porous silica nanoparticles for redox-responsive drug release. *Materials Science and Engineering: C*, *69*, 330-336.

152. Stöber, W., Fink, A., & Bohn, E. (1968). Controlled growth of monodisperse silica spheres in the micron size range. *Journal of colloid and interface science*, *26*(1), 62-69.

153. Tadanaga, K., Morita, K., Mori, K., & Tatsumisago, M. (2013). Synthesis of monodispersed silica nanoparticles with high concentration by the Stöber process. *Journal of sol-gel science and technology*, *68*, 341-345.

154. Ravat, V., Mantri, D. B., Selvam, P., & Aghalayam, P. (2009). Platinum group metals substituted MCM-41 molecular sieves: Synthesis, characterization and application as novel catalysts for the reduction of NO by CO. *Journal of Molecular Catalysis A: Chemical*, *314*(1-2), 49-54.

155. Tu, J., Boyle, A. L., Friedrich, H., Bomans, P. H., Bussmann, J., Sommerdijk, N. A. & Kros, A. Mesoporous Silica Nanoparticles with Large Pores for the.

156. Bharti, B., Meissner, J., Klapp, S. H., & Findenegg, G. H. (2014). Bridging interactions of proteins with silica nanoparticles: The influence of pH, ionic strength and protein concentration. *Soft Matter*, *10*(5), 718-728.

157. Lundqvist, M., & Ingmar Sethson, A. (2004). Bengt-Harald Jonsson Protein Adsorption onto Silica Nanoparticles: Conformational Changes Depend on the Particles' Curvature and the Protein Stability. *Langmuir*, *20*, 10639-10647.

158. Xu, C., Lei, C., & Yu, C. (2019). Mesoporous silica nanoparticles for protein protection and delivery. *Frontiers in chemistry*, *7*, 290.

159. Barberis, E., Baiocco, S., Conte, E., Gosetti, F., Rava, A., Zilberstein, G. & Manfredi, M. (2018). Towards the non-invasive proteomic analysis of cultural heritage objects. *Microchemical Journal*, *139*, 450-457.

160. Salvador, C., Silva, M., Rosado, T., Vaz Freire, R., Bordalo, R., Candeias, A., & Caldeira, A. T. (2016). Biodeterioration of easel paintings: development of new mitigation strategies.

161. Cartechini, L., Vagnini, M., Palmieri, M., Pitzurra, L., Mello, T., Mazurek, J., & Chiari, G. (2010). Immunodetection of proteins in ancient paint media. *Accounts of chemical research*, *43*(6), 867-876.

162. Liu, Y., Li, Y., Chang, R., Zheng, H., Li, M., Hu, Z., ... & Wang, B. (2016). Identification of proteinaceous binders in ancient tripitaka by the use of an enzyme-linked immunosorbent assay. *Analytical Sciences*, *32*(7), 735-740.

163. Salvador, C., Branco, A., Candeias, A., & Caldeira, A. T. (2017). Innovative approaches for immunodetection of proteic binders in art.

164. Giuffrida, M. G., Mazzoli, R., & Pessione, E. (2018). Back to the past: deciphering cultural heritage secrets by protein identification. *Applied microbiology and biotechnology*, *102*, 5445-5455.

165. Palmieri, M., Vagnini, M., Pitzurra, L., Brunetti, B. G., & Cartechini, L. (2013). Identification of animal glue and hen-egg yolk in paintings by use of enzyme-linked immunosorbent assay (ELISA). *Analytical and bioanalytical chemistry*, *405*, 6365-6371.

166. Cao, N., Zhao, Y., Sang, B., Wang, Z., Cao, L., Sun, L., & Zou, X. (2016). Fabrication of autofluorescent porous silica nanoparticles for redox-responsive drug release. *Materials Science and Engineering: C*, *69*, 330-336.

167. Stöber, W., Fink, A., & Bohn, E. (1968). Controlled growth of monodisperse silica spheres in the micron size range. *Journal of colloid and interface science*, *26*(1), 62-69.

168. Tadanaga, K., Morita, K., Mori, K., & Tatsumisago, M. (2013). Synthesis of monodispersed silica nanoparticles with high concentration by the Stöber process. *Journal of sol-gel science and technology*, *68*, 341-345.

169. Ravat, V., Mantri, D. B., Selvam, P., & Aghalayam, P. (2009). Platinum group metals substituted MCM-41 molecular sieves: Synthesis, characterization and application as novel catalysts for the reduction of NO by CO. *Journal of Molecular Catalysis A: Chemical*, *314*(1-2), 49-54.

170. Doménech-Carbó, A. (2018). Solid-to-solid transformations in organic electrosynthesis. *Modern Electrosynthetic Methods in Organic Chemistry*, 167-179.

171. Mills, J. S., & White, R. (1987). Natural resins and lacquers. *The Organic Chemistry of museum objects*, 83-110.

172. Thompson, D. V. (1956). *The materials and techniques of medieval painting* (Vol. 327). Courier Corporation.

173. Giocanti, H., Nowik, W., & Vieillescazes, C. (2011, May). Un exemple de nuancier architectural de Le Corbusier: appartement 725 de la Cité Radieuse (Marseille). In *Colloque «From Can to Canvas»*.

174. Benoit, C., Grimaud, P., Badet, C., Mognetti, E., & May, R. (2010, April). De la restauration à l'exposition: à la recherche de sens et de cohérence. La restauration de L'Apothéose de saint Roch de Michel Serre exposée au grand public. In *CeROArt. Conservation, exposition, Restauration d'Objets d'Art* (No. 5). Association CeROArt asbl.

175. GIOCANTI, H. (2020). La restauration des monuments d'Espira-de-Conflent et de Finestret (Pyrénées-Orientales, France). *Monuments et décors de la Semaine Sainte en Méditerranée: Arts, rituels, liturgies*, 181.

176. Friedstein, H. G. (1981). A short history of the chemistry of painting. *Journal of Chemical education,* 58(4), 291.

177. Eastlake, C. L. (2001). *Methods and materials of painting of the great schools and masters*. Courier Corporation.

178. Weil, P. D. (2007). TECHNICAL ART HISTORY AND ARCHEOMETRY II AN EXPLORATION OF CARAVAGGIO'S PAINTING TECHNIQUES. *Revista Brasileira de Arqueometria, Restauração e Conservação*, 1, 106-110.

179. Viñas, S. M. (1998). Original written sources for the history of mediaeval painting techniques and materials: a list of published texts. *Studies in conservation*, 43(2), 114-124.

180. Roy, A., Smith, P., & Bomford, D. (1998). Painting techniques history, materials and studio practice: contributions to the Dublin Congress 7-11 September 1998. *(No Title)*.

181. Speed, H. (1987). *Oil Painting Techniques and Materials*. Courier Corporation.

182. Chiavari, G., Galletti, G. C., Lanterna, G., & Mazzeo, R. (1993). The potential of pyrolysis—gas chromatography/mass spectrometry in the recognition of ancient painting media. *Journal of analytical and applied pyrolysis*, *24*(3), 227-242.

183. Colombini, M. P., Fuoco, R., Giacomelli, A., & Muscatello, B. (1998). Characterization of proteinaceous binders in wall painting samples by microwave-assisted acid hydrolysis and GC-MS determination of amino acids. *Studies in conservation*, *43*(1), 33-41.

184. Carbini, M., Stevanato, R., Rovea, M., Traldi, P., & Favretto, D. (1996). Curie-point Pyrolysis-Gas Chromatography/Mass Spectrometry in the Art Field. 2—The Characterization of Proteinaceous Binders. *Rapid communications in mass spectrometry*, *10*(10), 1240-1242.

185. Bauer, W. J., Badoud, R., & Löliger, J. (2010). *Science et technologie des aliments: Principes de chimie des constituants et de technologie des procédés*. PPUR Presses polytechniques.<

186. https://www.ecofoyer.fr/amenagement-interieur/peinture-caseine/%20:

References for Case Studies

1. TOLLON Bruno, The sculpted altarpieces in Roussillon and French Cerdagne in the 18th century, Postgraduate thesis, University of Toulouse le Mirail, 1972, p.62.

2. CCRP archives: Municipality of Rivesaltes, Saint-André parish church: study prior to the restoration, Christ altarpiece. Departmental Center for Conservation-Restoration of Heritage, directed by Anne Rigaud, 2016.

3. CORTADE, Eugène (abbot), Baroque Altarpieces of Roussillon, Imprimerie SINTHE, Perpignan, 1973, p.192, 199.

4. DALMAU Guillaume, "The gilder Félix Escribà, biographical approach", Around a restored work, the baroque altarpiece of the Mas Girvès de Llo, exhibition catalog, 2020, p.130.

5. DALMAU Guillaume, "Gilding works for the brotherhood of Sanch de Rivesaltes", Around a restored work, the baroque altarpiece of Mas Girvès de Llo, exhibition catalog, 2020, p.215.

6. LUGAND Julien, Painters and gilders in Roussillon (1650-1730), Thesis for obtaining a doctorate in Art History, Under the supervision of Professor Bruno Tollon, University of Toulouse - Le Mirail, Department of History of 'Art, December 2004, volume II, p.451, p.487.

7. A.D.66, 53J11: Pre-inventory of the Artistic Wealth of France. Municipality of Rivesaltes. Saint-André parish church. Typed pre-inventory, carried out by Jean Nougaret, October-November 1968.

8. Francine Arnal, Bernard Sournia, D. De Maistre, summer 1967 / winter 1968. A.D.66, 90J11: account book of the Sanch de Rivesaltes brotherhood

SOURCES

1.A.D. 66: 53 J 211 - Pre-inventory: Palace of the Kings of Majorca, Saint Dominic, Saint-François, Carmes.

BIBLIOGRAPHY:

1.CORTADE, Eugène (abbot), Baroque altarpieces of Roussillon, Imprimerie SINTHE, Perpignan, 1973, p.156.

2.REYNAL, Jean. "The altarpiece of Mas Girvès". In Exhibition catalog: "Millennium of North Catalan Art". General Council of Pyrénées-Orientales. Perpignan. p.135.
3.Ch. BODIN, Ch. DE CASTAIGNER and G. DALMAU, notice of the work published in the exhibition catalog: Around a restored work, the baroque altarpiece of Mas Girvès de Llo, 2020, p.13-49.
4.DALMAU Guillaume, "The gilder Félix Escribà, biographical approach", Around a restored work, the baroque altarpiece of the Mas Girvès de Llo, exhibition catalog, 2020, p.133.